

Politecnico di Torino

Master of Science Thesis

Reconfigurable Array Antennas

focusing on Beam Forming Network and Phase Shift



Author:
Mahyar Zeinalpour

Supervisors
Prof. Giuseppe Vecchi
Dr. Giorgio Giordanengo

A thesis submitted in fulfillment of the requirements for the
degree of Master of Science in Telecommunications Engineering
in the
Department of Electronics and Telecommunications

Superiore Mario Boella Institute

July 16, 2018

Acknowledgments

I would like to pay my regards to my supervisors prof. Giuseppe Vecchi and Dr Giorgio Giordanengo for providing me the opportunity to have wonderful experience in the field of Antenna. Their knowledge, presence made me possible to take always the proper path in order to obtain the final outcome of this work.

Secondly, my whole hearted gratitude to my family and friends for their constant support and motivation. They know that without their support I would not be here in this moment. This result is much of theirs as it is mine

Contents

1	Introduction	4
1.1	Objectives and Motivations	4
1.2	Thesis Outline	4
1.3	Thesis Contribution	5
2	Phased Antenna Arrays	6
2.1	Architecture	7
2.2	Phase Shifters	7
	What does Phase Shift mean?	8
	Switched Line	9
	Loaded Line	9
	Reflection Type	10
2.3	Analysis of commercial phase shifters	10
2.3.1	Scattering Matrix	11
2.3.2	Insertion Loss	12
2.3.3	Return Loss	13
2.3.4	VSWR	13
2.3.5	Bandwidth	13
2.3.6	Phase Shifters Categories	14
2.4	Analysis of Phase Shifter	18
2.4.1	N-Port Network	18
2.4.2	2-Port Coupler Phase Shifter	19
2.4.3	4-Port Coupler Phase Shifter	21
	General Properties of 4-Port Network	21
	Quadrature Hybrid Analysis	24
	Analysis of 4-Port Coupler (Quadrature Coupler) with Varactor as load	30
3	Phase Shifter Analysis and Design	34
3.1	Theoretical Analysis	34
3.1.1	Impedance Transforming Hybrid Coupler	36
3.1.2	Reflection Load	38
	Varactor diode	38

	Inductance L_S	40
	Shunt Resistance R_P	40
3.1.3	Theoretical Results	43
	Phase Shifter with $r_Z = 1$	44
	Phase Shifter with $r_Z = 2.5$	47
	Comparisons	49
3.2	Simulation	52
3.2.1	Simulation of Branch-Line Coupler with $r_Z = 1$	52
	Results of Phase Shifter With Using R_P in the Network Load	54
	Results of Phase Shifter Without Using R_P in the Network Load	55
3.2.2	Simulation of Branch-Line Coupler with $r_Z = 2.5$	57
	Results of Phase Shifter With Using R_P in the Network Load	59
	Results of Phase Shifter Without Using R_P in the Network Load	61
	Conclusion	63
3.3	Design and Improvements	63
3.3.1	Theoretical Analysis	63
3.3.2	Simulation	70
	Design of Branch-Line Coupler with $r_Z = 1.3$	70
	Load Network	71
	Simulation Results of Phase Shifter	71
	Simulation Results of Removing R_P from Load Network	73
	Simulation Results of using $L_S = 1.3nH$ and $R_P = 140, 156.4, 170\Omega$ and without R_P	75
	Simulation Results of using $L_S = 1.9nH$ and $R_P = 140, 156.4, 170\Omega$ and removing R_P	78
	Simulation Results of using $L_S = 2nH$ and $R_P = 140, 156.4, 170\Omega$ and removing R_P	81
4	Realization And Measurements	85
5	Conclusions And Perspectives	89

Chapter 1

Introduction

1.1 Objectives and Motivations

Phased antenna arrays have been traditionally used in military applications for several decades and are important components to realize detecting and tracking of the target especially in radars. As the commercial demand enhanced rapidly, the phased antenna array has been exploited in civil areas. In comparison to conventional mechanical scanning system, phased array system has some benefits: first, higher scanning rate. Second it's easy to change the direction of radiation beam. Third, the accuracy of phased array is much better than mechanical scanning. The principal motivation for developing phased array antennas has been the need to steer antenna beams rapidly to widely diverse angles. Clearly, electronic beam steering is required because mechanically rotating antennas do not have these capabilities. Consequently phased array antenna can replace the mechanical scanning in both military and civil utilization.

Although phased array antennas have great advantages, the technology of phased array has not been widely exploited in the commercial area. There are some drawbacks which restrict the phased array developments such as high cost, complex structure. So it is meaningful to find some novel ideas to decrease these restrictions.

1.2 Thesis Outline

This thesis is divided into 5 Chapters. Chapter 1 describes about the previous works and disadvantages and gives the motivations of the work performed in this thesis. Chapter 2 discusses the phased antenna arrays definition and its architectures, describing about phase shift meaning, analog phase shifter categories, analysis of commercial phase shifter and defining the key parameters such as insertion loss, return loss and relative phase shift and bandwidth, at the end of this Chapter analysis of N-port network, 2-port and

4-port coupler phase shifter are presented. Chapter 3 presents impedance transforming branch line coupler and reflective load and theoretical analysis and simulation of proposed phase shifter with two different impedance ratio r_Z at the end of this Chapter theoretical analysis and simulation of an improved phase shifter are presented to compensate disadvantages of previous proposed phase shifter. In Chapter 4 improved proposed phase shifter are manufactured to obtain agreement between theoretical analysis and simulation result with measurements and realization results. In Chapter 5 conclusion and perspective of this work are presented.

1.3 Thesis Contribution

Phase Antenna Array plays an important role in wireless communication and transmission. They are utilized in many application such as RADAR removing any mechanical dependency [1]. The crucial part of phased array are phase shifters changing the main beam scanning by variation of the exciting current phase [3]. So many researches are studied to find a solution for increasing the phase range while the insertion loss is low and constant [37][43] [51][52]. A novel approach to increase range of phase shift is to use impedance transforming branch line coupler and a single varactor series with an inductance considered as load which are connected to coupler output ports with a shunt resistor for eliminating variation of insertion loss which is resulted from parasitic resistance of the varactor diode. By increasing the impedance ratio of the coupler from $r_Z = 1$ to $r_Z = 4$, phase shift range can be increased from 100° to 240° respectively, while the size of coupler and insertion loss and insertion loss variation dramatically increased [43]. By changing the load network configuration which output ports of impedance transforming branch line coupler are connected to two reflections loads and choosing a proper impedance ratio of $r_Z = 1.3$, 360° relative phase shift range is achieved and insertion loss is relatively low in comparison to previous configuration load network with single varactor. In new load network configuration, each load has two series resonant varactors series with an inductance which are interconnected with a quarter wavelength transmission line [51]. So an improvement is achieved by proper impedance ratio of $r_Z = 1.3$ and load network configuration. By changing the series inductance, insertion loss can be reduced as much as possible, return loss can be better than $-20dB$ and bandwidth can be ISM band at center frequency of $f_0 = 2.45GHz$. By try and error approach, inductance value of $L_S = 1.9nH$ is eventually achieved.

Chapter 2

Phased Antenna Arrays

Phased Antenna Array is a system in which several individual antennas are arranged and connected together to produce the radiation pattern can be strengthened in a desired direction and minimum in an undesired one (directional radiation pattern) to meet more demanding specifications (high directivity and high gain). The direction of phased array radiation beam can be electronically steered in space to any point without moving antenna which eliminates any need of mechanically movements associating to any single antenna that makes it efficient and cost-effective solution for complex radars and communication systems [1]. This unique ability of phased antenna array is being used in many applications such as military and civilian radars.[2], [3].

Electronic scanning of the main beam is accomplished by changing the phase of exciting currents in each element antenna of the array which is the most interesting part of the array antennas that's why we call it phased array antenna [3].

Figure 2.1 shows two typical Array antennas.

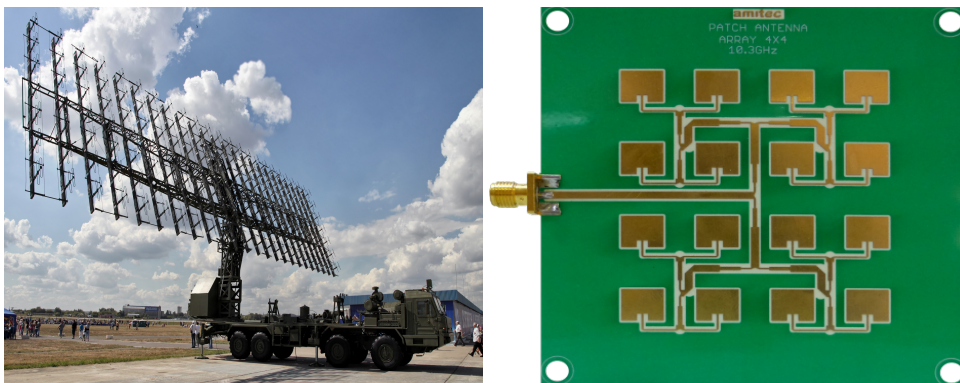


Figure 2.1: Typical Array Antennas

2.1 Architecture

The block diagram of an N-element phased array is shown in Figure 2.2. N identical antennas are equally spaced by a distance d along an axis [2].

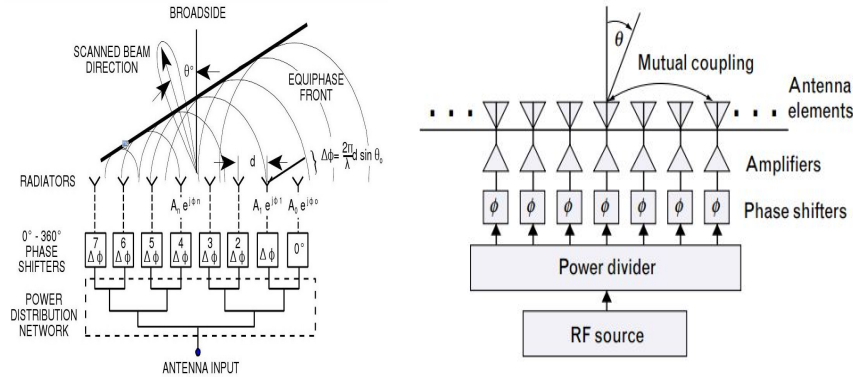


Figure 2.2: Typical Phased Array Antennas Architecture

As we can see from the above block diagram, the main parts of an array antenna are [4]:

1. Source
2. Power Divider (Power Distribution Network)
3. Phase Shifters
4. Amplifiers
5. Antenna elements (Radiators)

Figure 2.2 demonstrates the concept of a phased array antenna architecture that uses phase shifters to electronically steer the Antenna beam over the scan sector to point in a desired direction. The Radio Frequency (RF) source produces a waveform that is divided into individual paths, each containing a phase shifter and amplifier [4].

Phase Shifter which is the major part of this Architecture is the main goal of this article which will be described in following Section in details.

2.2 Phase Shifters

As mentioned previously the main part of the Phased Antenna Array is Phase Shifter. Phase shifters are devices in which the phase of radio frequency source is shifted by propagating through transmission line [5]. Phase shifters are being used in many applications such as Beam Forming Networks (BFN) and phased array antennas.

What does Phase Shift mean?

The phase of a signal is meaningless until it is compared to another one. A phase shift denotes an amount which a signal has shifted from the another signal or original one and can change from 0 to 360 degrees. Figure 2.3 shows two signals with the same amplitude but with a difference phase [6].

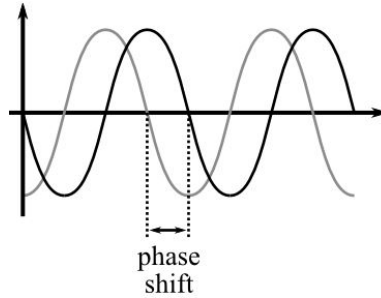


Figure 2.3: Phase Shift

Design of the phase shifter depends on the required phase shift, equipments and the range of frequencies[7].

By controlling the phase difference between the elements of array antenna, the maximum radiation can be produced in any required direction to create a scanning array. This is the basic idea of electronic scanning phased array system. Since the scanning phase must be continuous (Analog), the system should be able to keep constantly varying the phase between the elements. In practice for creating phase shift we can use ferrite (by using magnetic field within ferrite) or diode phase shifters (by changing the bias voltage of the diode)[8].

Figure 2.4 below demonstrates a typical example of phase shifter which is called incremental switched-line pin diode phase shifter.

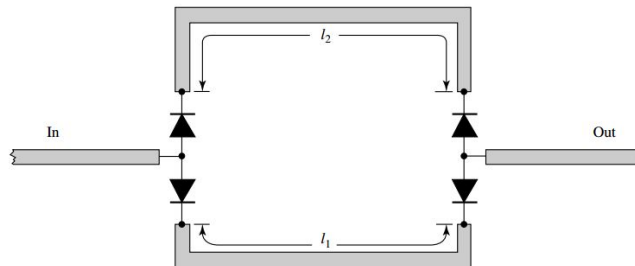


Figure 2.4: Incremental switched-line phase shifter using PIN diodes

As we can see in this Figure, there exist 4 PIN-diodes which by controlling the bias of each diode, the length path of l_1 and l_2 will be switched off

and on. So the phase shift in this case can be calculated as below[8]:

$$\Delta\phi = k(l_2 - l_1) \quad (2.1)$$

$$k = \frac{2\pi}{\lambda} \quad (2.2)$$

For obtaining entire range of phase shift (0 - 180°), several such Incremental switched-line phase shifters would be exploited. The basic design of a phase shifter utilizing PIN diodes are typically classified into three categories: *Switched Line*, *Loaded Line*, and *Reflection Type*[8].

Switched Line

Switched Line phase shifter, as mentioned above, can be easily computed from difference in electrical length of reference and delay arm (l_1 , l_2 in Figure 2.4)[9], however they are usually designed for binary phase shifts of $\Delta\phi = 180^\circ, 90^\circ, 45^\circ, 22.5^\circ$ [8].

Loaded Line

Loaded Line phase shifter are usually utilized for 45° phase shift or lower phase shift bits[8]. Figure 2.5 shows the structure of this kind of phase shifter.

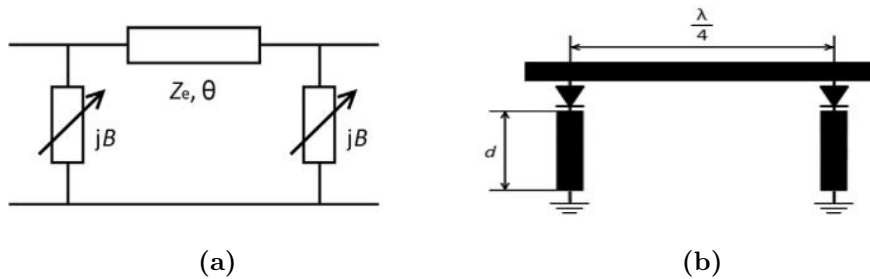


Figure 2.5: (a) Basic loaded-line phase shifter, and (b) Main-line PIN diode mounted type loaded-line phase shifter design

As shown in Fig 2.5a loaded Line phase shifter consists of Two similar susceptance loads which are connected to $\lambda/4$ transmission line. Susceptance values are controlled by switches like pin diodes. They have a change in the phase of the signal when switched into the circuit, while they affect the amplitude of the signal very little. The loads must have a very high reflection coefficient in order to minimize the loss of the phase shifter (they should utilize purely reactive elements). Obviously the loads must not be too close to a short circuit in phase angle, or the phase shifter will suffer extreme loss. By spacing the reactive loads approximately a quarter-wavelength apart,

the amplitude perturbation can be minimized and equalized in both states. By changing the length of d , the value of susceptance would be changed (Figure 2.5b)[10][11][12]

Reflection Type

Reflection Type phase shifter is a kind of phase shifter which provides a continuous phase shift and consists of a coupler which splits input power equally into two signals at port 2 and 3 with 90° out of phase and loads network including varactor diodes and inductors which reflects the input power and they are combined in phase (for identical loads) at the coupler output (port 4)[13][14].

The coupler can be a Lange Coupler, a Hybrid Coupler, or a Rat-Race Coupler which will be describe later in details.

Figure 2.6 demonstrates the structure of reflection type phase shifter.

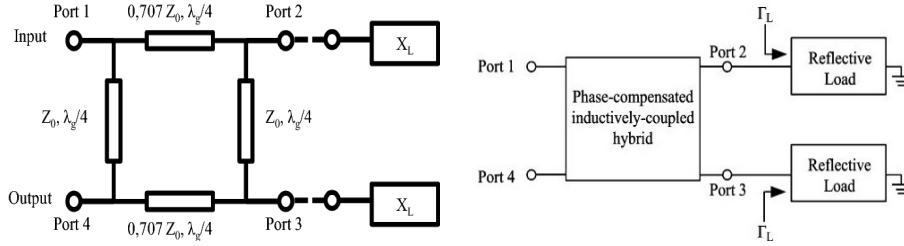


Figure 2.6: Typical Schematic of reflection type phase shifter

As we can see in this Figure port 2 and 3 of 90° hybrid coupler are connected to identical reflective loads (X_L). Input signal (at port 1) is reflected from port 2 and 3. Port 4 which is the output port of the coupler (isolated from port 1) combines this reflection signal. Phase shift between port 1 and port 4 is calculated as below [15] :

$$\Delta\varphi = -2\tan^{-1}(X_L/Z_0) \quad (2.3)$$

Reflective Load (X_L) should be variable to cover the whole range of phase shift from 0 to 360 degrees. There are so many articles with many approaches to find entirely covering phase shift with low insertion loss. Designing of this kind of phase shifter is the objective part of this article described in following Chapter[16][17]

2.3 Analysis of commercial phase shifters

before going to describe about commercial phase shifters for better understanding the details, some expressions and key parameters are described.

2.3.1 Scattering Matrix

Scattering matrix provides a complete description of N-port network. The scattering matrix relates the voltage waves incident on the ports to those reflected from the ports[14]. In fact scattering matrix (S-parameter) gives us useful information about the microwave network behavior which we are studying Figure 2.7 below shows an arbitrary N-port microwave network with specified voltages and currents on it.

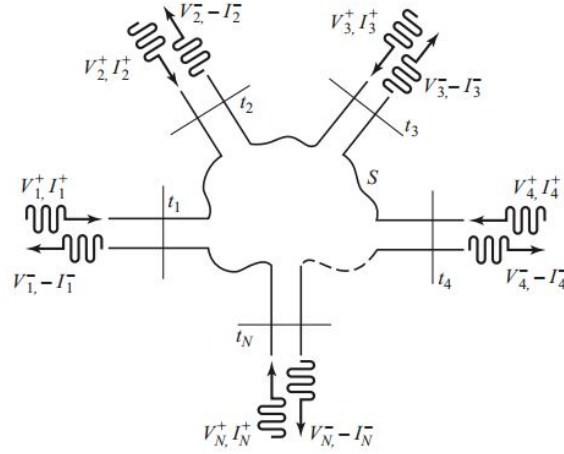


Figure 2.7: An arbitrary N-port microwave network

By considering this network V_n^+ represents the amplitude of the incident voltage wave to the port n and V_n^- represent the amplitude of the reflected voltage from the port n. The relationship between Voltage matrix (incident and reflected matrix) and scattering matrix can be defined as below:

$$[V^-] = [S] [V^+] \quad (2.4)$$

Where V^- is the reflected voltage wave and V^+ is the incident voltage wave vector and S is the Scattering matrix. The elements of S are all complex number (real and imaginary part) for consideration of both magnitude and phase. Element of Scattering Matrix can be defined as below[14]:

$$S_{ij} = \frac{V_i^-}{V_j^+} \Big|_{V_k^+ = 0, k \neq j} \quad (2.5)$$

Where i represents the port of the reflected wave (output port) and j represents the port of the incident wave (input port). The incident waves on all ports except the j th port are set to zero, which means that all ports should be terminated in matched loads to avoid reflection[14]. So S_{ii} represents the reflection coefficient which means all other ports except port i are terminated in matched loads. S_{ii} refers to the ratio of the amplitude of the signal

that reflects from port i to the amplitude of the signal incident on that port. Parameters along the diagonal of the S-matrix are referred to as reflection coefficients [18]. And also S_{ij} represents the transmission coefficient from port j to port i when all other ports are terminated in matched loads[14].

Reflection coefficient in Transmission Line theory can also be defined when the transmission line terminated in an arbitrary load impedance Z_L . This problem will illustrate wave reflection on transmission lines[14], Figure 2.8 below shows this principle:

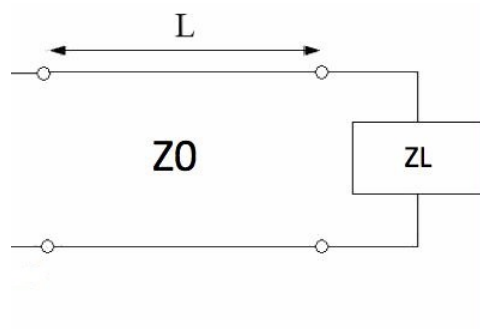


Figure 2.8: Transmission Line with Z_L as a load
The Reflection Coefficient (Γ) can be computed as:

$$\Gamma = \frac{Z_L - Z_0}{Z_L + Z_0} \quad (2.6)$$

2.3.2 Insertion Loss

Insertion Loss is defined as the loss of power received by an arbitrary load from an arbitrary generator when a two-arm waveguide junction is inserted in place of a lossless transducer which transfers all of the available power to the load [19] and is usually expressed in decibels. Insertion loss can be defined as :

$$IL(dB) = 10 \log_{10} \frac{P_T}{P_R} \quad (2.7)$$

Which P_T is the power transmitted to the load before insertion and P_R is the power received by the load after insertion. In case of the 2-port microwave network, the insertion loss is defined as below:

$$IL(dB) = -20 \log_{10} |S_{21}| \quad (2.8)$$

Which S_{21} stands for the transmission coefficient.

2.3.3 Return Loss

Return Loss in transmission line can happen when all of the available power from generator is not delivered to the mismatched load and this loss is called *ReturnLoss(RL)*[14]. For 2-port microwave network return loss is defined as a portion of incident power of port i is reflected from port i . So whatever the absolute value of return loss is larger means the port is more matched. The standard output for the return loss is a positive value, so a large return loss value actually means that the power in the reflected wave is small compared to the power in the incident wave and indicates a better impedance match [20]. Return Loss is defined in dB and calculated as:

$$RL(dB) = -20\log |\Gamma| \quad (2.9)$$

2.3.4 VSWR

VSWR stands for Voltage Standing Wave Ratio which states how much is transmitted from source to load through a transmission line so if the load is not mismatched with the source, a fraction of transmitted power is reflected. This reflection caused destructive interference leading to peaks and valleys in the voltage at various times and distances along the line. It is also a function of return loss ($VSWR = \frac{1+\Gamma}{1-\Gamma} = \frac{V_{max}}{V_{min}}$). The smaller VSWR means load is well matched to the transmission line and the more power is delivered to the load. The minimum value of VSWR is 1.0 (no reflected power) (or, as commonly expressed, 1:1). [14], [20], [21]

2.3.5 Bandwidth

Bandwidth is the Range of frequencies over which important performance parameters are acceptable[3]. Antenna Bandwidth can be found over a given return loss. Bandwidth is usually difference between upper and lower frequencies in a range of continuous frequency band and as a percent of center frequency (f_C) is[3] :

$$B_P = \frac{f_U - f_L}{f_C} \times 100\% \quad (2.10)$$

Which f_U is upper frequency and f_L is lower frequency. Bandwidth can also be defined as B_r ratio[3]:

$$B_r = \frac{f_U}{f_L} \quad (2.11)$$

For Antenna bandwidth over a given return loss is simply calculated as:

$$BW = f_U - f_L \quad (2.12)$$

All required key parameters for better understanding which phase shifter is proportional to our application needs have been defined. Following Sections describes the commercial phase shifters categories according to different applications.

2.3.6 Phase Shifters Categories

Phase shifters are used to change the transmission phase angle (phase of S_{21}) of a two-port network. There are several important key parameters and characteristics to define the performance of any phase shifter[22].

1. **Center frequency of operation**
2. **Bandwidth** We have to specify the bandwidth of phase shifters such as ISM which the frequency range of 2.4 GHz to 2.5 GHz with center frequency of 2.45 GHz
3. **Insertion Loss:** Low insertion loss denotes better performance of phase shifters, while the loss of phase shifters can be compensated by amplifiers
4. **Phase Range (Degrees)** This is the phase shift range of the device. Based on the way the device is configured, it will only be able to provide a phase shift within this range
5. **VSWR or Return Loss** As previously described shows how much load is matched with the source
6. **Amplitude:** Phase shifters have equal amplitude for all phase states.
7. **Reciprocal Networks:** This means they work effectively on signals passing through them in either direction
8. **Switching time (for digital operation) or time required for 360° phase change (for analog operation)** The time interval from the 50% point of the TTL control signal to within 10° of final phase shift. This applies to a change in either direction between any two phase states which differ by more than 22.5° . [23]
9. **Switching Power or Energy (for digital operation) or dc holding power (for analog operation)**

These characteristics are used to describe the electrical performance of phase shifters[22]

Most of companies providing RF phase shifter use passive reciprocal phase shifters. For better understanding passive or other networks, we need to study the various types of phase shifters categorized as below:

- **Active vs. Passive Phase Shifters:** Active phase shifters provide gain and amplify while phase shifting and make it potential to work against the loss of the phase shift elements and they are nonreciprocal. On the contrary Passive phase shifters attenuate while phase shifting (Lossy) and are reciprocal. As passive phase shifters are reciprocal, so they work well on signals passing on different directions[24], [25]
- **Analog vs. Digital Phase Shifters** Analog phase shifters provide a continuous variable phase shift which are controlled by a voltage. These analog phase shifters can be controlled with tuning diodes such as varactors that change capacitance with voltage, or nonlinear dielectrics such as barium strontium titanate, or ferro-electric materials such as yttrium iron garnet. A mechanically-controlled analog phase shifter is really just a mechanically lengthened transmission line, often called a trombone line. Analog phase shifters have been used in radar systems and more recently to down-tilt (steer) antennas used in cellular base stations. Digital phase shifters provide a discrete set of phase states that are controlled by two-state phase bits. As the order bit of 360 degree in digital phase shifters is divided into smaller binary steps, so the highest order bit is of 180 degree, then 90 degree and then of 45 degree. A phase shifter with 45 degree Least Significant Bits (LSB) would be a three bit shifter. Similarly, a six bit shifter will have 5.6 degree LSB. Analog phase shifters are readily convertible to digital control by the addition of suitable D/A converters and appropriate linearizing circuits. And digital phase shifter converts a continuous analog input voltage into discrete steps. [25], [26], [27], [28]

Analog Phase shifter advantages:

- Lower loss
- Lower cost of parts

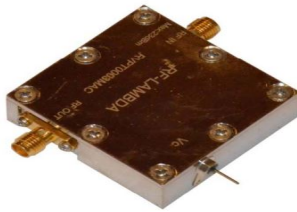
Digital Phase shifter advantages:

- Immunity to noise on control lines
- More uniform performance, unit-to-unit
- Ability to achieve flat phase over wide bandwidth
- Less susceptible to phase pulling when embedded in networks that are not perfectly impedance matched
- simple to assemble
- Potentially higher power handling and linearity

After identifying various types of phase shifter, it becomes clearer to analyze our needs and requirements for any applications After analyzing our needs,

we can make a contact with any well-known microwave company providing phase shifters for required components.

Figures below illustrate examples of commercial analog and digital phase shifters [29]



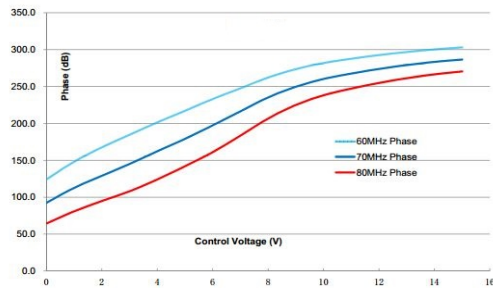
(a) Analog Phase Shifter



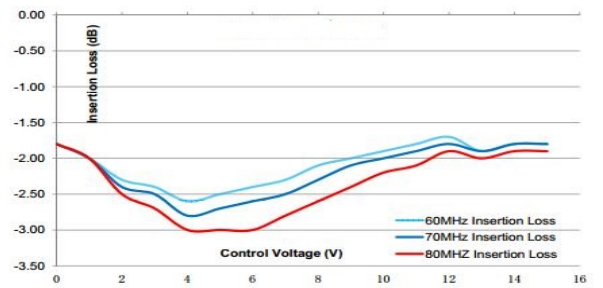
(b) Digital Phase Shifter

Figure 2.9: (a) Analog Voltage Control Phase Shifter 60-80 MHz 180° Full Band, and (b) 2-4 GHz Digital 4/5/6 Bits 360° Step Phase Shifter

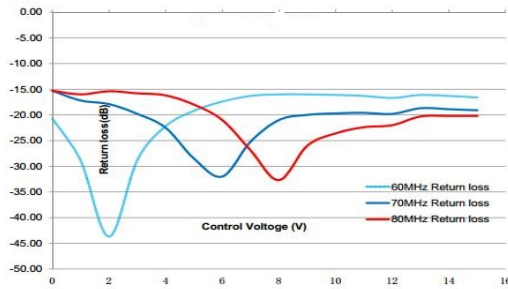
Figure 2.9 shows two kinds of analog and digital phase shifter. For digital phase shifter 4/5/6 bits step means 22.5° 11.25° 5.625° . Figures 2.10 below shows the characteristics (Phase, Insertion Loss, Return Loss) of above Analog Phase Shifter.



(a) Phase



(b) Insertion Loss



(c) Return Loss

Figure 2.10: Characteristics of Analog Phase Shifter (a).Phase, (b).Insertion Loss, (c).Return Loss

2.4 Analysis of Phase Shifter

A phase shifter is a two-port microwave device which shifts the phase of an input signal. These devices are used in phased antenna arrays. Figure 2.11 below illustrates a simplified phase shifter.

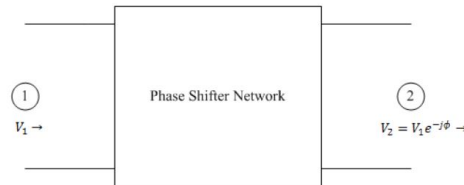


Figure 2.11: Simplified Phase Shifter

Most usual methods to implement Phase Shifters are based on switched line, loaded line, and reflection type (as described in Section 2 of this Chapter). In this article the main object is to implement phase shifter using Reflection Type method that provides continuous phase shift of 0° to 360° . Reflection Type phase shifter uses a 90° hybrid coupler and two reflective load networks consisting of varactor diodes and inductors. Hybrid coupler play an important role in phase shifter which may have three ports, four ports, or more, and may be (ideally) lossless. Directional couplers can be designed for arbitrary power division between output, while hybrid junctions usually divide input power into two equal output power and have 90° or 180° phase difference between output ports.[14].

2.4.1 N-Port Network

For Analyzing hybrid Coupler phase shifter at first we should know about N-Port Networks and their properties. Figure 2.12 below shows the N-port Network with inputs and outputs [30]

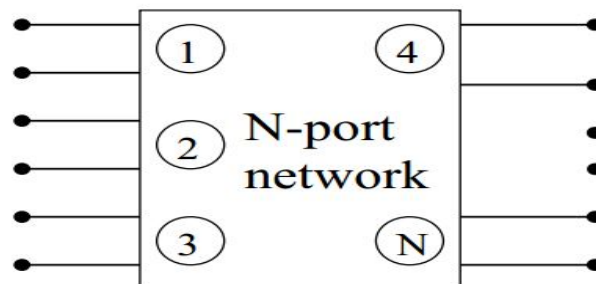


Figure 2.12: N-port Network

For this kind of network Scattering matrix gives us an useful information about the behavior of the any Microwave Network under study. For N-Port Network scattering matrix can be defined as below:

$$[s] = \begin{bmatrix} S_{11} & S_{12} & S_{13} & \dots & S_{1N} \\ S_{21} & S_{22} & S_{23} & \dots & S_{2N} \\ S_{31} & S_{32} & S_{33} & \dots & S_{3N} \\ \dots & \dots & \dots & \dots & \dots \\ S_{N1} & S_{N2} & S_{N3} & \dots & S_{NN} \end{bmatrix} \quad (2.13)$$

Which for 2 and 4 Ports Network we have N=2 and N=4 respectively.

Properties[14]:

1. For matched ports we have : $S_{ii}=0$
2. For reciprocal network (Symmetry) property we have : $S_{ij} = S_{ji}$
3. For Lossless network we have :

$$\sum_{i=1}^N |S_{ij}|^2 = 1$$

$$\sum_{k=1}^N S_{ki}S_{kj}^* = 0 \quad i \neq j$$

2.4.2 2-Port Coupler Phase Shifter

A 2-Port Network connected between source and load are considered as Figure 2.13. Several types of phase shift of 2-ports may be considered, as will be shown with reference to Figure 2.13.[31]: The Equation of Scattering

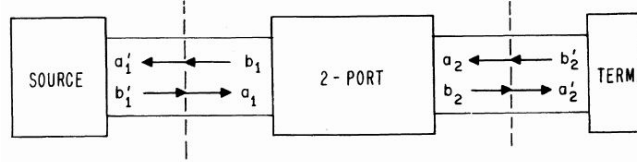


Figure 2.13: 2-Port Network

for this Network can be defined :

$$b_1 = S_{11}a_1 + S_{12}a_2 \quad (2.14)$$

$$b_2 = S_{21}a_1 + S_{22}a_2 \quad (2.15)$$

Two above Equations can be combined to form the S-parameter matrix for the two port system in the form found in the Equation below:

$$\begin{pmatrix} b_1 \\ b_2 \end{pmatrix} = \begin{bmatrix} S_{11} & S_{12} \\ S_{21} & S_{22} \end{bmatrix} \begin{pmatrix} a_1 \\ a_2 \end{pmatrix} \quad (2.16)$$

Each element of S-matrix of above Equations states for properties of the 2-port Network.[32] S_{11} is the input reflection coefficient, S_{12} is the reverse

voltage gain, S_{21} is the forward voltage gain, and S_{22} is the output reflection coefficient. And can be defined as[33] :

$$S_{11} = \frac{b_1}{a_1} = \left. \frac{\text{reflectedwave}}{\text{incidentwave}} \right|_{a_2=0} \quad (2.17)$$

$$S_{12} = \frac{b_1}{a_2} = \left. \frac{\text{reflectedwave}}{\text{incidentwave}} \right|_{a_1=0} \quad (2.18)$$

$$S_{21} = \frac{b_2}{a_1} = \left. \frac{\text{reflectedwave}}{\text{incidentwave}} \right|_{a_2=0} \quad (2.19)$$

$$S_{22} = \frac{b_2}{a_2} = \left. \frac{\text{reflectedwave}}{\text{incidentwave}} \right|_{a_1=0} \quad (2.20)$$

The phase shift of a 2-Port is the argument phase of S_{21} or S_{12} which is difference between b_2 and a_1 . For the reciprocal 2-port network $S_{21}=S_{12}$. By using scattering Equations 2.14 and 2.15 the Phase Difference between b_2 and a_1 is :

$$\varphi_{b_2, a_1} = \arg \frac{b_2}{a_1} = \arg \frac{S_{21}}{1 - S_{22}\Gamma_L} \quad (2.21)$$

which $\Gamma_L = \frac{a_2}{b_2}$

When the is non reflecting (matched Load) we have :

$$[\varphi_{b_2, a_1}]_{\Gamma_L=0} = \arg S_{21} = \varphi_{21} \quad (2.22)$$

Equation 2.22 above demonstrates that if the load is matched the phase shift of the 2-Port is the argument of S_{12} or S_{21} .

For computation of Differential Phase Shift, we should consider the initial and final conditions. By assuming the source is matched with transmission line (non reflecting and $\Gamma_s = 0$) the differential phase shift is :

$$[\Delta\varphi]_{\Gamma_s=0} = \arg \left[\frac{S_{21}^f}{S_{21}^i} \cdot \frac{(1 - S_{22}^i\Gamma_L)}{(1 - S_{22}^f\Gamma_L)} \right] \quad (2.23)$$

Superscript of i and f in above Equation stands for initial and final stage respectively.

If the load is non reflection ($\Gamma_L = 0$ and $\Gamma_s = 0$)

$$[\Delta\varphi]_{\Gamma_s=\Gamma_L=0} = \arg \left[\frac{S_{21}^f}{S_{21}^i} \right] = \varphi_{21}^f - \varphi_{21}^i \quad (2.24)$$

Two above Equations 2.23 and 2.24 state that the phase difference in general not only depends on the characteristic of the 2-port but also the characteristic of the load and source[32].

It has been showed that the argument of S_{12} or S_{21} can be used as the characteristic phase shift of 2-port and for variable phase shift the differential phase shift $\Delta\varphi$ equals the change in φ_{21} or φ_{12} between initial and final stages. And also this is important to insert the phase shifter into nonreflecting system ($\Gamma_L = \Gamma_s = 0$)[34], [35]

2.4.3 4-Port Coupler Phase Shifter

4-Port Coupler Phase Shifter is a kind of the phase shifter which has 4 ports, like reflection type phase shifter, including directional or power divider coupler and a load network connecting to the output ports of its coupler. In this Section, 4-port coupler is analyzed and in the next Section 4-port coupler with varicap as a load will be analyzed.

Power divider and directional coupler are passive microwave components which are used for power division (input power is divided into two or more equal or unequal power) or power combining (two or more input power are combined at output port). Output signal from power dividers are in-phase signal with usually an equal power, Directional couplers can be designed for arbitrary power division, while hybrid junctions usually have equal power division. Hybrid junctions have either a 90° or a 180° phase shift between the output ports.[14]. Figure 2.14 below illustrates the power combiner and divider. Which α is known as the division ratio.

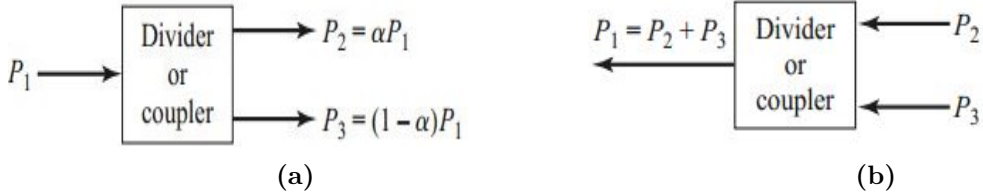


Figure 2.14: (a) Power division. (b) Power combining.

General properties of 4-port Network will be discussed first and then Couplers and Hybrids will be analyzed and designed.

General Properties of 4-Port Network

Scattering matrix of a 4-port Network contains 16 elements which each element describe its performance and S-matrix should be symmetric and unitary. A 4-port network can be lossless, reciprocal and matched at all port. So the form of scattering matrix has the following form:

$$[S] = \begin{bmatrix} 0 & S_{12} & S_{13} & S_{14} \\ S_{12} & 0 & S_{23} & S_{24} \\ S_{13} & S_{23} & 0 & S_{34} \\ S_{14} & S_{24} & S_{34} & 0 \end{bmatrix} \quad (2.25)$$

to satisfy unitary condition we have $|S_{13}|=|S_{24}|$ and $|S_{12}| = |S_{34}|$ by using $S_{14}=S_{23}=0$ directional coupler will be resulted. By considering $S_{12}=S_{34}=\alpha$, $S_{13} = \beta e^{j\theta}$ and $S_{24} = \beta e^{j\phi}$ where α and β are real and θ, ϕ are phase constant. So the new form of matrix 2.25 is :

$$[S] = \begin{bmatrix} 0 & \alpha & \beta e^{j\theta} & 0 \\ \alpha & 0 & 0 & \beta e^{j\phi} \\ \beta e^{j\theta} & 0 & 0 & \alpha \\ 0 & \beta e^{j\phi} & \alpha & 0 \end{bmatrix} \quad (2.26)$$

Further application of unitary condition yields: $\theta + \phi = \pi \pm 2n\pi$
by letting $n=0$, we have 2 choices which are used in practice :

1. $\theta=\phi=\pi/2$

$$[S] = \begin{bmatrix} 0 & \alpha & j\beta & 0 \\ \alpha & 0 & 0 & j\beta \\ j\beta & 0 & 0 & \alpha \\ 0 & j\beta & \alpha & 0 \end{bmatrix} \quad (2.27)$$

2. $\theta=0, \phi=\pi$

$$[S] = \begin{bmatrix} 0 & \alpha & \beta & 0 \\ \alpha & 0 & 0 & -\beta \\ \beta & 0 & 0 & \alpha \\ 0 & -\beta & \alpha & 0 \end{bmatrix} \quad (2.28)$$

These are two matrices which are the directional coupler characteristics. When an incident wave like a_1 is directed to port 1 (all port are matched):

$$\begin{bmatrix} 0 & \alpha & \beta & 0 \\ \alpha & 0 & 0 & -\beta \\ \beta & 0 & 0 & \alpha \\ 0 & -\beta & \alpha & 0 \end{bmatrix} \begin{bmatrix} a_1 \\ 0 \\ 0 \\ 0 \end{bmatrix} = \begin{bmatrix} 0 \\ \alpha a_1 \\ j\beta a_1 \\ 0 \end{bmatrix} \quad (2.29)$$

Above Equation means when an incident power to port 1 is delivered to port 2 and 3 while no power is delivered to port 4 (isolation port). Figure 2.15 below shows this:

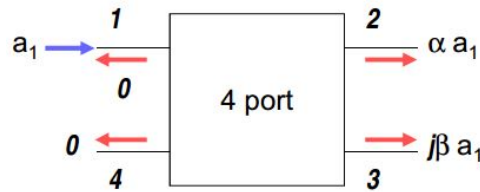


Figure 2.15: 4-Port network with incident power at port 1

$$P_1 = \frac{1}{2} |a_1|^2 \quad P_2 = \alpha^2 P_1 \quad P_3 = \beta^2 P_1$$

for lossless condition of the 4-port network:

$$\alpha^2 + \beta^2 = 1$$

By repeating above Equations at port 4, the same results will be obtained. We can conclude that any reciprocal, lossless, matched 4-port network is a Directional Coupler. Figure 2.16 shows that input power at port 1 is coupled to port 3 (coupled port) with the coupling factor of $|S_{13}| = |\beta|^2$ and the rest of the input power is delivered to port 2 (through port) with the coefficient of $|S_{12}|^2 = \alpha^2 = 1 - \beta^2$ and no power is delivered to port 4 (isolated port)[14].

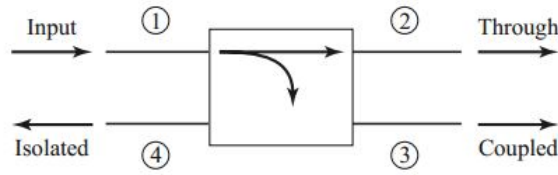


Figure 2.16: Directional Coupler

The following 3 quantities are used to characterize the quality of a directional coupler:

$$\text{Coupling} = C = 10 \log \frac{P_1}{P_3} = -20 \log |S_{13}| = -20 \log \beta \text{ dB} \quad (2.30)$$

The coupling factor indicates the fraction of the input power that is coupled to the output port

$$\text{Directivity} = D = 10 \log \frac{P_3}{P_4} = 20 \log \frac{\beta}{|S_{14}|} \text{ dB} \quad (2.31)$$

The directivity is the ability to transfer power from the input port to the coupled port and to reject the power that can come from the through port, due to reflections on this. From point of view, it is a parameter that defines the technical and technological quality of directional coupler. The higher value of this parameter is the greater the technical quality of the component will be.

$$\text{Isolation} = I = 10 \log \frac{P_1}{P_4} = -20 \log |S_{14}| \text{ dB} \quad (2.32)$$

The isolation is a measure of input power which is delivered to port 4.

$$\text{Insertion loss} = L = 10 \log \frac{P_1}{P_2} = -20 \log |S_{12}| \text{ dB} \quad (2.33)$$

The insertion loss accounts for the input power delivered to the through port, diminished by power delivered to the coupled and isolated ports.

For an ideal coupler Isolation and Directivity is infinite.

Hybrid Couplers are directional coupler with C=3 dB (equal split) which implies $\alpha = \beta = \frac{1}{\sqrt{2}}$. There are two kinds of hybrid coupler :

1. Quadrature Hybrid which there is 90° phase shift between port 2 and 3 when input power is directed to port 1 (Symmetric coupler). They are usually implemented in microstrip or stripline form. The form of S-Matrix is :

$$[S] = \frac{1}{\sqrt{2}} \begin{bmatrix} 0 & 1 & j & 0 \\ 1 & 0 & 0 & j \\ j & 0 & 0 & 1 \\ 0 & j & 1 & 0 \end{bmatrix} \quad (2.34)$$

2. The Magic T or rat-race hybrid which there is 180° phase shift between port 2 and 3 when input power is directed to port 1 (Anti-Symmetrical coupler). Its form of S-Matrix is :

$$[S] = \frac{1}{\sqrt{2}} \begin{bmatrix} 0 & 1 & 1 & 0 \\ 1 & 0 & 0 & -1 \\ 1 & 0 & 0 & 1 \\ 0 & -1 & 1 & 0 \end{bmatrix} \quad (2.35)$$

In this article we use Quadrature Hybrid Coupler for designing phase shifter. Following Section will describe the Quadrature Hybrid Analysis.

Quadrature Hybrid Analysis

As described above Quadrature Hybrid is a type of 4-port 3dB coupler with 90° phase shift between through and coupled port. Quadrature Hybrid is also well known as Branch-Line Hybrid Coupler. Figure below shows a typical geometry of branch-line coupler.

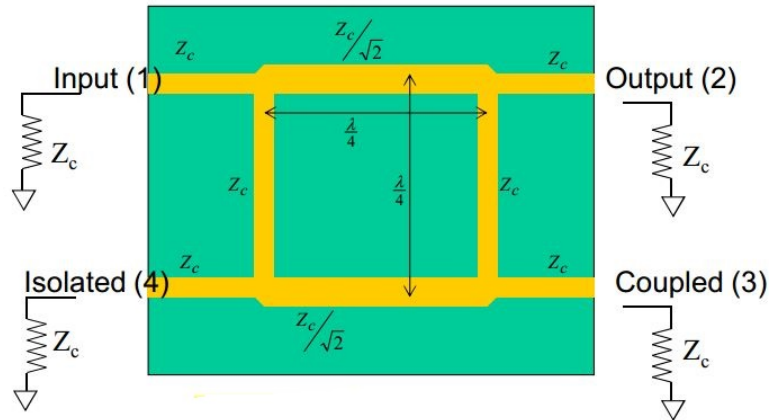


Figure 2.17: Geometry of a Branch-Line Coupler

As we can see in this Figure, all ports are matched by Z_C characteristic impedances so input power at port 1 is evenly divided between port 2 and 3 with 90° phase difference between them and no power is delivered to port 4 (isolated port). Figure 2.18 below demonstrates S-parameters versus normalized frequency for branch-line coupler which $Z_C = 50\Omega$.

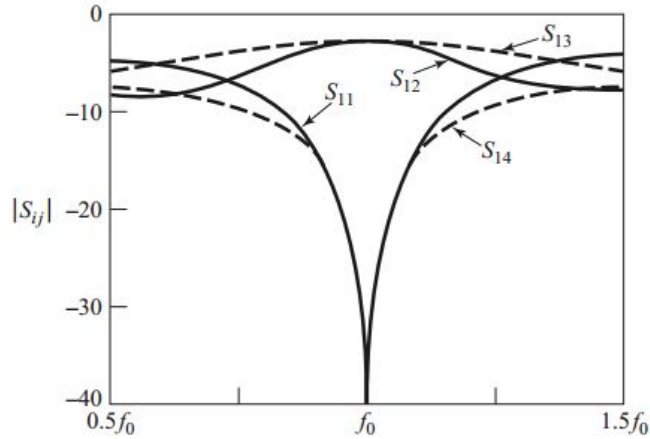


Figure 2.18: Scattering Parameters

As Figure 2.18 shows, S_{12} and S_{13} are power division at input 2 and 3 which are 3dB at f_0 and S_{14} is perfect isolation at f_0 and S_{11} is perfect return loss due to the matched port at 1 at f_0 .

The operation of the branch-line coupler can be analyzed using even and odd mode analysis because of its symmetrical nature.

The first step of this analysis is to normalize the impedances of the coupler as Figure below:

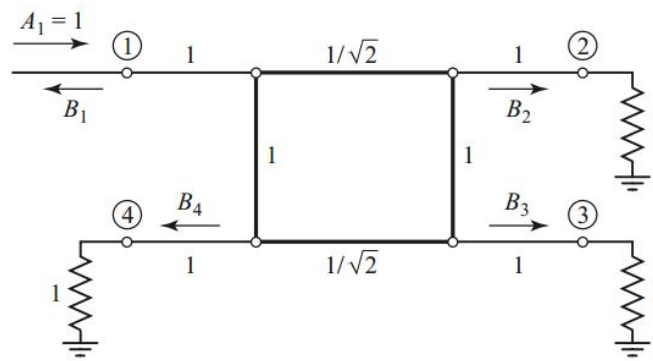


Figure 2.19: Normalized Form of Branch-Line Coupler

in order to find the Scattering matrix of the coupler, it should be excited at one port and other ports are loaded with matched load. When the reflected wave is found, the S-parameters are calculated by 2.5 formula. So

signal of unit amplitude is applied at port 1 (other ports also can be selected) and divides in the network. The method of even and odd is used for the analysis of symmetrical 4-port coupler such as branch-line coupler, so the Figure 2.19 can be split into the superposition of even mode and odd mode excitation [36].

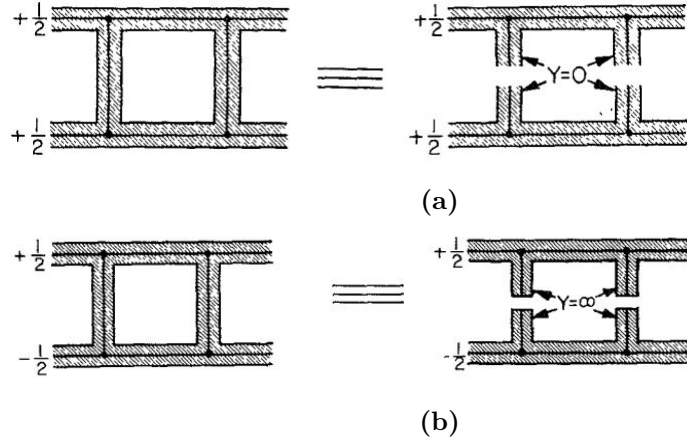


Figure 2.20: (a). Even mode (b). Odd mode

As we can see from above Figure, in even mode two equal in phase signals with amplitude of $\frac{1}{2}$ are applied at port 1 and 4 and due to the symmetry maximum voltage and no current can happen at the line of symmetry and this implies open circuited stub with length of $\lambda/8$ (Figure 2.21). In odd mode two equal out of phase signal with amplitude of $\pm\frac{1}{2}$ are applied at port 1 and 4 and in this case zero voltage and maximum current occurs at the line of symmetry and this also implies short circuited stubs at this line with length of $\lambda/8$.

Because of symmetry and antisymmetry of the excitation, 4-Port network can be split into a set of two identical decoupled two-port networks and now one of them needs to be analyzed. And because the amplitudes of the incident signal for these two-port are $\pm\frac{1}{2}$, the vector amplitudes of the signals emerging from the branch-line coupler can be expressed as:

$$\begin{aligned}
 S_{11} &= \frac{1}{2}\Gamma_e + \frac{1}{2}\Gamma_o \\
 S_{21} &= \frac{1}{2}T_e + \frac{1}{2}T_o \\
 S_{31} &= \frac{1}{2}T_e - \frac{1}{2}T_o \\
 S_{41} &= \frac{1}{2}\Gamma_e - \frac{1}{2}\Gamma_o
 \end{aligned} \tag{2.36}$$

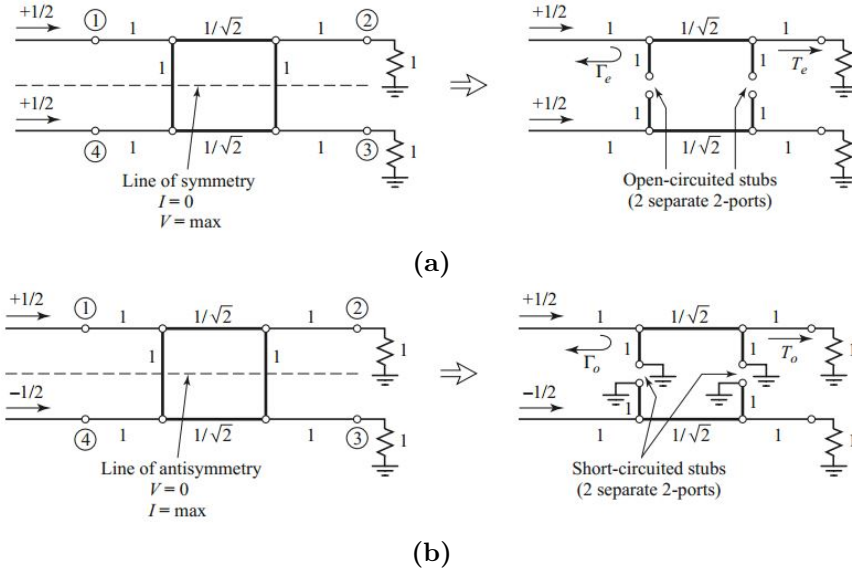


Figure 2.21: (a).Even mode with open circuited stubs (b).Odd mode with short circuited stubs

So for the even mode, reflection and transmission coefficient are $\frac{1}{2}\Gamma_e$ and $\frac{1}{2}T_e$ respectively which subscript e stands for even mode. And also for even mode we have $\frac{1}{2}\Gamma_o$ and $\frac{1}{2}T_o$ for reflection and transmission coefficient respectively.

To find Scattering parameters of one of two-port network, transmission matrices (ABCD) are used to cascade the subs and $\lambda/4$ Section. So the transmission matrix for even mode analysis is :

$$\begin{bmatrix} A & B \\ C & D \end{bmatrix}_e = [T_1][T_2][T_1] \quad (2.37)$$

Which T_1 is transmission matrix for open-circuited $\lambda/8$ stubs which is :

$$\begin{bmatrix} 1 & 0 \\ 0 & j \end{bmatrix} \quad (2.38)$$

And T_2 is transmission matrix for $\lambda/4$ transmission line which is :

$$\begin{bmatrix} 0 & j/\sqrt{2} \\ j/\sqrt{2} & 0 \end{bmatrix} \quad (2.39)$$

So by using 2.38 and 2.39 into 2.37 ABCD matrix is :

$$\begin{bmatrix} A & B \\ C & D \end{bmatrix}_e = \frac{1}{\sqrt{2}} \begin{bmatrix} -1 & j \\ j & -1 \end{bmatrix} \quad (2.40)$$

Similarly using above Equations for odd mode we get :

$$\begin{bmatrix} A & B \\ C & D \end{bmatrix}_o = \frac{1}{\sqrt{2}} \begin{bmatrix} 1 & j \\ j & 1 \end{bmatrix} \quad (2.41)$$

For calculation of Γ_{eo} and T_{eo} for even and odd mode we need to convert ABCD parameters to S-Parameter which S_{11} and S_{12} give us reflection coefficient (Γ) and transmission coefficient (T) :

$$\begin{aligned} S_{11} &= \frac{A + B/Z_0 - CZ_0 - D}{A + B/Z_0 + CZ_0 + D} \\ S_{12} &= \frac{2}{A + B/Z_0 + CZ_0 + D} \end{aligned} \quad (2.42)$$

Where Z_0 is the characteristic impedance of the network.

So by using 2.40 into 2.42 we obtain for even mode:

$$\begin{cases} \Gamma_e = 0 \\ T_e = \frac{-1}{\sqrt{2}}(1 + j) \end{cases} \quad (2.43)$$

And by using 2.41 into 2.42 for odd mode:

$$\begin{cases} \Gamma_o = 0 \\ T_o = \frac{1}{\sqrt{2}}(1 - j) \end{cases} \quad (2.44)$$

So by using 2.43 and 2.44 into 2.36 we acquire:

$$S_{11} = 0 \quad (2.45a)$$

$$S_{21} = \frac{-j}{\sqrt{2}} \quad (2.45b)$$

$$S_{31} = \frac{-1}{\sqrt{2}} \quad (2.45c)$$

$$S_{41} = 0 \quad (2.45d)$$

Each Equation in (2.45) has a meaning. 2.45a shows that no reflected power at input port (matched port), 2.45b shows half power amplitude of input power with -90° phase difference between input and through port, 2.45c shows half power amplitude of input power with -180° phase difference between input and coupled port so the phase shift between through and coupled port (output ports) is 90° . 2.45d shows no power is delivered to isolation port[14].

Thanks to the symmetry 4-port network we can complete the Scattering matrix of the branch-line coupler[14]:

$$[S] = \frac{1}{\sqrt{2}} \begin{bmatrix} 0 & -j & -1 & 0 \\ -j & 0 & 0 & -1 \\ -1 & 0 & 0 & -j \\ 0 & -1 & -j & 0 \end{bmatrix} \quad (2.46)$$

Figure 2.22 shows a photograph of Hybrid Branch-line coupler which is implemented on microstrip.

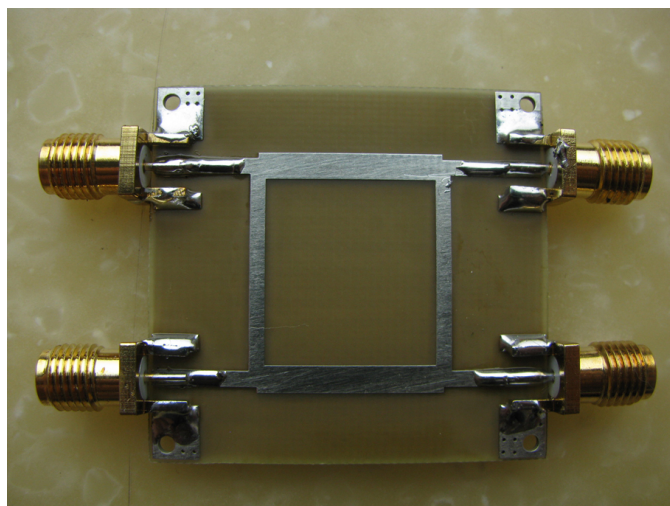


Figure 2.22: Microstrip Hybrid Branch line Coupler

Analysis of 4-Port Coupler (Quadrature Coupler) with Varactor as load

A network load can be connected to the through and coupled ports of the Hybrid coupler, in this case, power is applied to input port and the isolation port is used as output port. The phase shift between input port and output port depends on the reflection coefficient on through and coupled port, which is connected to network load.[37]. So the configuration of load is more important in the design of reflection type phase shifter. To avoid having any mismatch on input port the network load must be identical on through and coupled ports.

To obtain a variable phase shift we should use a kind of reflective loads which give us phase changes with range of 360° . In this article varactor diode control voltage is used as load which by changing its voltages different phase changes are accomplished. In the following the varactor performance will be described.

Varactor diode

Varactor diodes are semiconductor devices (p-n junction diode) that are used in many applications. These kind of semiconductor which are also known as Varicap diodes act as a variable capacitor under changing reverse bias. Enable much higher ranges of capacitance change to be gained as a result of the way in which they are manufactured [38]. there are different types of varactor from relatively standard varieties to abrupt or hyperabrupt varactor diodes. The symbol of varactor diode is shown as below:



Figure 2.23: Varactor Symbol

The capacitance of varactor diode is found as:

$$C_T = \epsilon \frac{A}{W_d} \quad (2.47)$$

Where C_T is a total capacitance of the junction and ϵ is Permittivity of the semiconductor material and A is Cross-sectional area of the junction and W_d is the Width of depletion layer. As reverse voltage of the varactor diode increases, the width W_d of depletion layer increases therefore the total capacitance of the junction decreases and vice versa. By changing voltage we can have different capacitances. So varactor diode can be easily changed by changing the voltage of reverse bias that's why varactor diode is sometimes

called voltage controlled capacitor. In terms of applied reverse voltage the total capacitance can be expressed as below [39] :

$$C_T = \frac{C_{j0}}{\left(1 + \frac{V}{\Phi}\right)^\Gamma} \quad (2.48)$$

Where C_{j0} is the capacitance value at 0 Volt, Φ is the built in potential which constant value and for GaAs is 1.3 V and for silicon is 0.7 V and Γ which is a tuning slope is usually 0.5 for an ideal abrupt varactor diode and V is reverse voltage in volt. The Figure demonstrates that capacitance is inversely proportional to reverse voltage[40].

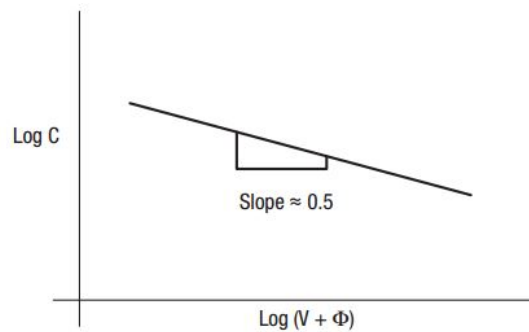


Figure 2.24: Characteristic Curve of a varactor diode

The equivalent circuit of varactor diode is shown in Figure below including a series of RLC circuit with a parallel capacitance (C_d) [41]

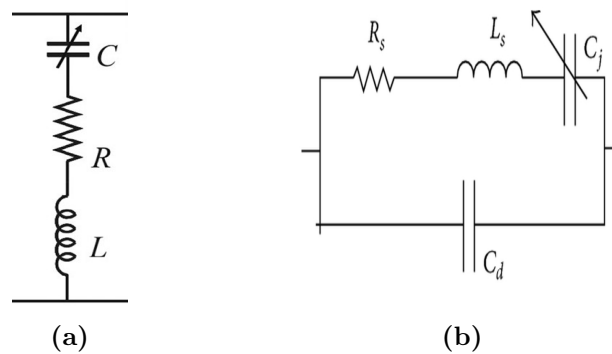


Figure 2.25: Equivalent Circuit of varactor diode (a).Simplified equivalent circuit (b).Full equivalent circuit

Hybrid Coupler with Reflective Load

The general block diagram of a phase shifter including 90° Hybrid coupler with varactor diode as reflective load is depicted in Figure 2.26[37].

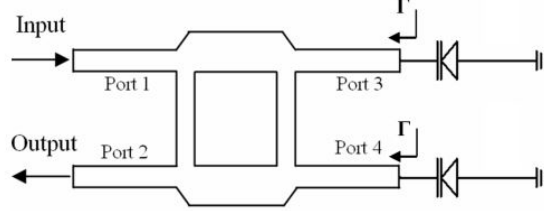


Figure 2.26: Simple structure of phase shifter with 90° Hybrid coupler loaded by varactor diode

As we can see from above Figure 2.26 two identical varactor diodes are connect to port 3 and 4 to avoid mismatching on input port (port 1). Any incident signal (coming from Port 1) will be reflected by the reactance loads producing a variable phase shift between the ports 1 and 2 [42]. For calculating phase shift between port 1 and 2 we have to compute the S-parameters of the coupler (Γ and S_{12}). The phase shift between port 1 and 2 depends on the reflection coefficient on port 3 and 4 connected to the load impedance. So the reflection coefficient can be calculated as[37] :

$$\Gamma = \frac{Z_L - Z_0}{Z_L + Z_0} = \frac{1 - jZ_0C(V)\omega}{1 + jZ_0C(V)\omega} \quad (2.49)$$

Where Z_0 is the characteristic impedance and $C(V)$ is the variable capacitance of varactor diode. The reactance of varactor diode varies with bias voltage and will change the reactance of the load. We can define another S-parameter of the coupler (S_{12}) as :

$$S_{12} = j\alpha^2 |\Gamma_L| e^{j\varphi_{12}} \quad (2.50)$$

Where α represents the extra loss of branch-line coupler ($\alpha = 0$ representing the 3dB ideal coupler) and φ_{12} is the phase angle of reflection coefficient [43]. The phase angel of S_{12} represents the phase shift of the coupler that can be found as:

$$\begin{cases} \angle S_{12} = \frac{\pi}{2} + \varphi_{12} \\ \arg(S_{12}(V)) = \frac{\pi}{2} - 2\arctan^{-1}(Z_0C(V)\omega) \end{cases} \quad (2.51)$$

And Insertion loss can be defined as :

$$\begin{aligned} IL &= 10\log\alpha^2 |\Gamma_L|^2 \\ &= 10\log\alpha^2 \frac{1 + (Z_0C(V))^2}{1 + (Z_0C(V))^2} = 0dB \end{aligned} \quad (2.52)$$

All calculations above have been obtained by assuming that varactor diode is a variable capacitance which has been obtained no insertion loss, but in practice varactor diode is composed of RLC circuit (simplified equivalent circuit Figure 3.6a) so the reflection coefficient is[42][44] :

$$\begin{aligned}\Gamma &= \frac{Z_L - Z_0}{Z_L + Z_0} \\ &= \frac{R + jX_L - Z_0}{R + jX_L + Z_0}\end{aligned}\quad (2.53)$$

And phase shift of the coupler can be found as:

$$\angle S_{12} = \frac{\pi}{2} + \tan^{-1}\left(\frac{X_L}{R - Z_0}\right) - \tan^{-1}\left(\frac{X_L}{R + Z_0}\right)\quad (2.54)$$

Insertion Loss is :

$$IL(dB) = 10 \log \frac{(R - Z_0)^2 + X_L^2}{(R + Z_0)^2 + X_L^2}\quad (2.55)$$

Where X_L is equal to $\omega L - \frac{1}{\omega C(V)}$

Chapter 3

Phase Shifter Analysis and Design

3.1 Theoretical Analysis

A new approach for designing phase shifter is to employ Impedance Transforming Hybrid (90°) Coupler. Unlike the conventional quadrature hybrid which has the same impedance at all four ports, this new patented design provides input and isolation ports at 50 Ohms and the -3dB ports at an impedance other than 50 Ohms, for example, 25 Ohms. This kind of coupler play an important role in phase shifters. The Figure below 3.1 shows the geometry of impedance transforming of quadrature hybrid [45]

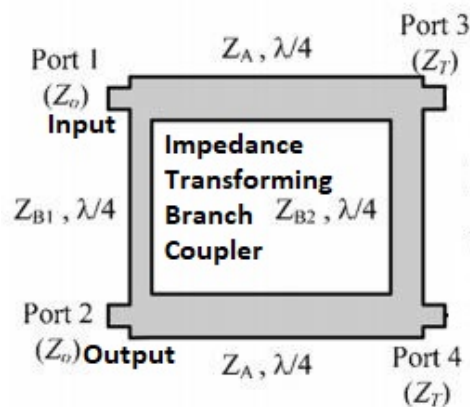


Figure 3.1: Geometry of Impedance Transforming Branch-Line coupler

For this kind of hybrid, each arm of the coupler has different impedance

based on the application, for general case we have

$$\begin{cases} Z_{B1} = Z_0 \\ Z_{B2} = \frac{Z_0}{r_Z} \\ Z_A = \frac{r_Z Z_0}{\sqrt{2r_Z}} \\ Z_T = \frac{Z_0}{r_Z} \end{cases} \quad (3.1)$$

Where Z_0 is Impedance characteristic and r_Z is called impedance ratio and when $r_Z=1$ conventional branch-Line coupler is obtained [46]. Each arm of the coupler has $\frac{\lambda}{4}$ length (Electrical length) which is equal 90° phase shift (or phase length).

$$\varphi = \beta l = \frac{2\pi}{\lambda} \frac{\lambda}{4} = \frac{\pi}{2} \quad (3.2)$$

The important part of designing phase shifter is network load which determines the range of phase shift. Schematic below 3.2 demonstrates the structure of phase shifter including a 3-dB impedance transforming hybrid coupler connecting to a network load [49] [43]. Network load consists of two

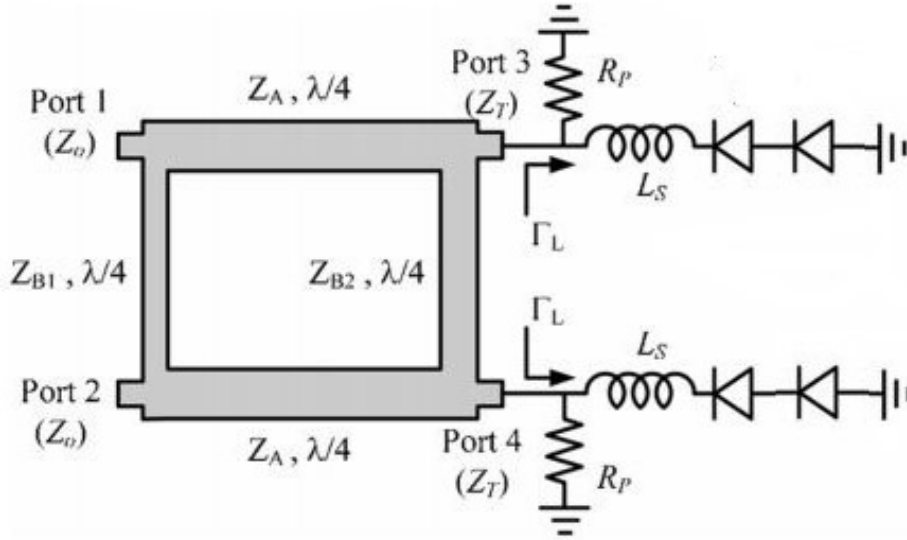


Figure 3.2: Schematic of proposed phase shifter

identical reflection load which are connected to port 3 and 4 including a varactor diode which is series with an inductance L_S and a resistance R_P which is connected in parallel with varactor and inductance.

In the following Section each part of the phase shifter is analyzed.

3.1.1 Impedance Transforming Hybrid Coupler

As described above in impedance transforming hybrid coupler, the impedance of input port is different from output port, this is the prominent difference between this kind of coupler and conventional one ($r_Z = 1$). In the following Sections we will see that by increasing the impedance ratio (r_Z) phase shift will be changed and it also affect insertion loss which are main characteristics of the phase shifter.

For design purpose, the frequency operation is considered at $f_0=2.45\text{GHz}$ which is the **center frequency** of the phase shifter. By considering this frequency, we should calculate each arm length of hybrid coupler. Hybrid coupler is microstrip line which is implemented on the top of specific substrate which has dielectric constant ϵ_r of 3.38 and thickness of 0.508mm and loss tangent ($tg\delta$) of 0.0028, so for given the dimensions of microstrip branch line coupler, the characteristic impedance can be calculated as: [8], [14]

$$Z_0 = \begin{cases} \frac{60}{\sqrt{\epsilon_e}} \ln \left(\frac{8h}{W} + \frac{W}{4h} \right), & \text{for } W/h \leq 1 \\ \frac{120\pi}{\sqrt{\epsilon_e} [W/h + 1.393 + 0.667 \ln(W/h + 1.444)]}, & \text{for } W/h \geq 1 \end{cases} \quad (3.3)$$

Where ϵ_e is the effective dielectric constant of a microstrip line and is approximately calculated by:

$$\epsilon_e = \frac{\epsilon_r + 1}{2} + \frac{\epsilon_r - 1}{2} \frac{1}{\sqrt{1 + 12h/W}} \quad (3.4)$$

For a given characteristic impedance Z_0 and dielectric constant ϵ_r , the W/d ratio can be found :

$$\frac{W}{h} = \begin{cases} \frac{8e^A}{e^{2A}-2} & \text{for } W/h < 2 \\ \frac{2}{\pi} \left[B - 1 - \ln(2B - 1) + \frac{\epsilon_r - 1}{2\epsilon_r} \left\{ \ln(B - 1) + 0.39 - \frac{0.61}{\epsilon_r} \right\} \right] & \text{for } W/h > 2 \end{cases} \quad (3.5)$$

Where

$$A = \frac{Z_0}{60} \sqrt{\frac{\epsilon_r + 1}{2}} + \frac{\epsilon_r - 1}{\epsilon_r + 1} \left(0.23 + \frac{0.11}{\epsilon_r} \right) \quad (3.6)$$

$$B = \frac{377\pi}{2Z_0\sqrt{\epsilon_r}} \quad (3.7)$$

Figure 3.3 below shows the geometry of a microstrip line :

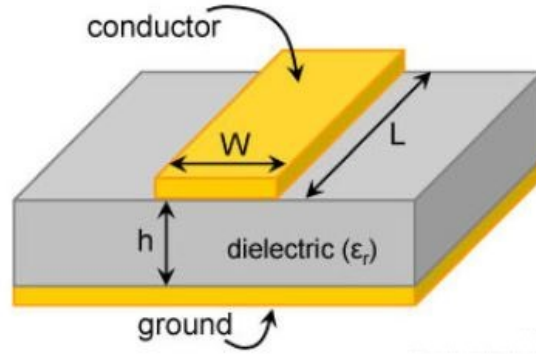


Figure 3.3: Geometry of Microstrip Transmission Line

In order to calculate the length of the each branch of the coupler in Figure 3.2 Equations below are given :

$$\varphi = \beta l = \sqrt{\epsilon_e} k_0 l \quad (3.8)$$

Where :

$$k_0 = \frac{2\pi f_0}{c} = \frac{2\pi \times 2.45 \times 10^9}{3 \times 10^8} = 51.312 \quad (3.9)$$

and

$$l = \frac{\varphi}{\sqrt{\epsilon_e} 51.312} \quad (3.10)$$

Where φ is the phase shift (or phase length) of each arm of the coupler in terms of radian. The electrical length of the coupler is $l = \frac{\lambda}{4}$. In order to convert the electrical length to phase length :

$$\varphi = \beta l = \frac{2\pi \lambda}{\lambda} \frac{\lambda}{4} = \frac{\pi}{2} \quad (3.11)$$

By using Equations from 3.3 to 3.7 and substitution $h = 0.508^{mm}$ and $\epsilon_r = 3.38$, and using Equation 3.1 dimensions for conventional coupler ($r_z = 1$) can be found in Table below:

Table 3.1: Dimensions of conventional branch line coupler ($r_z = 1$)

	Z_0	Z_A	Z_{B1}	Z_{B2}	Z_T
Impedance (Ω)	50	35.35	50	50	50
Width (mm)	1.186	1.975	1.186	1.186	1.186
Length (mm)	18.7393	18.355	18.7393	18.7393	18.7393

3.1.2 Reflection Load

Reflection Load which is used in this article consists of : a varactor diode, an Inductance (L_S) and a shunt resistant (R_P) making insertion loss constant. All load components are describe in detail as below:

Varactor diode

Varactor diodes as previously described is the main component of the load. Type of varactor diode in this article is Hyperabrupt Junction Tuning Varactor (SMVA1248-079LF). The SMVA1248-079LF silicon hyperabrupt junction varactor diode is designed for use in voltage controlled oscillators (VCOs) with low tuning voltage operation and is ideal for in-vehicle infotainment applications. This varactor is characterized for capacitance and resistance over temperature [47] (all information about varactor diode in this article is taken from data-sheet released by skyworks company (www.skyworksinc.com)).



Figure 3.4: Picture of Varactor Diode

The typical capacitance values according to reverse voltage are listed in Table below 3.2:

Table 3.2: Capacitance VS Reverse Voltage

V_R (V)	0	1	2	2.5	3	3.5	4	5
C_T (pF)	22.62	12.33	6.27	3.93	2.57	1.95	1.71	1.49

The Spice model of the varactor diode is depicted in Figure below. As shown, parasitic resistance and inductance are included in varactor diode, the value of these parasitic components are listed in Table 3.3

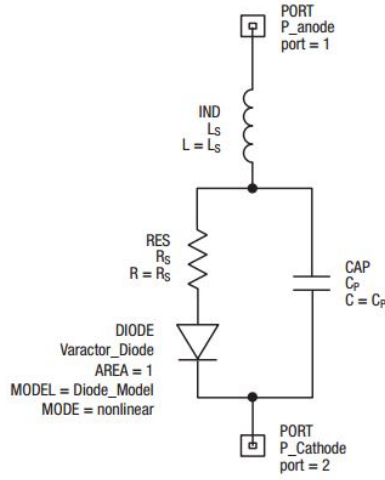


Figure 3.5: Varactor Diode Spice Model

In the Spice model structure of varactor a parallel capacitance is used that is negligible due to the low value of capacitance so the simplified model of varactor diode like 3.6a can be used (voltage-controlled capacitance C_V with parasitic resistance and inductance in series configuration). Spice model parameters value are listed in Table below [[47]:

Table 3.3: Spice Model Parameters Value

C_{J0} (pF)	V_J (V)	M	C_P (V)	R_S (Ω)	L_S (nH)
22.12	138	100	0.87	2.4	0.7

The varactor Dimensions are given in Figures below, (Dimensions are in inches and millimeters shown in parentheses).

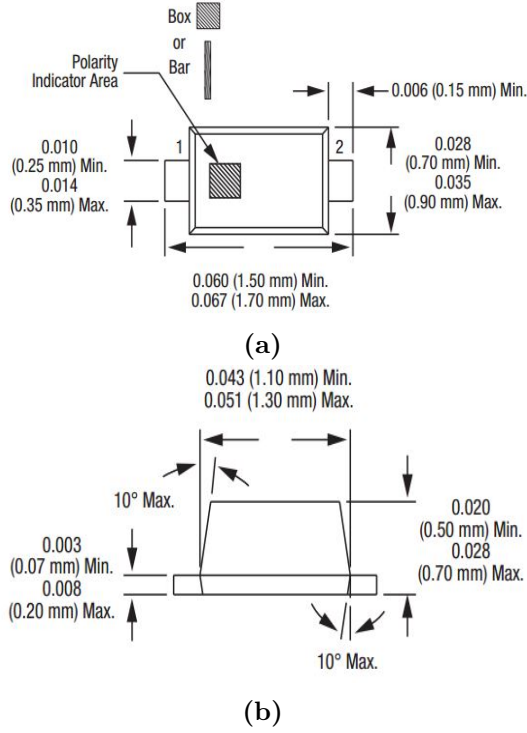


Figure 3.6: Dimensions of varactor diode (a).Top View (b).Side view

Inductance L_S

The total inductance are counted as parasitic inductance and external inductance so the total inductance (L_S) of the load is the summation of parasitic inductance and external inductance.

For finding optimal L_S we should find it as below:

$$j\omega L_S + \frac{1}{j\omega C_{V,max}} + j\omega L_S + \frac{1}{j\omega C_{V,min}} = 0 \quad (3.12)$$

So L_S can be obtained [43] :

$$L_S = \frac{C_{V,max} + C_{V,min}}{2\omega^2 C_{V,max} C_{V,min}} \quad (3.13)$$

Where $C_{V,min}$ and $C_{V,max}$ are minimum and maximum varactor capacitance at $V=0$ (V) and $V=5$ (V) respectively. So the value of L_S is obtained as $L_S=1.509\text{nH}$.

Shunt Resistance R_P

Shunt resistance R_P which is also called equalization resistance is used to minimize the insertion loss variation [44]. By considering the network load

of Figure 3.2 for calculation this resistor, we need to compute the reflection coefficient (return loss) at first:

$$|\Gamma| \equiv |\Gamma| e^{j\varphi_{21}} = \frac{(2r_Z R_S R_P - 2R_S Z_0 - R_P Z_0) + j2X_L(r_Z R_P - Z_0)}{(2r_Z R_S R_P + 2R_S Z_0 + R_P Z_0) + j2X_L(r_Z R_P + Z_0)} \quad (3.14)$$

Where X_L is equal to $\omega L_S - 1/\omega C_V$ so the insertion loss (IL) between input and output can be found as[43]:

$$\begin{aligned} IL &= \alpha^2 |\Gamma|^2 \\ &= \alpha^2 \frac{(2r_Z R_S R_P - 2R_S Z_0 - R_P Z_0)^2 + (2X_L(r_Z R_P - Z_0))^2}{(2r_Z R_S R_P + 2R_S Z_0 + R_P Z_0)^2 + (2X_L(r_Z R_P + Z_0))^2} \end{aligned} \quad (3.15)$$

The insertion loss is changed by varying the varactor reactance X_L . In order to eliminate the insertion loss variation, $|\Gamma|$ must be kept constant and independent on X_L if:

$$\frac{(2r_Z R_S R_P - 2R_S Z_0 - R_P Z_0)^2}{(2r_Z R_S R_P + 2R_S Z_0 + R_P Z_0)^2} = \frac{(2X_L(r_Z R_P - Z_0))^2}{(2X_L(r_Z R_P + Z_0))^2} \quad (3.16)$$

By solving Equation 3.16 the optimal shunt resistance $R_{P,optimal}$ can be obtained as:

$$R_{P,optimal} = \frac{Z_0^2}{4r_Z^2 R_S} \left[1 + \sqrt{1 + \left(\frac{4r_Z R_S}{Z_0} \right)^2} \right] \quad (3.17)$$

For small parasitic resistance of varactor diode $r_Z R_S \ll Z_0$ the optimal resistance $R_{P,optimal}$ is reduced to [50][52]:

$$R_{P,optimal} = \frac{Z_0^2}{2r_Z^2 R_S} \quad (3.18)$$

By substituting Equation 3.17 into Equation 3.15 constant insertion loss can be obtained. Figure below demonstrates the value of R_P for different port impedance ratio r_Z .

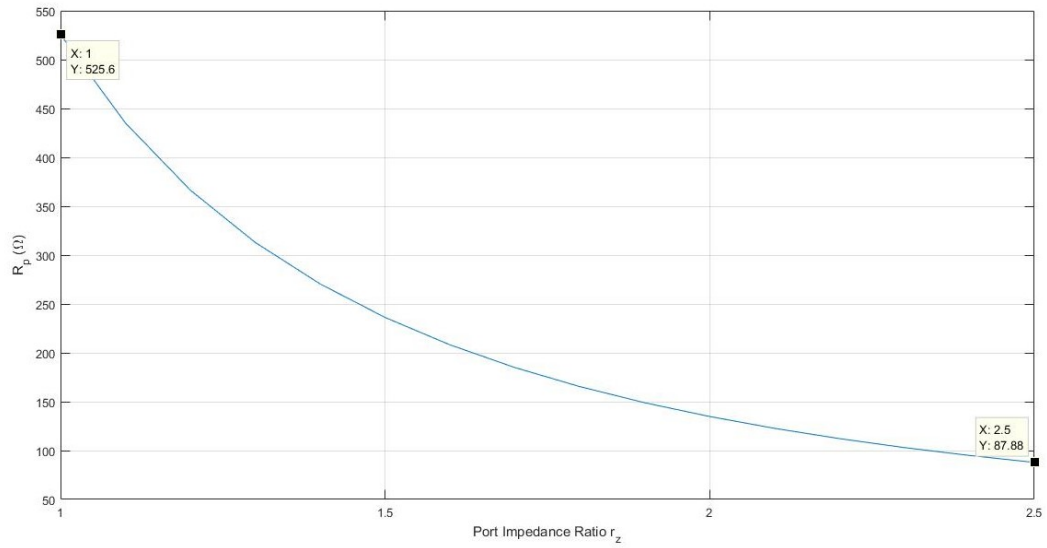


Figure 3.7: R_P vs r_Z

As we can see from Figure 3.7 the value of R_P at $r_Z = 1$ is 525.6 Ω and at $r_Z = 2.5$ is 87.88 Ω

Following Sections Theoretical predictions and simulation results of proposed phase shifter are discussed.

3.1.3 Theoretical Results

All components of phase shifter (Branch-line coupler and load network) have been discussed previously. Now the phase shifter behavior and effects of each component such as R_P , r_Z on insertion loss and relative phase shift between input and output ports are discussed using MATLAB. Before behavior analysis, insertion loss and phase shift formulas with using R_P and without using R_P are given as followings:

- **Insertion Loss and Relative Phase Shift with using R_P**

The reflection coefficient for the phase shifter can be defined as below:

$$\Gamma = \frac{(2r_Z R_S R_P - 2R_S Z_0 - R_P Z_0) + j2X_L(r_Z R_P - Z_0)}{(2r_Z R_S R_P + 2R_S Z_0 + R_P Z_0) + j2X_L(r_Z R_P + Z_0)} \quad (3.19)$$

Where $X_L = \omega L_S - 1/\omega C_V$. The scattering parameter S_{21} is defined as :

$$S_{21} = j\alpha^2 |\Gamma| e^{j\varphi_{21}} \quad (3.20)$$

Where α represents the extra loss of the 3-dB branch-line coupler (for ideal 3 dB coupler $\alpha = 1$). The phase angle of S_{21} is relative phase shift between port 1 and 2 so :

$$\begin{aligned} \angle S_{21} &= \frac{\pi}{2} + \varphi_{21} \\ &= \frac{\pi}{2} + \tan^{-1} \left(\frac{2X_L(r_Z R_P - Z_0)}{2r_Z R_S R_P - 2R_S Z_0 - R_P Z_0} \right) \\ &\quad - \tan^{-1} \left(\frac{2X_L(r_Z R_P + Z_0)}{2r_Z R_S R_P + 2R_S Z_0 + R_P Z_0} \right) \end{aligned} \quad (3.21)$$

So the maximal relative phase shift is obtained by phase difference between $C_{V,max}$ and $C_{V,min}$ causing $X_{L,max}$ and $X_{L,min}$ respectively So:

$$\Delta\varphi_{max} = \left| \angle S_{21}(X_{L,max}) - \angle S_{21}(X_{L,min}) \right| \quad (3.22)$$

Insertion Loss in dB is :

$$\begin{aligned} IL(dB) &= 10 \log_{10} |\Gamma|^2 \\ &= 10 \log_{10} \frac{(2r_Z R_S R_P - 2R_S Z_0 - R_P Z_0)^2 + (2X_L(r_Z R_P - Z_0))^2}{(2r_Z R_S R_P + 2R_S Z_0 + R_P Z_0)^2 + (2X_L(r_Z R_P + Z_0))^2} \end{aligned} \quad (3.23)$$

- **Insertion Loss and Relative Phase Shift without using R_P**

The reflection coefficient for the phase shifter can be defined as below:

$$\Gamma = \frac{(2R_S r_Z - Z_0) + j2X_L r_Z}{(2R_S r_Z + Z_0) + j2X_L r_Z} \quad (3.24)$$

Where $X_L = \omega L_S - 1/\omega C_V$. The relative phase shift is :

$$\angle S_{21} = \frac{\pi}{2} + \tan^{-1} \left(\frac{2X_L r_Z}{2R_S r_Z - Z_0} \right) - \tan^{-1} \left(\frac{2X_L r_Z}{2R_S r_Z + Z_0} \right) \quad (3.25)$$

The insertion loss in dB is :

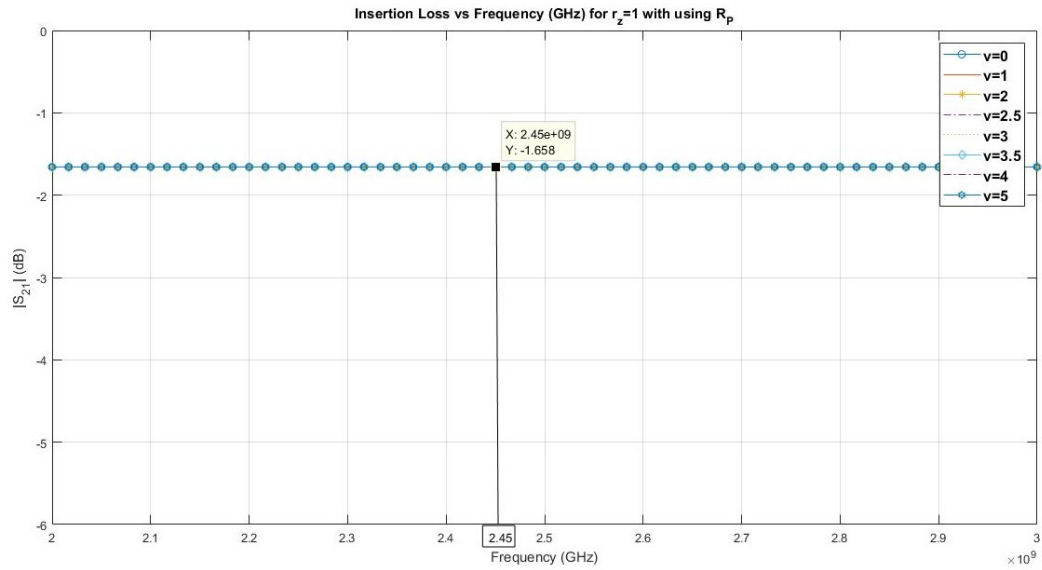
$$IL(dB) = 10 \log_{10} \left(\frac{(2R_S r_Z - Z_0)^2 + (2X_L r_Z)^2}{(2R_S r_Z + Z_0)^2 + (2X_L r_Z)^2} \right) \quad (3.26)$$

The behavior of phase shifter for $r_Z = 1$ and $r_Z = 2.5$ are discussed in this study.

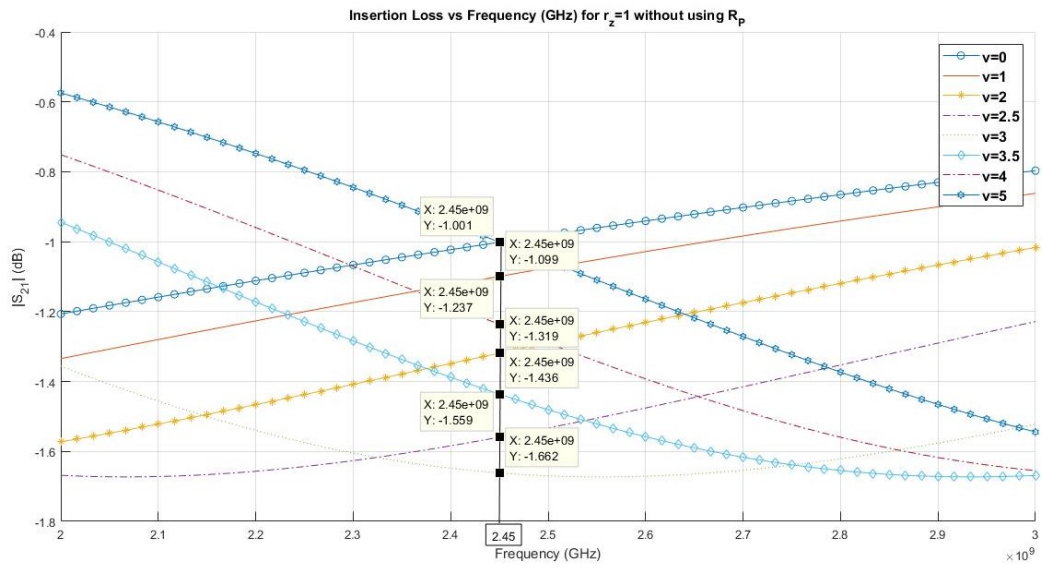
Notice: All results are obtained by assuming that phase shifter is ideal ($\alpha = 1$)

Phase Shifter with $r_Z = 1$

Insertion Loss is depicted in Figure below at center frequency $f_0 = 2.45GHz$ over frequency rang of 2-3 GHz.



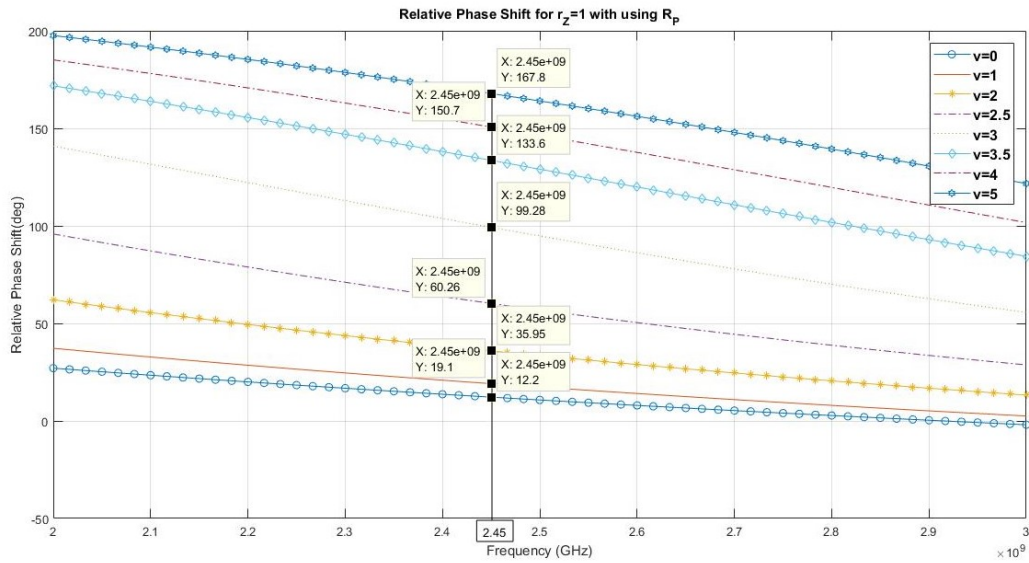
(a)



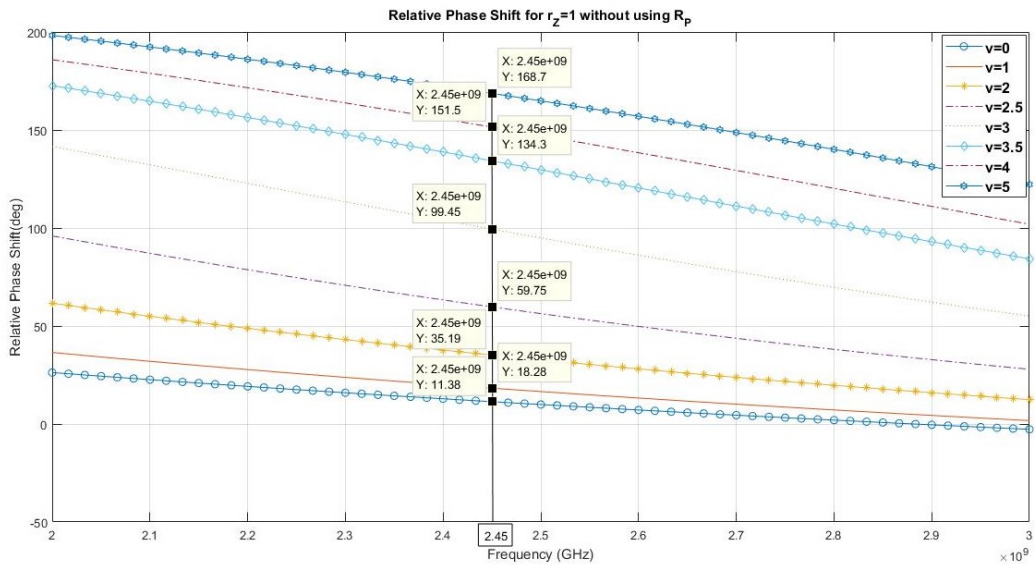
(b)

Figure 3.8: Insertion Loss for $r_z = 1$ (a). With using R_P (b). Without using R_P

As we can see from Figure 3.8, insertion loss for using R_P is constant for different voltages and lower than -1.65 dB and for without using R_P , there is a slight variation over the frequency rang of 2-3 GHz



(a)



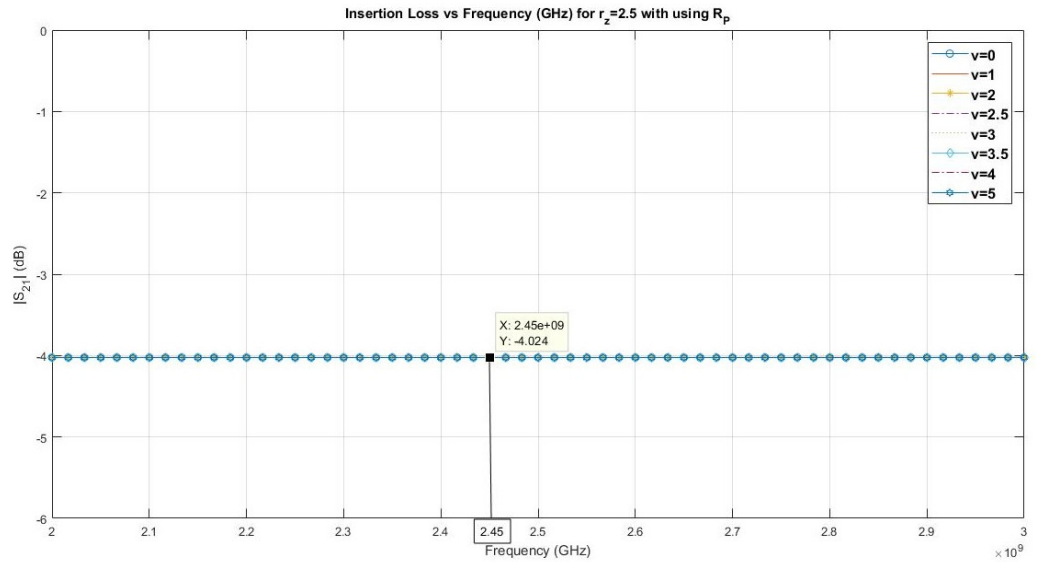
(b)

Figure 3.9: Relative Phase shift for $r_z = 1$ (a). With using R_P (b). Without using R_P

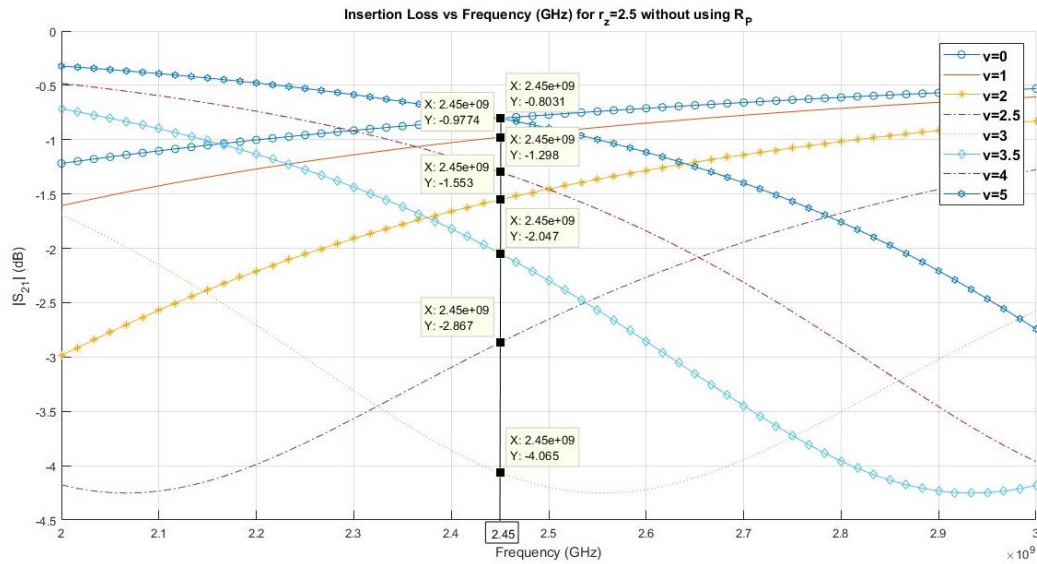
The relative phase shift is depicted in Figure above 3.9 and it varies from 12.12° to 167.8° for with using R_P and from 11.38° to 168.7° for without using R_P at $V=0$ and $V=5$ respectively. It can be understood from Figure above that R_P has not so much effect on relative phase shift.

Phase Shifter with $r_Z = 2.5$

Insertion loss for $r_Z = 2.5$ with and without using R_P at center frequency $f_0 = 2.45\text{GHz}$ over frequency range of 2-3 GHz, are shown at Figure below.



(a)

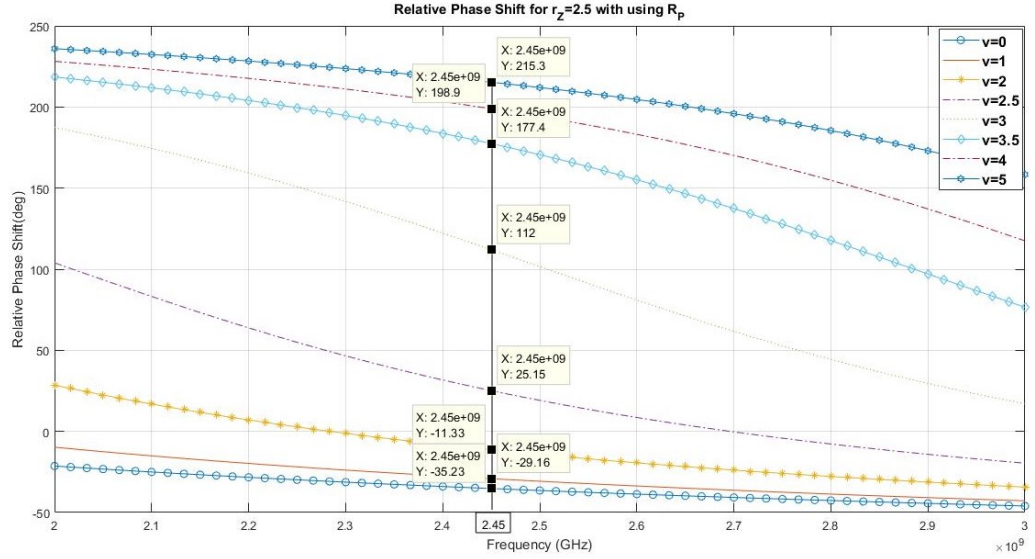


(b)

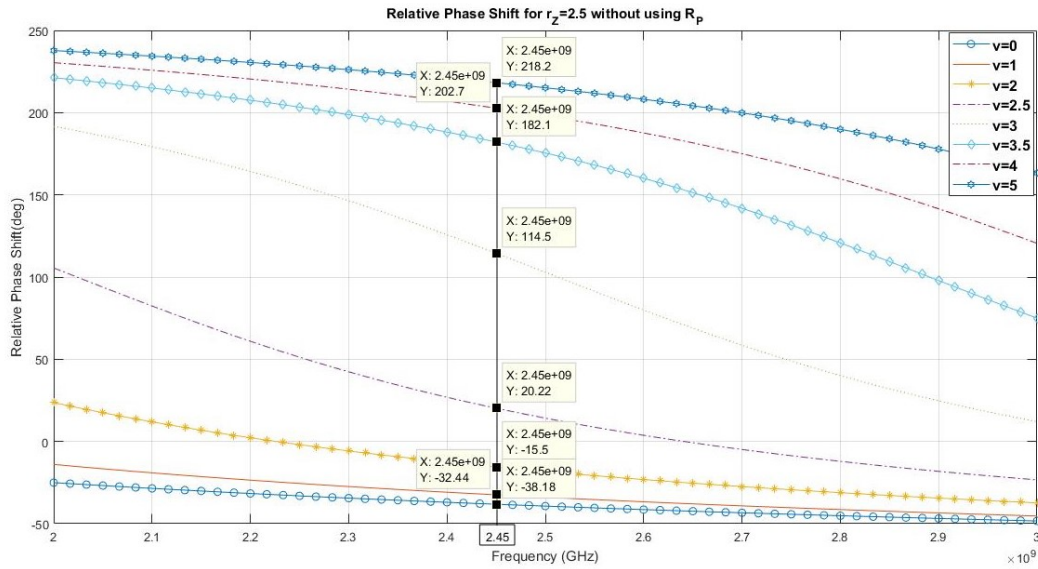
Figure 3.10: Insertion Loss for $r_Z = 2.5$ (a). With using R_P (b). Without using R_P

As shown in Figure 3.10 insertion loss with using R_P is -4 dB and with-

out using R_P varies from -0.8 dB to -4 dB (3.2 dB variation). It can be understood that R_P has a great effect on insertion loss.



(a)



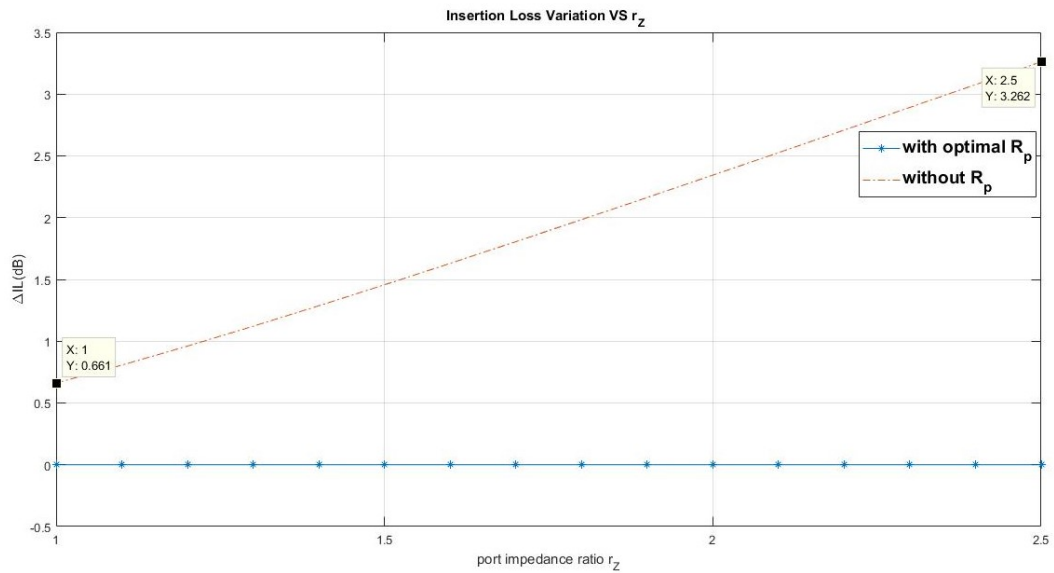
(b)

Figure 3.11: Relative Phase Shift for $r_Z = 2.5$ (a).with using R_P (b). Without using R_P

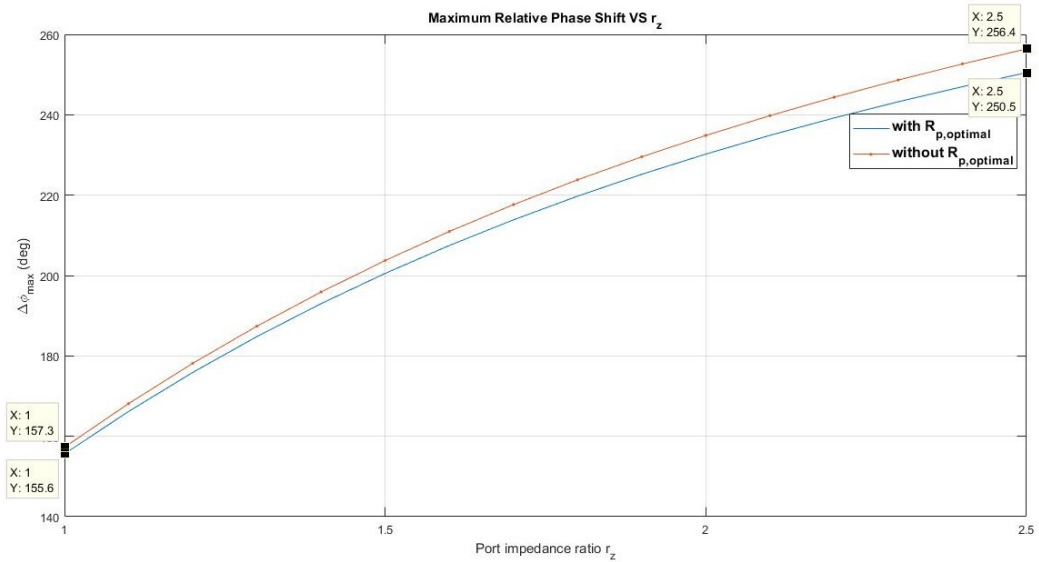
The relative phase shift are depicted in Figure 3.11 and it changes from -35.23° to 215.3° (250.55° phase shift) with using R_P and from -38.18° to 218.2° (256.38° phase shift) without using R_P .

Comparisons

From above results, it can be understood as r_Z increases, insertion loss and insertion loss variation and maximum relative phase shift increase as well. These are demonstrated in Figure below:



(a)

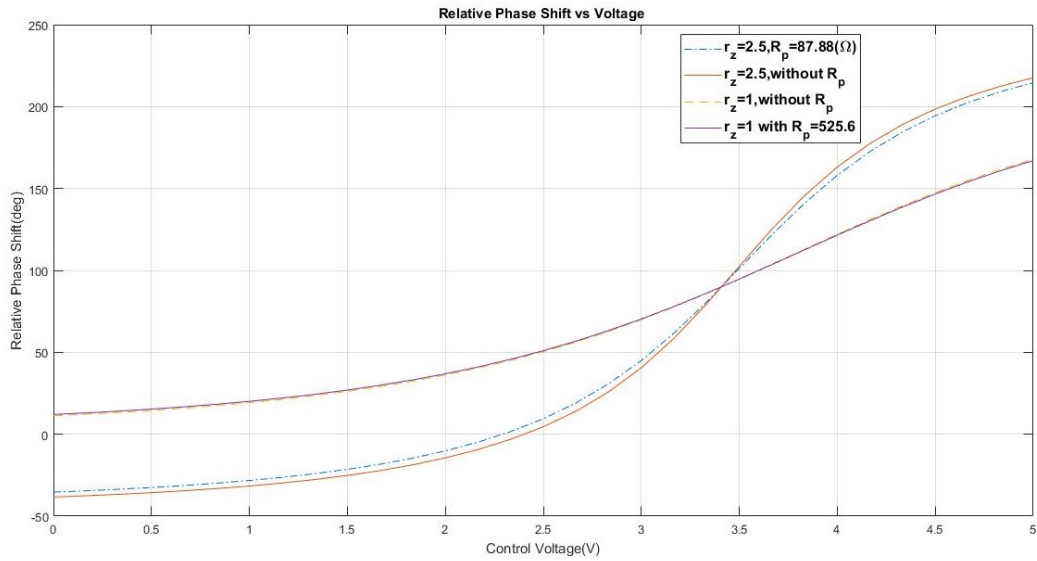


(b)

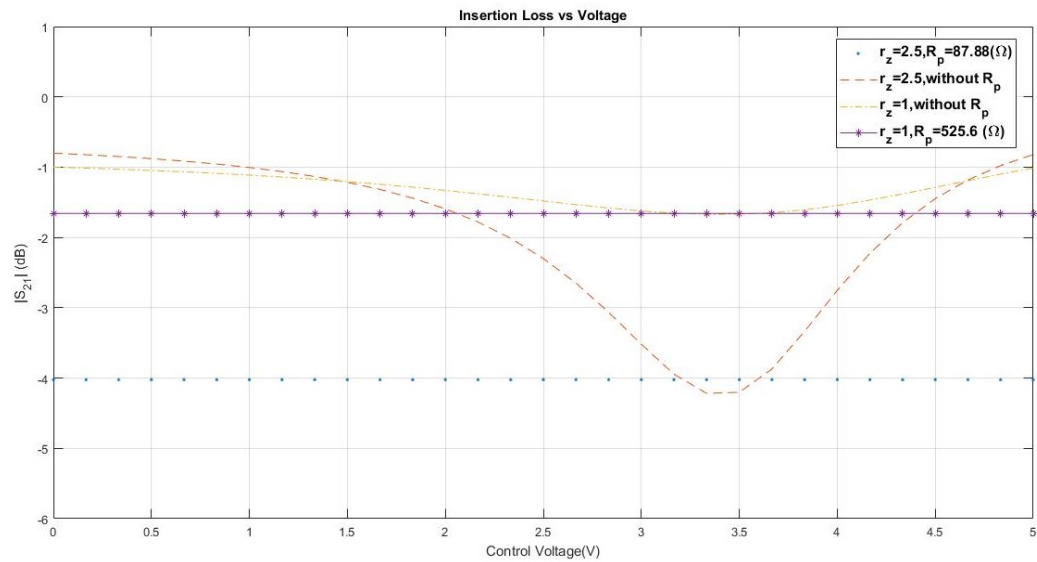
Figure 3.12: (a). Insertion Loss Variation VS r_Z (b). Maximum Relative Phase Shift VS r_Z

As shown in Figure 3.12a for load network with using R_P there is no variation over insertion loss from $r_Z = 1$ to $r_Z = 2.5$ but without using R_P , the insertion loss variation is increased along with the r_Z

In Figure 3.12b can be seen which R_P has a negligible effect on maximal relative phase shift at $r_Z = 1$ but there is a slight reduction (5.9°) at $r_Z = 2.5$.



(a)



(b)

Figure 3.13: (a). Insertion Loss Variation VS Voltage (b). Relative Phase Shift VS Voltage

Figures 3.13a and 3.13b compare the insertion loss variation and relative phase shift as a function of voltage for different value of r_Z with and without using R_P

Table 3.4 shows comparisons between $r_Z = 1$ and $r_Z = 2.5$.

Table 3.4: Theoretical results comparison between $r_Z = 1$ and $r_Z = 2.5$ for this work

	This work $r_Z = 1$ with R_P	This work $r_Z = 1$ without R_P	This work $r_Z = 2.5$ with R_P	This work $r_Z = 2.5$ without R_P
f_0 (GHz)	2.45	2.45	2.45	2.45
$R_P(\Omega)$	525.6	-	87.88	-
Insertion Loss (dB)	-1.658	min:-1 max:-1.662	-4.024	min:-0.8 max:-4.065
Insertion Loss Variation (ΔIL)	0	0.661	0	3.265
Maximal Relative Phase Shift (Degree)	155.6	157.3	250.5	256.4

In order to make a comparison between this work and reference [43], Table 3.5 is created.

As shown in Table for $r_Z = 1$, this work has greater maximal phase shift but in terms of insertion loss, reference [43] has a bit better performance. This work with $r_Z = 2.5$ and reference [43] with $r_Z = 4$ have the same maximal phase shift but in terms of insertion loss reference [43] has better performance while this work has smaller branch line coupler size.

Table 3.5: Theoretical results comparison between this work and reference [43]

	This work $r_Z = 1$	Reference [[43]] $r_Z = 1$	This work $r_Z = 2.5$	Reference [[43]] $r_Z = 4$
f_0 (GHz)	2.45	2	2.45	2
$R_P(\Omega)$	525.6	1252	87.88	82
Insertion Loss (dB)	-1.658	-1.3	-4.024	-3.2
Maximal Relative Phase Shift (Degree)	155.6	106.3	250.5	252.4

3.2 Simulation

All theoretical calculations have been done in previous Section (Theoretical analysis). In this Section, simulation will be carried out by CST Studio in the following. At first, simulation of impedance transforming branch-line coupler with $r_Z = 1$ connected to its specified configuration load network will be discussed and then the same procedure by changing the port impedance ratio to $r_Z = 2.5$ will be simulated and discussed.

3.2.1 Simulation of Branch-Line Coupler with $r_Z = 1$

Figures 3.14 below show the branch-line coupler which its port impedance ratio is $r_Z = 1$.

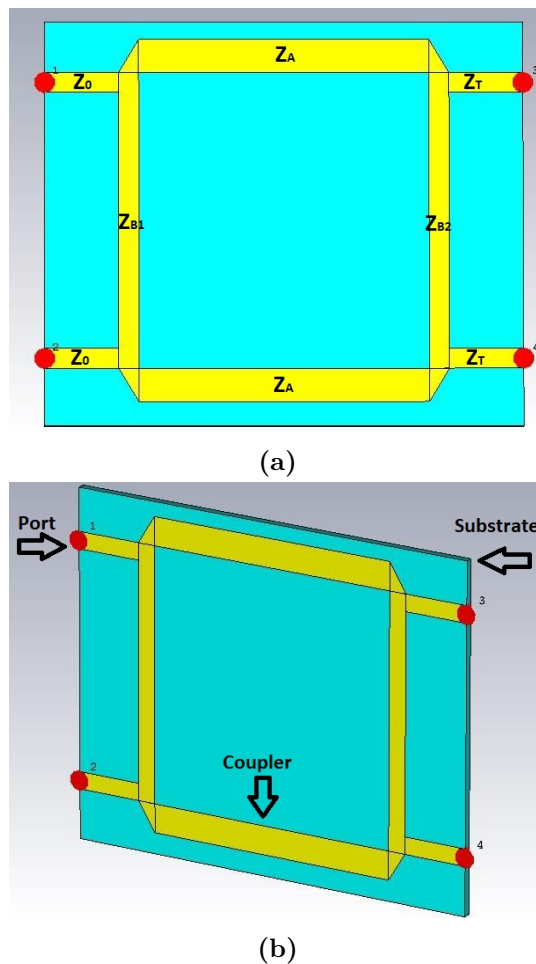


Figure 3.14: Picture of branch-line coupler with $r_Z = 1$ (a). Specified Impedance on each arm (b). Demonstrated components

According to the formulas from 3.1 to 3.11 the dimensions of coupler can be calculated and shown in Table 3.6 below:

Table 3.6: Dimensions of branch-line coupler with $r_Z = 1$

	Z_0	Z_A	Z_{B1}	Z_{B2}	Z_T
Impedance (Ω)	50	35.35	50	50	50
Width (mm)	1.186	1.975	1.186	1.186	1.186
Length (mm)	4.3975	17.24	17.59	17.59	4.3975

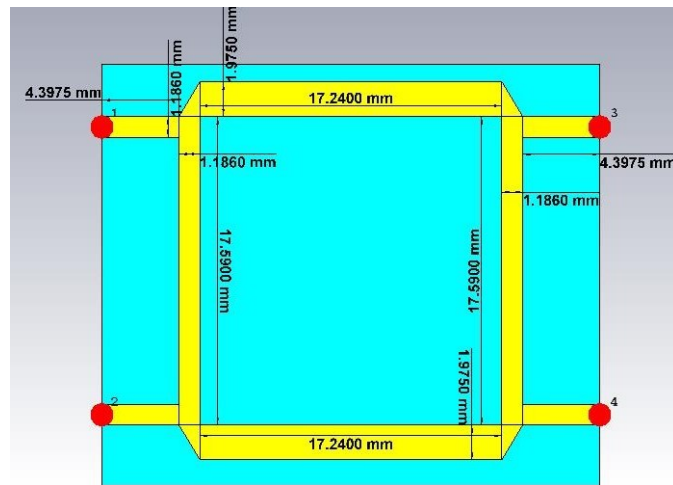


Figure 3.15: Branch-Line Coupler with $r_Z = 1$ with specified dimensions

In order to obtain insertion loss (S_{21}) and relative phase shift ($\angle S_{21}$) and also return loss (S_{11}) between port 1 and 2, Symmetrical loads are connected to port 3 and 4. Figure below shows the load network in CST studio

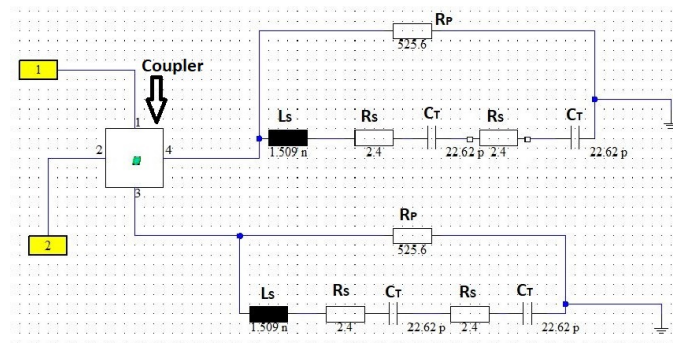


Figure 3.16: Network Load of Branch-Line Coupler

Results are discussed with and without using optimal shunt resistance of R_P in the following Section are given:

Results of Phase Shifter With Using R_P in the Network Load

As demonstrated in the theoretical analysis Section, R_P has effect on insertion loss and relative phase shift. Figures below are depicted to show the insertion loss, relative phase shift and also return loss for proposed phase shifter.

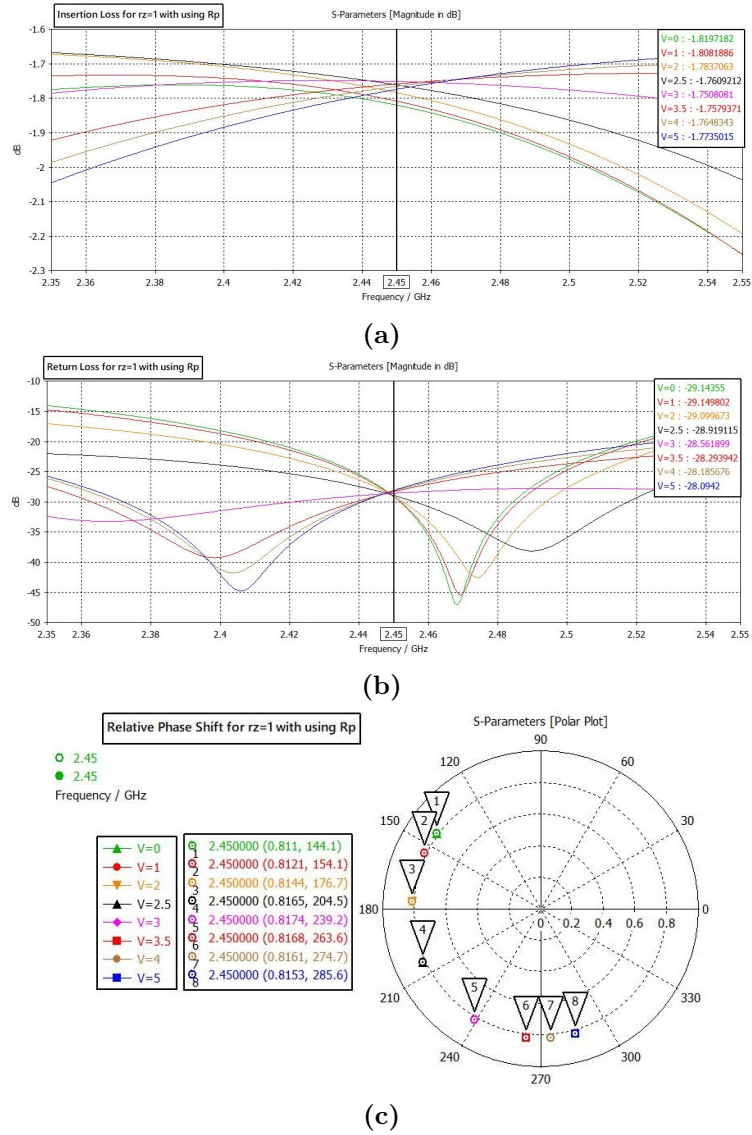


Figure 3.17: Results of proposed phase shifter with $r_Z = 1$ and using R_P (a). Insertion Loss (b). Return Loss (c). Relative Phase Shift

In order to make a sense of results, Table below is created.

Table 3.7: Tabular results of proposed phase shifter with $r_Z = 1$ and using R_P

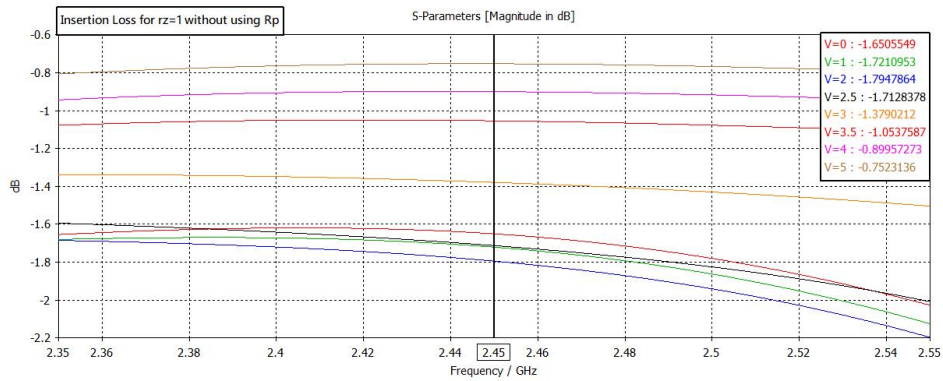
f_0 (GHz)	Insertion Loss (dB)	Insertion Loss Variation (ΔIL)	Maximal Relative Phase Shift (degree)	Return Loss (dB)	R_P (Ω)	R_S (Ω)	L_S (nH)
2.45	Min:-1.75 Max:-1.82	0.07	141.5	<-25 dB	525.6	2.4	1.509

It can be found from results which using optimal shunt resistance of R_P makes almost insertion loss constant. By using this load network which is connected to port 3 and 4, relative phase shift between input and output port is increased from 90^0 to 141.5^0 . Results shown in Table 3.7 shows approximately agreement with the calculation predictions.

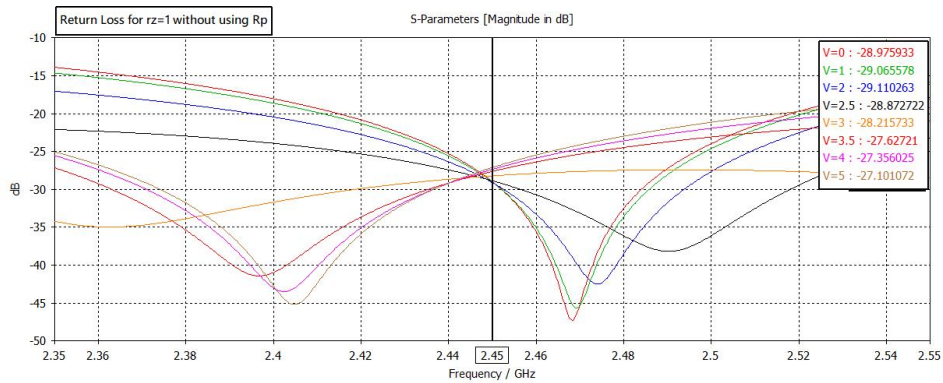
Removing shunt resistance R_P will be presented in following.

Results of Phase Shifter Without Using R_P in the Network Load

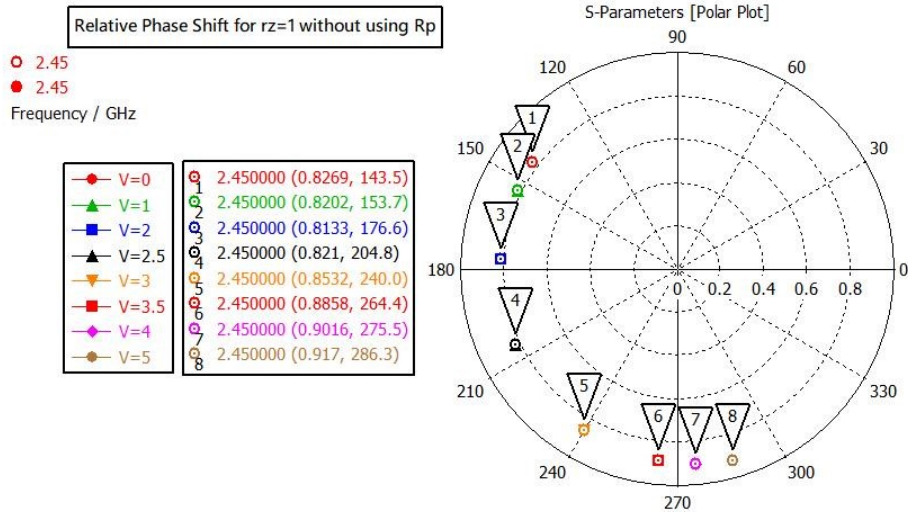
According to the theoretical predictions, by removing the shunt resistance R_P from load network, insertion loss variation (ΔIL) and maximal relative phase shift increase. Table and Figures below are demonstrated to show this fact.



(a)



(b)



(c)

Figure 3.18: Results of proposed phase shifter with $r_z = 1$ and without using R_p (a). Insertion Loss (b). Return Loss (c). Relative Phase Shift

Table 3.8: Tabular results of proposed phase shifter with $r_Z = 1$ and without using R_P

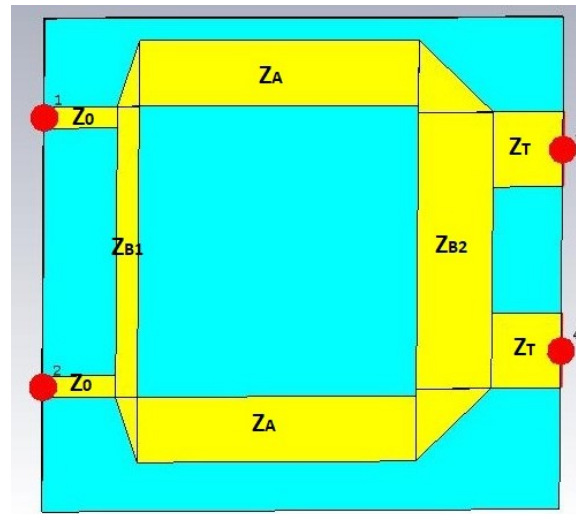
f_0 (GHz)	Insertion Loss (dB)	Insertion Loss Variation (ΔIL)	Maximal Relative Phase Shift (degree)	Return Loss (dB)	R_P (Ω)	R_S (Ω)	L_S (nH)
2.45	Min:-0.75 Max:-1.79	1.04	142.8	<-25 dB	525.6	2.4	1.509

As shown in Table 3.8, by removing R_P insertion loss variation increases and as demonstrated in theoretical analysis, maximal relative phase shift is a little bit more than load network with using R_P .

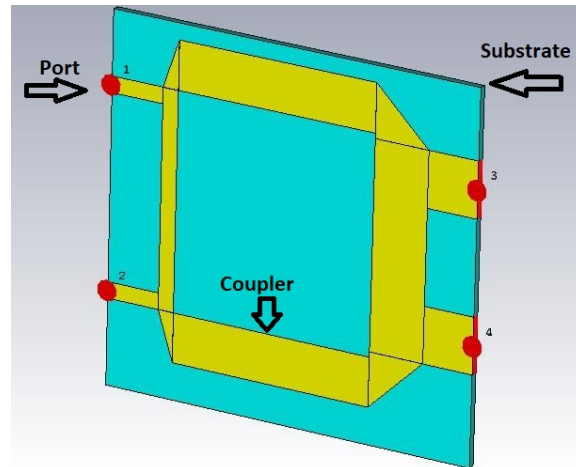
For both results of with and without using R_P , return loss are better than -25 dB

3.2.2 Simulation of Branch-Line Coupler with $r_Z = 2.5$

Figures 3.19 demonstrate the Impedance Transforming Branch-Line Coupler with the port impedance ratio of $r_Z = 2.5$.



(a)



(b)

Figure 3.19: Picture of branch-line coupler with $rZ = 2.5$ (a). Specified Impedance on each arm (b). Demonstrated components

Dimensions of this kind of coupler are shown in Table and Figure 3.9 below: Similar to coupler with impedance ratio of $r_Z = 1$, in the case

Table 3.9: Dimensions of branch-line coupler with $r_Z = 2.5$

	Z_0	Z_A	Z_{B1}	Z_{B2}	Z_T
Impedance (Ω)	50	22.36	50	20	20
Width (mm)	1.186	3.585	1.186	4.11	4.11
Length (mm)	3.9825	15.25	15.93	15.17	3.7925

of $r_Z = 2.5$ the same procedure will be carried out, to see the results and

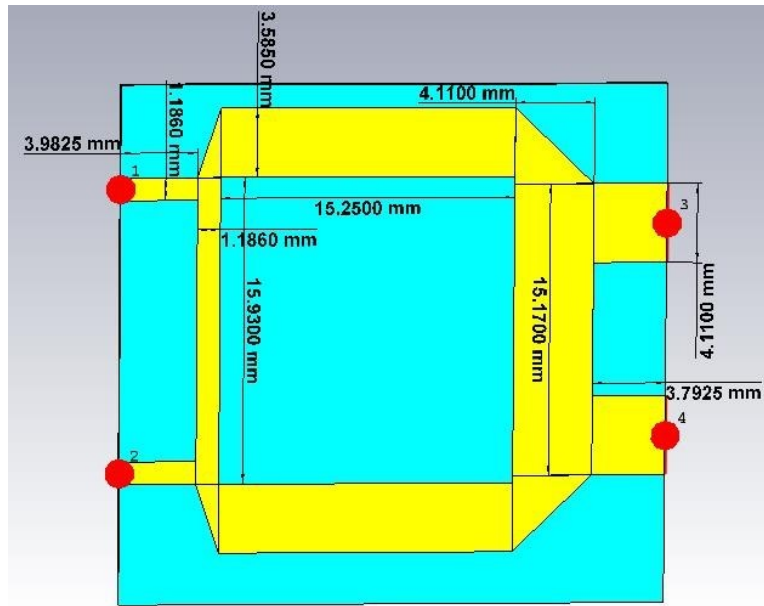


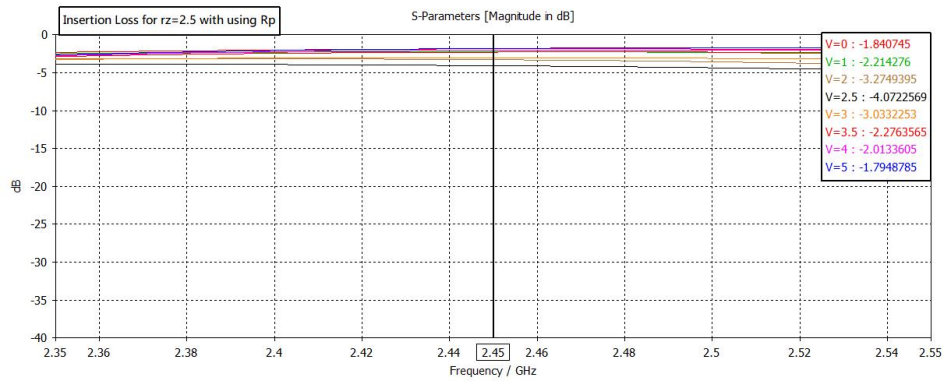
Figure 3.20: Branch-Line coupler with $r_Z = 2.5$ with specified dimensions

consequences of increasing port impedance ratio to $r_Z = 2.5$ and effect of R_P on this kind of coupler.

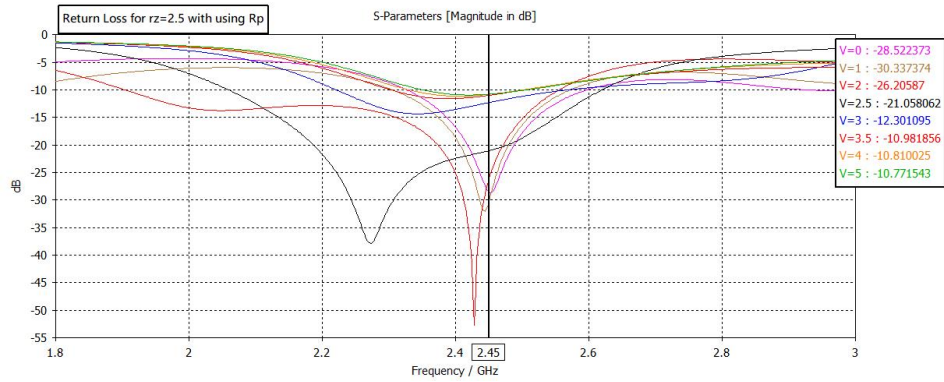
The load network shown in the Figure 3.16 is used. In following, results are discussed.

Results of Phase Shifter With Using R_P in the Network Load

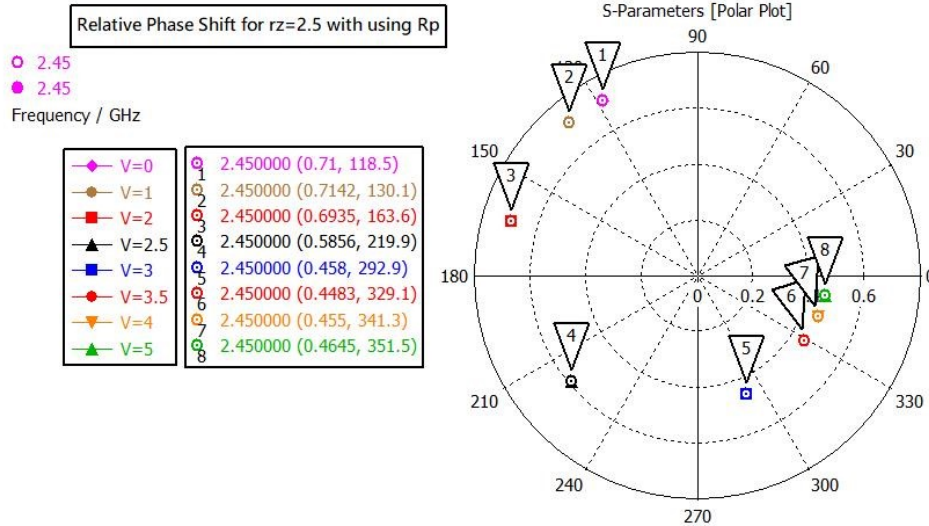
Insertion Loss(S_{21}), return loss (S_{11}), maximal relative phase shift ($\angle S_{21}$) are obtained from simulation.



(a)



(b)



(c)

Figure 3.21: Results of proposed phase shifter with $r_z = 2.5$ and using R_p (a). Insertion Loss (b). Return Loss (c). Relative Phase Shift

The above results are summarized in Table 3.10 below.

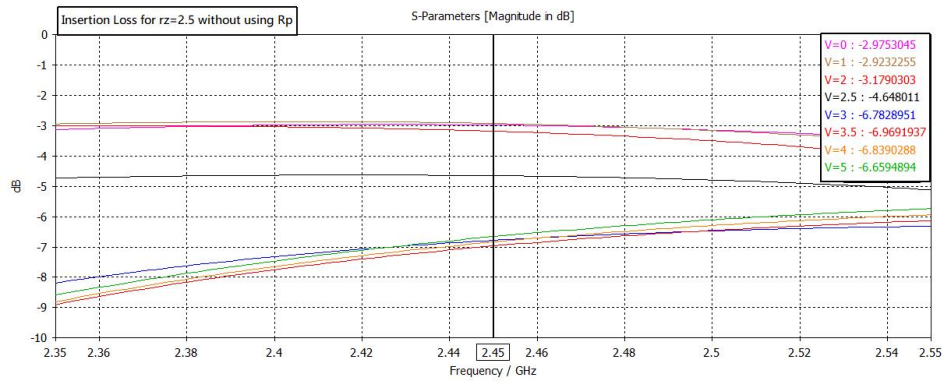
Table 3.10: Tabular results of proposed phase shifter with $r_Z = 2.5$ and using R_P

f_0 (GHz)	Insertion Loss (dB)	Insertion Loss Variation (ΔIL)	Maximal Relative Phase Shift (Degree)	Return Los (dB)	R_P (Ω)	R_S (Ω)	L_S (nH)
2.45	Min:-1.8 Max:-4.07	2.27	233	<-10	87.88	2.4	1.509

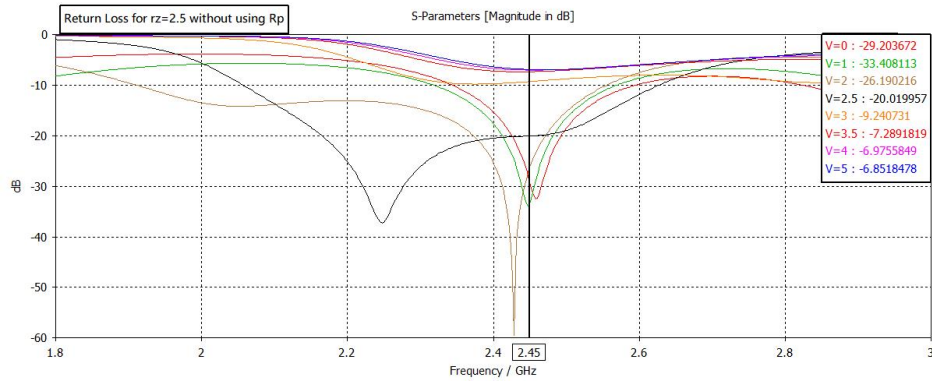
As seen in theoretical results by increasing impedance port ratio from $r_Z = 1$ to $r_Z = 2.5$ insertion loss variation and maximal relative phase shift increase as well.

Results of Phase Shifter Without Using R_P in the Network Load

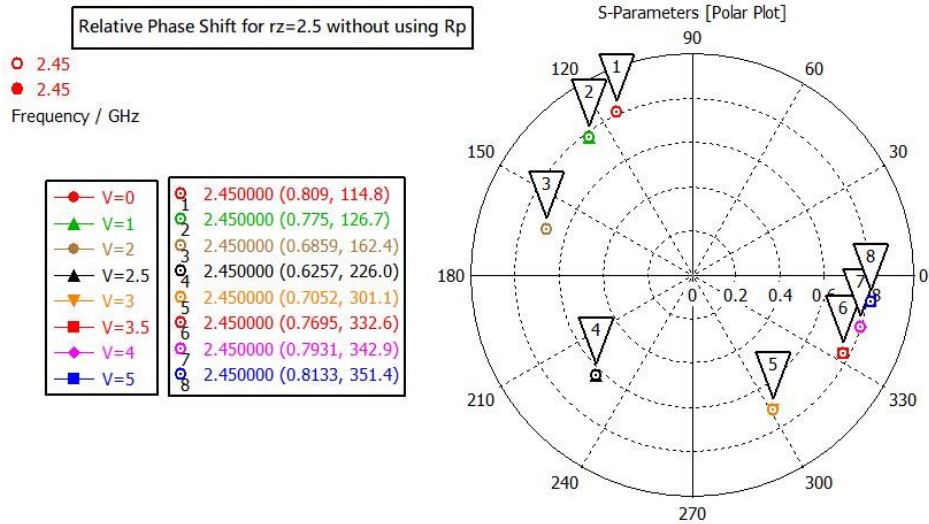
By removing the shunt resistance, as obtained in theoretical results, increasing the maximal relative phase shift and insertion loss variation are expected. Results below show this fact :



(a)



(b)



(c)

Figure 3.22: Results of proposed phase shifter with $r_z = 2.5$ and without using R_p (a). Insertion Loss (b). Return Loss (c). Relative Phase Shift

Table 3.11 below summarizes all above results:

Table 3.11: Tabular results of proposed phase shifter with $r_Z = 2.5$ and without using R_P

f_0 (GHz)	Insertion Loss (dB)	Insertion Loss Variation (ΔIL)	Maximal Relative Phase Shift (Degree)	Return Los (dB)	R_P (Ω)	R_S (Ω)	L_S (nH)
2.45	Min:-2.92 Max:-6.97	4.05	236.6	<-5	-	2.4	1.509

Conclusion

With a simple look at Tables 3.7 , 3.8, 3.10, 3.11, It can be understood that by increasing port impedance ratio r_Z from 1 to 2.5, insertion loss , insertion loss variation, maximal relative phase shift increase, but return loss is getting worse. In order to reach a compromise between return loss and other parameters such as insertion loss... and enhance the maximal relative phase shift to 360° , the proposed phase shifter should be improved.

In the next Section, design and improvement of proposed phase shifter are discussed

3.3 Design and Improvements

3.3.1 Theoretical Analysis

Previously, we have seen which insertion loss is relatively high at $r_Z = 2.5$ and maximal relative phase shift never reaches to 360° and return loss get worse by increasing r_Z . In this Section, these parameters are improved[51].

The new proposed phase shifter is composed of impedance transforming branch line coupler similar to previous design of phase shifter and two symmetrical reflection loads [48]which are connected to the coupler. Figure 3.23 below shows this new proposed phase shifter [51].

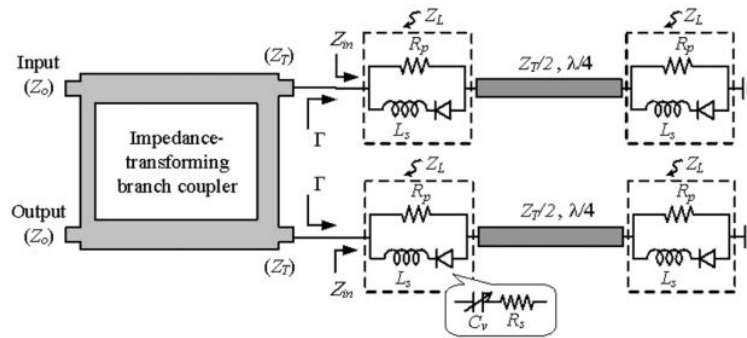


Figure 3.23: Schematic diagram of new proposed phase shifter with load network

For this configuration of load network the reflection coefficient (Γ) can be found as Equation below:

$$\Gamma = \left(\frac{(2r_Z R_s R_p - R_s Z_0 - R_p Z_0) + jX_L(2r_Z R_p - Z_0)}{(2r_Z R_s R_p + R_s Z_0 + R_p Z_0) + jX_L(2r_Z R_p + Z_0)} \right)^2 \quad (3.27)$$

Where X_L is equal to $\omega L_S - 1/\omega C_v$ which L_S is optimal shunt resistance making the insertion loss constant and C_v is capacitance of varactor at different voltage (0-5 volt) and r_Z denotes for port impedance ratio and is equal to $\frac{Z_0}{Z_T}$ and the value of R_s according to the varactor data sheet is 2.4 Ω and the value of R_P is obtained as Equation below [43] :

$$R_P = \frac{Z_0^2}{8r_Z^2 R_s} \left[1 + \sqrt{1 + \left(\frac{4r_Z R_s}{Z_0} \right)^2} \right] \quad (3.28)$$

Figure below demonstrates R_P as a function of r_Z .

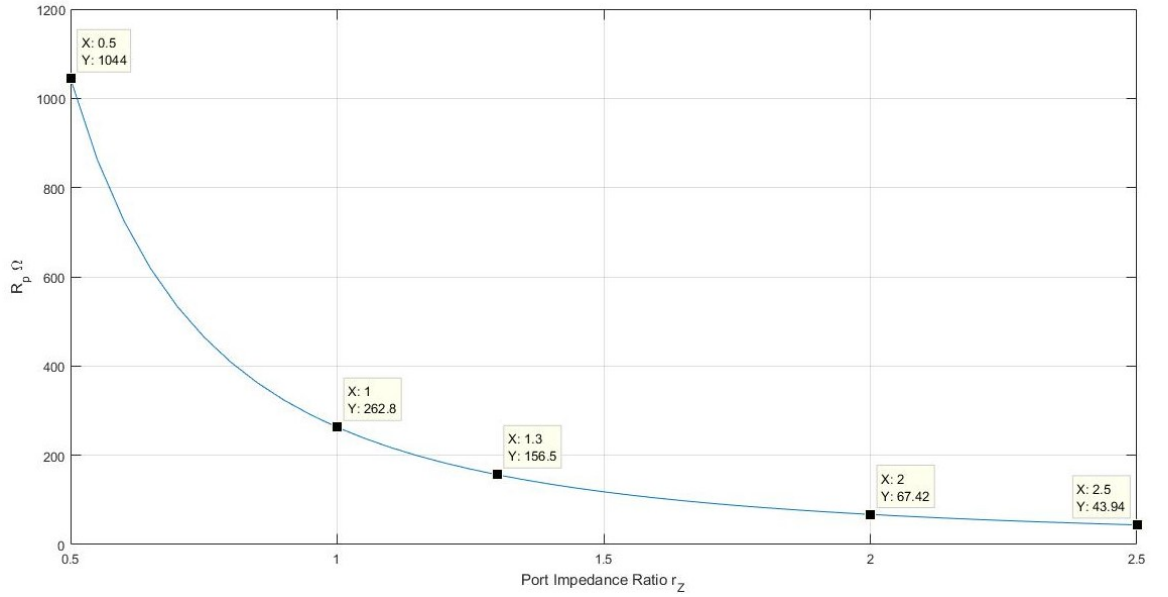


Figure 3.24: R_P vs r_Z

It can be seen that for $r_Z = 1.3$, R_P is 156.6 Ω .

Insertion Loss (S_{21}) is :

$$\begin{aligned} IL(dB) &= 20 \log_{10} |\Gamma|^2 \\ &= 20 \log_{10} \left(\frac{(2r_Z R_s R_p - R_s Z_0 - R_p Z_0)^2 + (X_L(2r_Z R_p - Z_0))^2}{(2r_Z R_s R_p + R_s Z_0 + R_p Z_0)^2 + (X_L(2r_Z R_p + Z_0))^2} \right) \end{aligned} \quad (3.29)$$

Relative Phase Shift ($\angle S_{21}$) can be calculated as :

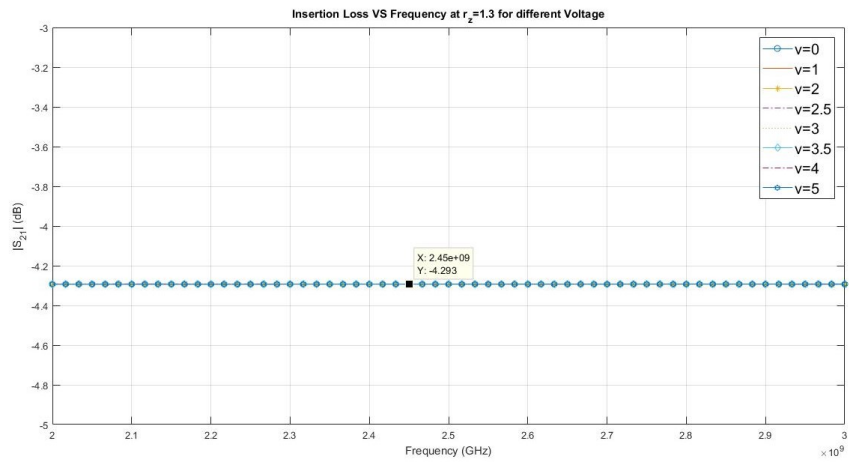
$$\begin{aligned}
\angle S_{21} &= \frac{\pi}{2} + \varphi_{21} \\
&= \frac{\pi}{2} + \tan^{-1} \left(\frac{X_L(2r_Z R_p - Z_0)}{2r_Z R_s R_p - R_s Z_0 - R_P Z_0} \right) \\
&\quad - \tan^{-1} \left(\frac{X_L(2r_Z R_p + Z_0)}{2r_Z R_s R_p + R_s Z_0 + R_P Z_0} \right)
\end{aligned} \tag{3.30}$$

Maximal Relative Phase Shift can be found as:

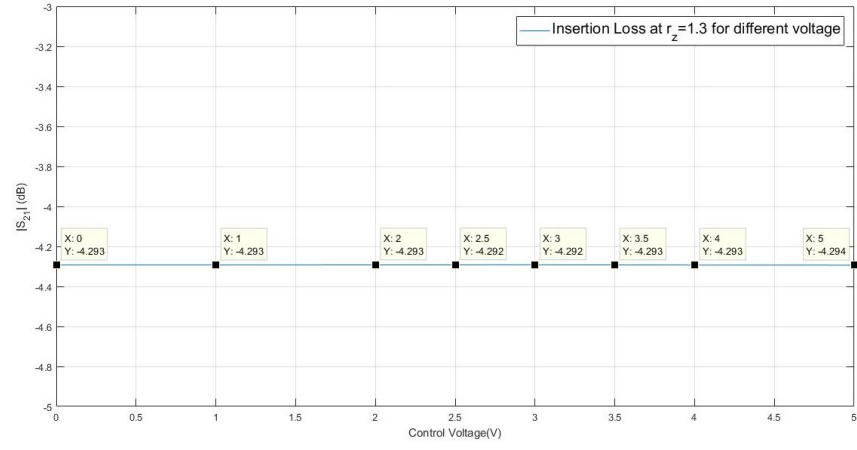
$$\Delta\varphi_{max} = \left| \angle S_{21}(X_{L,max}) - \angle S_{21}(X_{L,min}) \right| \tag{3.31}$$

Where $X_{L,max}$ and $X_{L,min}$ correspond to maximum and minimum reactance of the inductance and capacitance of varactor.

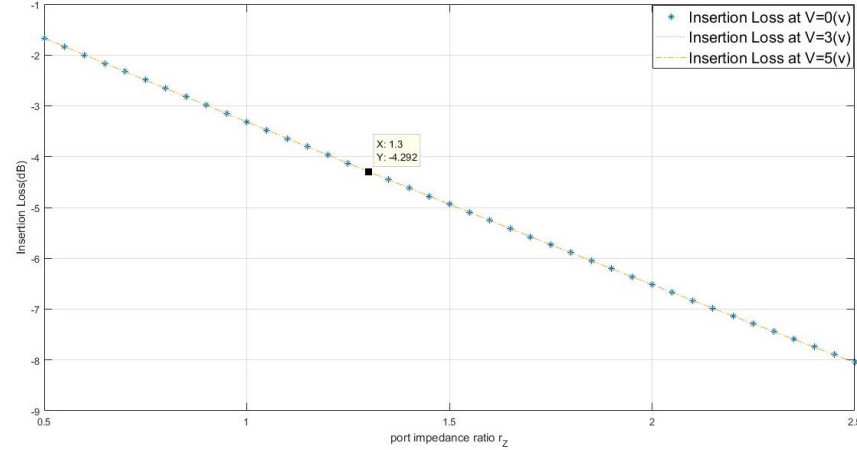
Figures below show the insertion loss as function of frequency rang of 2-3 GHz, control voltage and port impedance ratio r_Z .



(a)



(b)

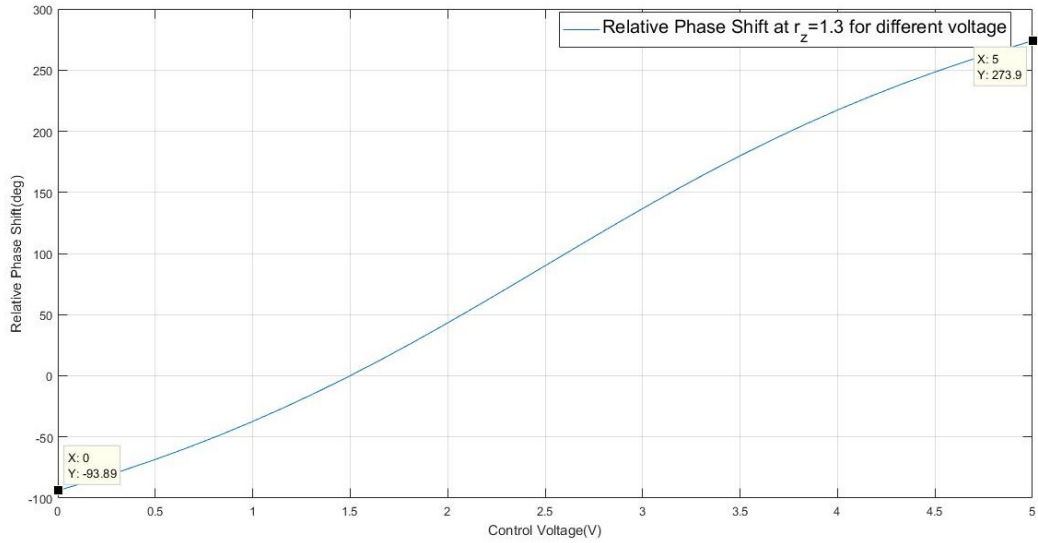


(c)

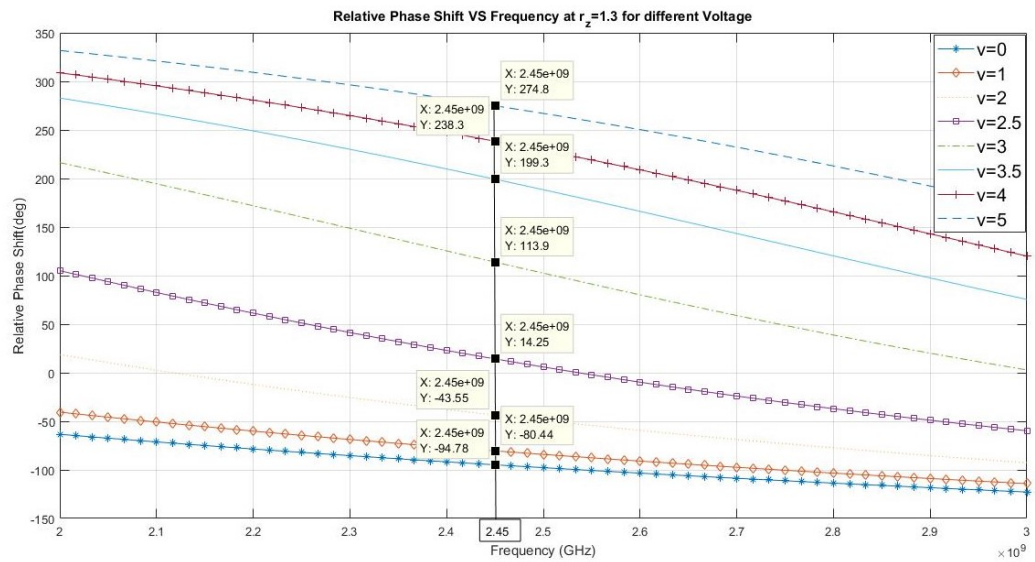
Figure 3.25: Results of insertion loss as function of (a). Frequency (b). Control Voltage (c). Port Impedance Ratio r_z

As can be found from above results insertion loss is constant and independent on varactor reactance (X_L) changing for frequency range of 2-3 GHz and different voltages of (0-5 volts). But it increases along port impedance ratio (r_Z).at $r_Z = 1.3$ Insertion Loss is -4.29 dB.

Relative Phase shift for different voltage and frequency at $r_Z = 1.3$ is shown at Figure 3.26 below :



(a)



(b)

Figure 3.26: Relative Phase Shift as function of: (a). Control Voltage (b). Frequency

Maximal relative phase shift as shown in Figure above is 387.8° . Maximal relative phase shift for different r_Z is depicted in Figure below:

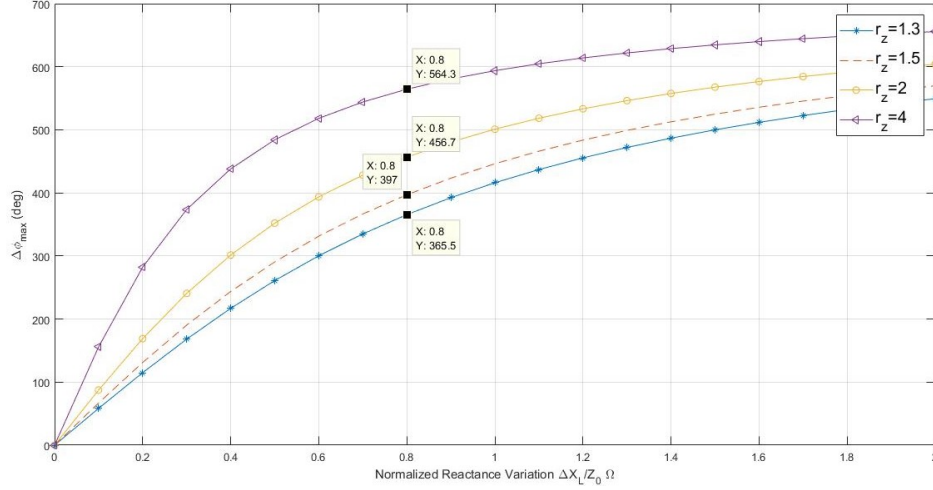


Figure 3.27: Maximal Relative Phase shift for different r_Z as function of normalized reactance $\frac{\Delta X_L}{Z_0}$

Varactor reactance variation for this work is :

$$\Delta X_L = \frac{C_{max} - C_{min}}{\omega C_{max} C_{min}} \quad (3.32)$$

Where C_{max} and C_{min} are 22.62 pF and 1.49 pF respectively. So reactance variation (ΔX_L) is 40.7 which normalized reactance is:

$$\frac{\Delta X_L}{Z_0} = 0.81 \quad (3.33)$$

Where Z_0 is 50Ω

Figure 3.27 demonstrates which for $r_Z = 1.3$, full 360° phase shift is covered in this work. Other port impedance ratio such as $r_Z = 1.5, 2, 4$ are covering more than 360° phase shift but as Figure 3.25c shows insertion loss become larger for all of them that is not efficient. Figure below shows comparison between reference [43] and [51] and this work.

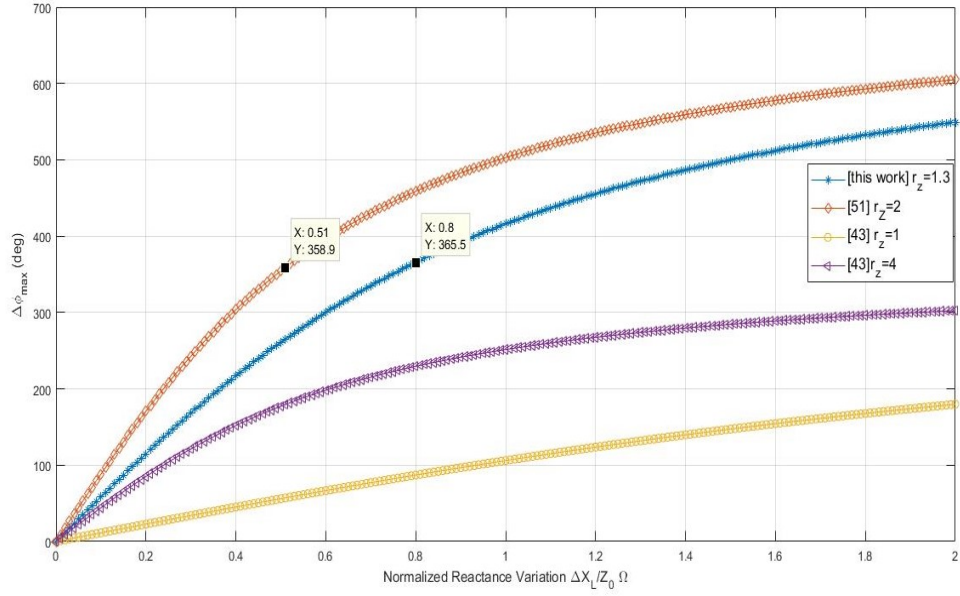


Figure 3.28: Maximal Relative Phase Shift ($\Delta\phi_{max}$) comparison between this work and references

As shown in Figure 3.28 for reference [51], $r_Z = 2$, in order to reach full 360° relative phase shift, required normalized reactance variation ($\Delta X_L/Z_0$) is almost 0.5 but according to Figure 3.25c insertion loss for $r_Z = 2$ is greater than $r_Z = 1.3$ which is not efficient. On the other hand for reference [43] relative phase shift never reach to full 360° for both $r_Z = 1$ and $r_Z = 4$.

Table below summarizes all information and compares this work with references.

Table 3.12: Theoretical results comparison between this work and reference [43], [51] and [52]

	This Work $r_Z = 1.3$	[[51]] $r_Z = 2$	[[52]] $r_Z = 1$	[[43]] $r_Z = 4$	[[43]] $r_Z = 1$
f_0 (GHz)	2.45	2	10	2	2
Insertion Loss (dB)	-4.29	-5.5	-4.8	-3.2	-1.3
Maximal Relative Phase Shift (degree)	365.5	360	360	252.4	106.3
$\Delta X_L/Z_0$	0.8	0.5	2	1	1
R_P (Ω)	156.5	80	714.3	82	1252
R_S (Ω)	2.4	2	3.5	2	2

Table 3.12 makes explicit Theoretical calculation comparisons between this work and reference [43], [51] and [52]. As shown in Table this work and reference [51] and [52] cover full 360° relative phase shift, although reference [43] has lowest insertion loss, it never achieves 360° relative phase shift. In terms of insertion loss, this work has better performance with lowest insertion loss.

3.3.2 Simulation

in this Section, simulation by CST studio will be done to see whether the simulation results would agree with calculation predictions or not.

Design of Branch-Line Coupler with $r_Z = 1.3$

The dimensions of the coupler should be calculated according to formulas from 3.1 to 3.11. Figures below show the picture of branch-line coupler with $r_Z = 1.3$ with calculated dimensions.

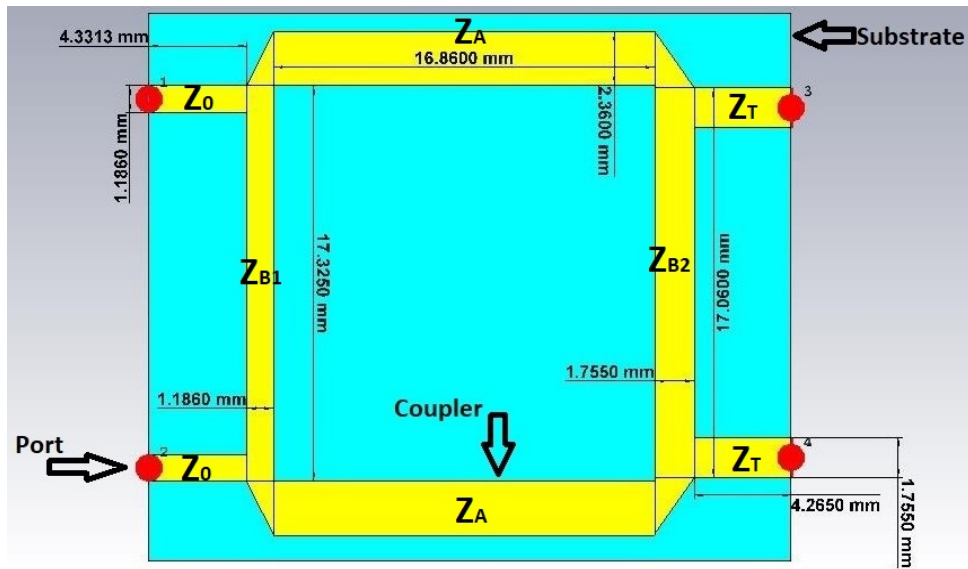


Figure 3.29: Picture of branch-line coupler with $r_Z = 1.3$ and specified dimensions

Table below shows dimensions of the coupler in tabular form.

Table 3.13: Dimensions of branch-line coupler with $r_Z = 1.3$

	Z_0	Z_A	Z_{B1}	Z_{B2}	Z_T
Impedance (Ω)	50	31	50	38.46	38.46
Width (mm)	1.186	2.36	1.186	1.755	1.755
Length (mm)	4.3313	16.86	17.325	17.06	4.2650

Load Network

As shown in Figure 3.23, the load network of new proposed phase shifter consists of two identical loads connected to port 3 and 4 of the coupler and each load consists of two series resonant varactors interconnected by a ($\lambda/4$) transmission line with impedance of 19.23Ω ($Z_T/2$) and with length and width of 16.462mm and 4.306mm . R_S and L_S are given 2.4Ω and 1.509nH respectively and C_T is the varactor capacitance according to Table 3.2. Figure below shows the load configuration in CST studio simulation.

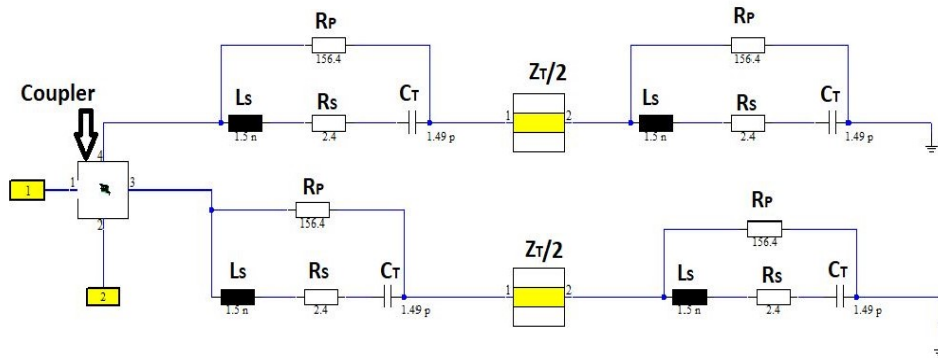
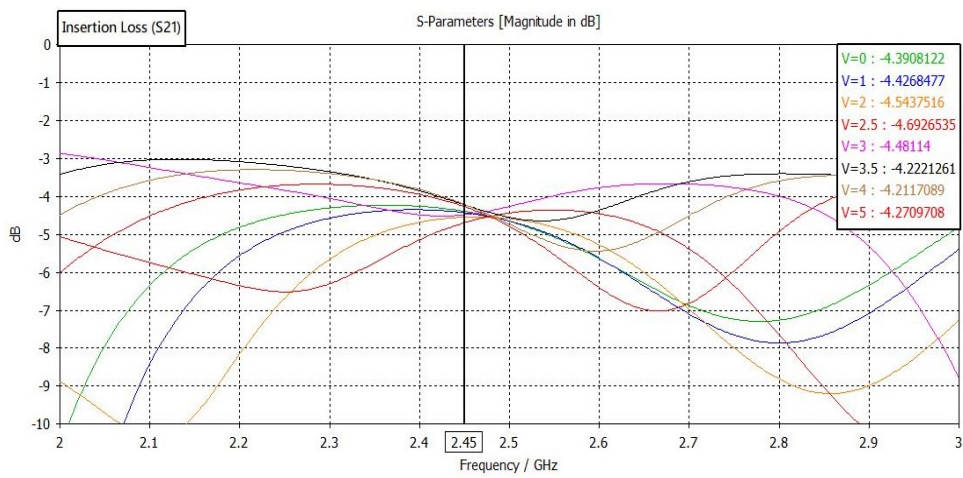


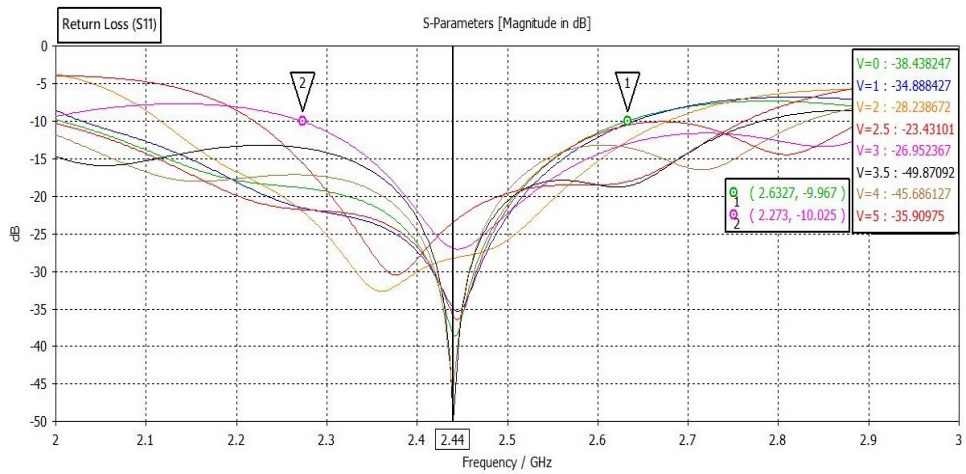
Figure 3.30: Load Network of new proposed phase shifter

Simulation Results of Phase Shifter

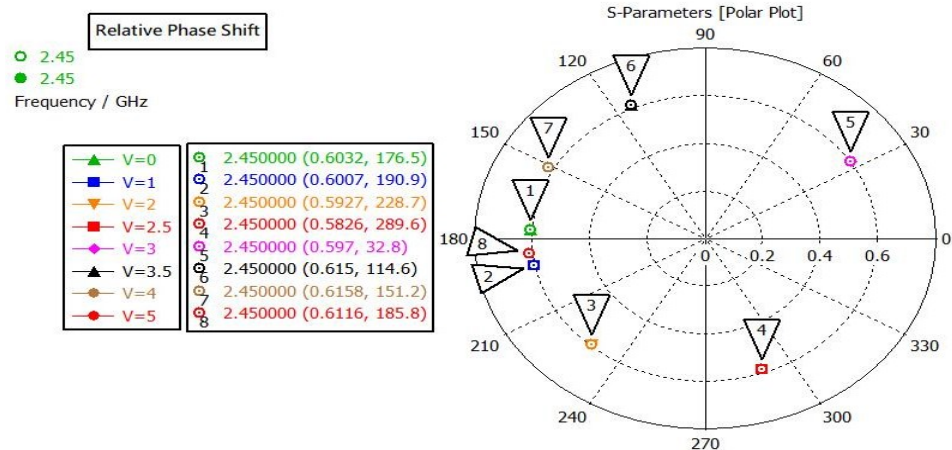
Figures of Insertion Loss (S_{21}), Relative Phase shift ($\angle S_{21}$) and return Loss (S_{21}) are depicted as below:



(a)



(b)



(c)

Figure 3.31: Simulation Results (a). Insertion Loss (b). Return Loss (c). Relative Phase Shift

Table below summarize all above results:

Table 3.14: Tabular Results of new proposed phase shifter with $r_Z = 1.3$

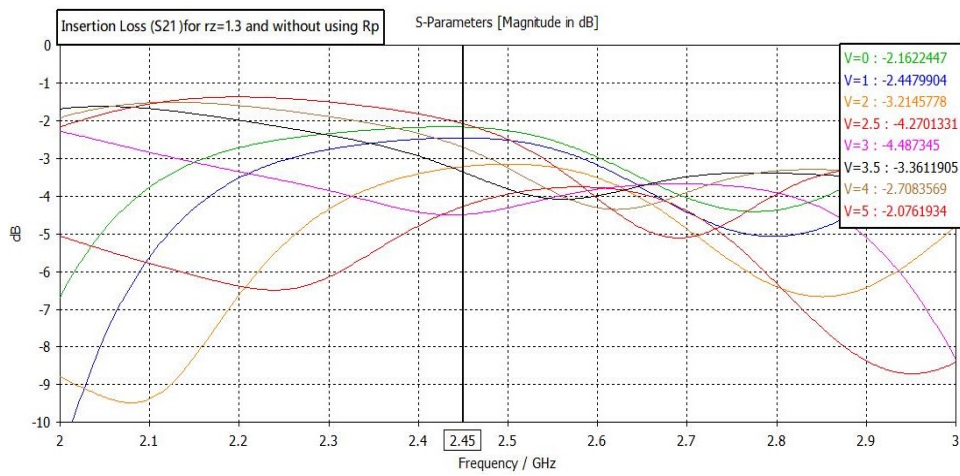
f_0 (GHz)	Insertion Loss (dB)	Insertion Loss Variation (ΔIL)	Maximal Relative Phase Shift (Degree)	Return Loss (dB)	Band Width (MHz)	R_P Ω	L_S (nH)
2.45	Min:-4.21 Max:-4.69	0.48	369.3	<-20	359.7	156.5	1.5

It is obvious which at center frequency $f_0 = 2.45$ GHz, Return Loss is better than -20 dB and Relative Phase Shift satisfies full 360° , and Insertion Loss excellently agree with theoretical calculation. In terms of bandwidth, new proposed phase shifter completely covers the industrial, scientific, and medical radio band (ISM) which is frequency range of 2.4 and 2.5 GHz.

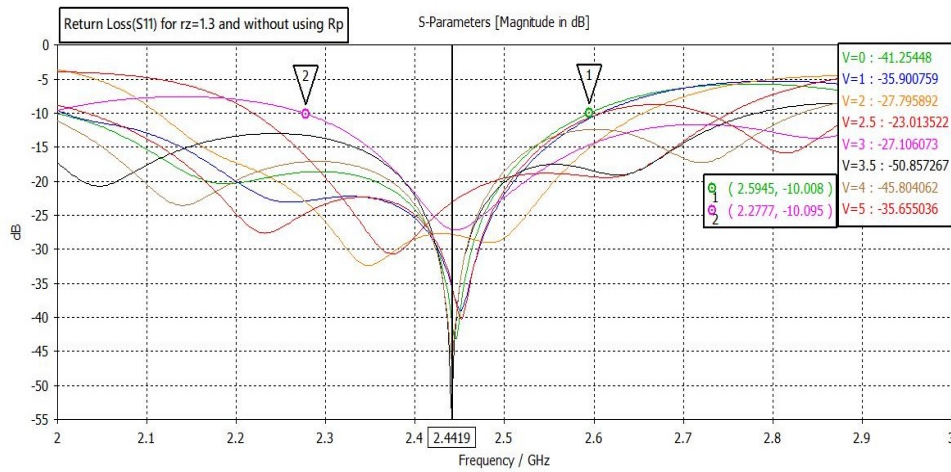
Simulation Results of Removing R_P from Load Network

In order to get more results, the shunt optimal resistance R_P is removed from the load network of Figure 3.30.

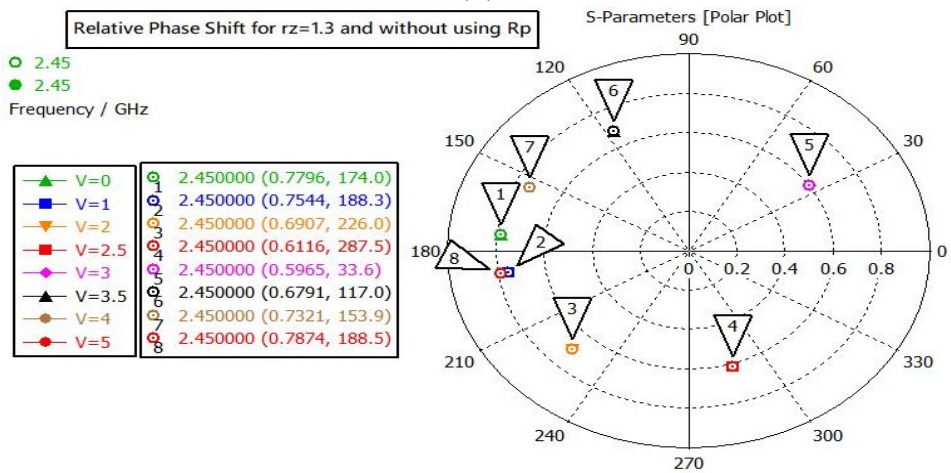
Insertion Loss (S_{21}), Return Loss (S_{11}), Relative Phase shift ($\angle S_{21}$) are depicted in Figures below:



(a)



(b)



(c)

Figure 3.32: Simulation Results for the Load Network without using R_P
 (a). Insertion Loss (b). Return Loss (c). Relative Phase Shift

As shown in Figure 3.32a, insertion loss variation obviously appears. Table 3.15 below summarize simulated results in tabular form:

Table 3.15: Tabular Results of new proposed phase shifter with removing R_P from load network

f_0 (GHz)	Insertion Loss (dB)	Insertion Loss Variation (ΔIL)	Maximal Relative Phase Shift (Degree)	Return Loss (dB)	Band Width (MHz)	R_P Ω	L_S (nH)
2.45	Min:-2.07 Max:-4.48	2.41	374.5	<-20	316.8	-	1.5

By a simple look at above Table, it can be found that, Maximal relative phase shifter get better than result of load network using R_P . Although bandwidth is a little bit lower than results in the Table 3.14, it still covers ISM band.

In order to see more results the value of L_S and R_P can be changed. In following, results with $L_s = 1.3^{nH}$, 1.9^{nH} , 2^{nH} and $R_P=140\Omega$, 156.5Ω , 170Ω , and without using R_P are obtained using simulation CST studio.

Simulation Results of using $L_S = 1.3nH$ and $R_P = 140, 156.4, 170\Omega$ and without R_P

Figures below show the Simulation results of Phase Shifter load network with $L_S = 1.3nH$ and using different various $R_P = 140, 156.4, 170\Omega$ and removing R_P . Insertion Loss (S_{21}), Return Loss (S_{11}) and Relative Phase Shift ($\angle S_{21}$) are depicted below:

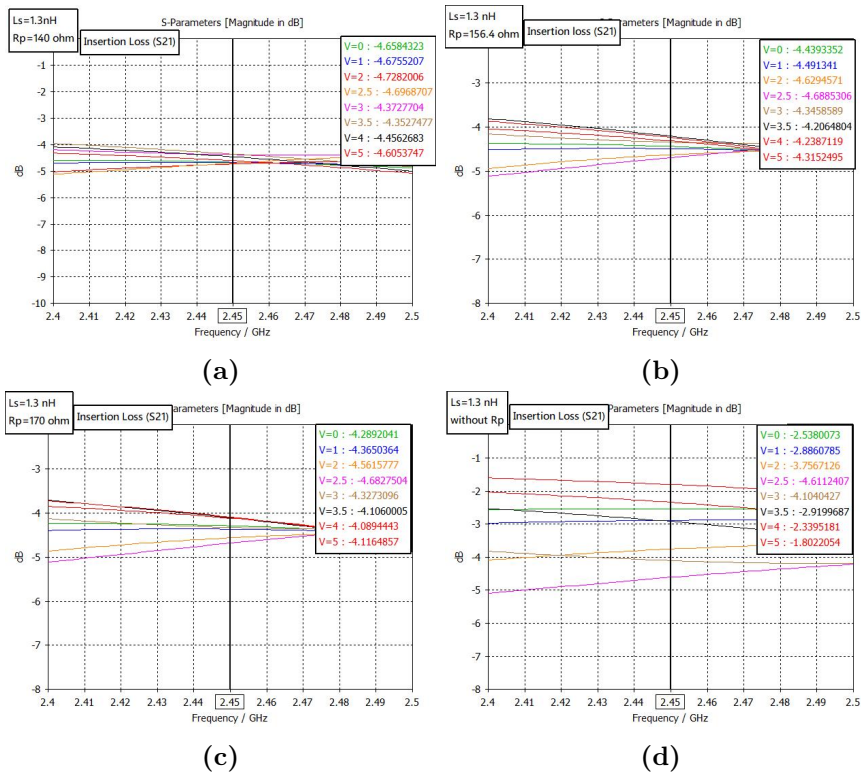


Figure 3.33: Insertion Loss results for Load Network with $L_S = 1.3 \text{ nH}$ and (a). $R_P = 140 \Omega$ (b). $R_P = 156.4 \Omega$ (c). $R_P = 170 \Omega$ (d). No R_P

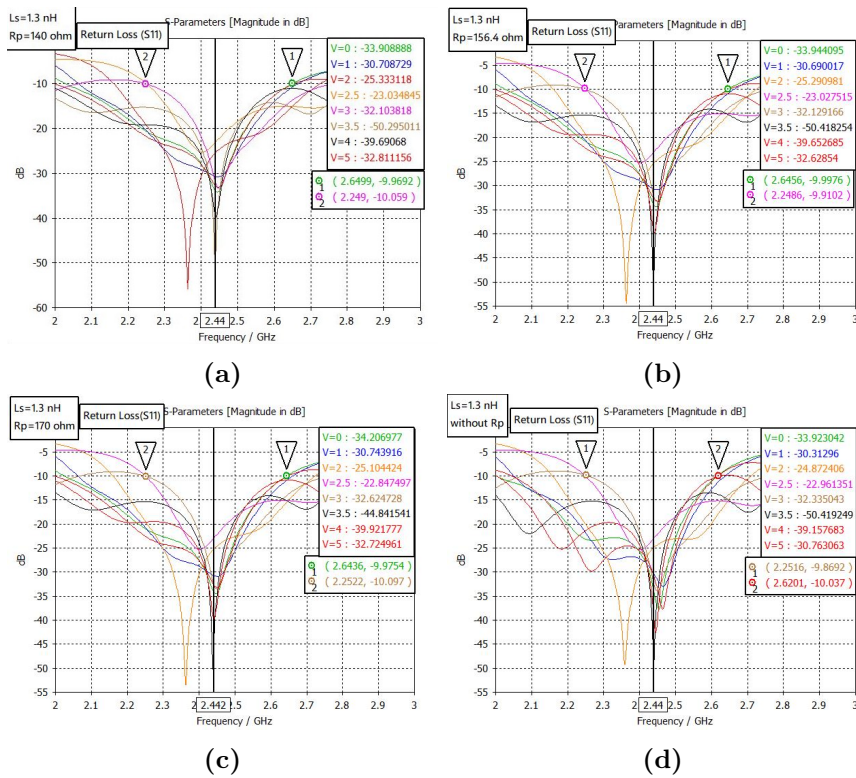


Figure 3.34: Return Loss results for Load Network with $L_S = 1.3\text{ nH}$ and (a). $R_P = 140\Omega$ (b). $R_P = 156.4\Omega$ (c). $R_P = 170\Omega$ (d). No R_P

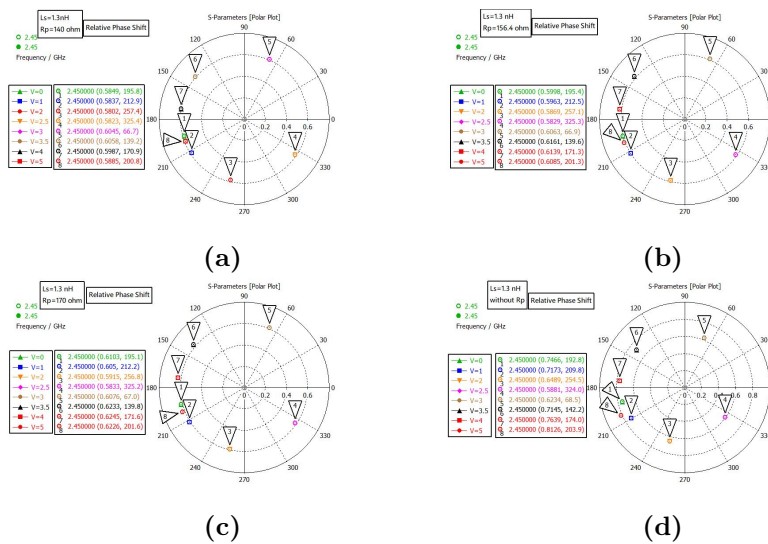


Figure 3.35: Relative Phase Shift results for Load Network with $L_S = 1.3\text{ nH}$ and (a). $R_P = 140\Omega$ (b). $R_P = 156.4\Omega$ (c). $R_P = 170\Omega$ (d). no R_P

Table 3.16 below summarizes all above results in tabular format:

Table 3.16: Tabular results for proposed phase shifter with load network with $L_S = 1.3nH$ and $R_P = 140, 156.4, 170\Omega$ and removing R_P

R_P (Ω)	140	156.4	170	no R_P
Insertion Loss (dB)	Min:-4.35 Max:-4.73	Min:-4.2 Max:-4.69	Min:-4.08 Max:-4.68	Min:-1.8 Max:-4.61
Insertion Loss Variation (ΔIL) (dB)	0.38	0.49	0.6	2.81
Maximal Relative Phase Shift (Degree)	365	365.9	366.5	377.1
Return Loss (dB)	<-20	<-20	<-20	<-20
Bandwidth (MHz)	400.9	397	391.4	368.5

As we can see in Table 3.16, by increasing R_P , maximum and minimum insertion loss and bandwidth decrease while insertion loss variation (ΔIL) and maximal relative phase shift increase.

Simulation Results of using $L_S = 1.9nH$ and $R_P = 140, 156.4, 170\Omega$ and removing R_P

By changing the value of inductance L_S to 1.9nH, new results are obtained. Insertion Loss (S_{21}), Return Loss (S_{11}) and Relative Phase Shift ($\angle S_{21}$) for various values of R_P are depicted belows:

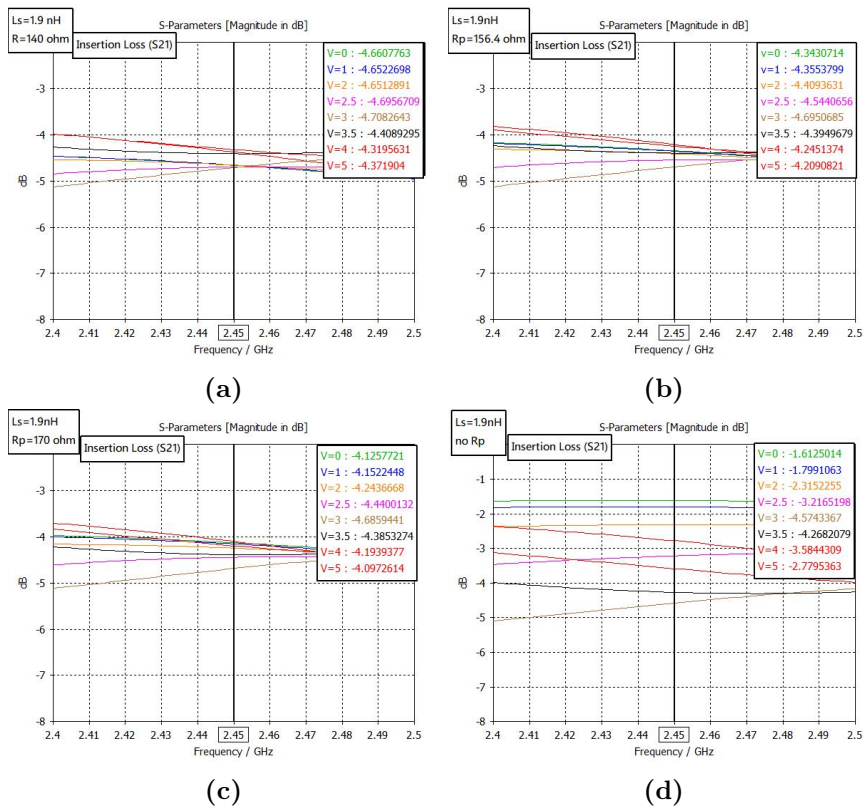


Figure 3.36: Insertion Loss results for Load Network with $L_S = 1.9\text{ nH}$ and (a). $R_P = 140\ \Omega$ (b). $R_P = 156.4\ \Omega$ (c). $R_P = 170\ \Omega$ (d). no R_P

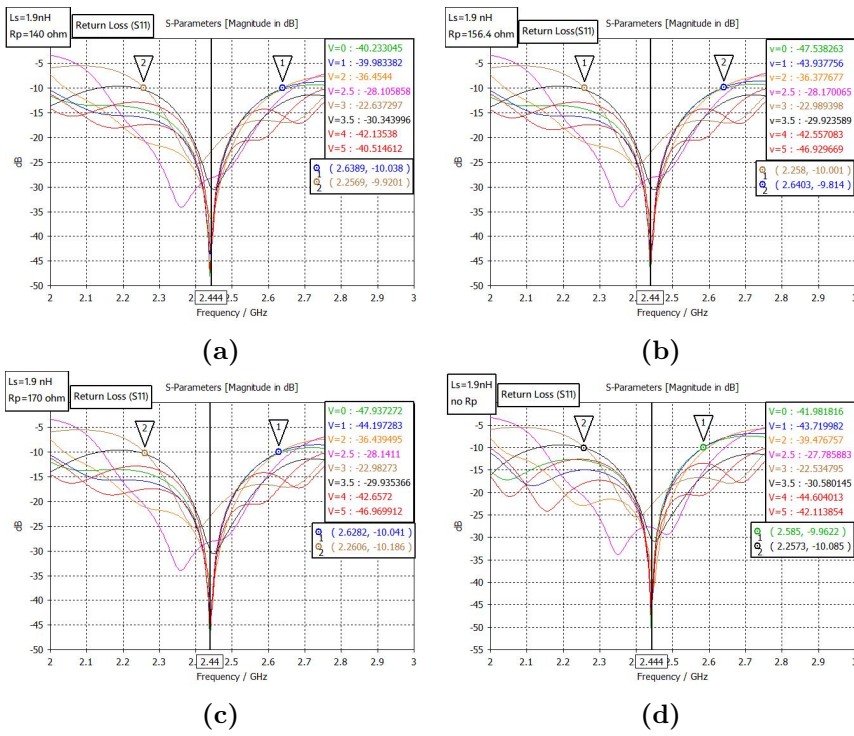


Figure 3.37: Return Loss results for Load Network with $L_S = 1.9 \text{ nH}$ and (a). $R_P = 140 \Omega$ (b). $R_P = 156.4 \Omega$ (c). $R_P = 170 \Omega$ (d). no R_P

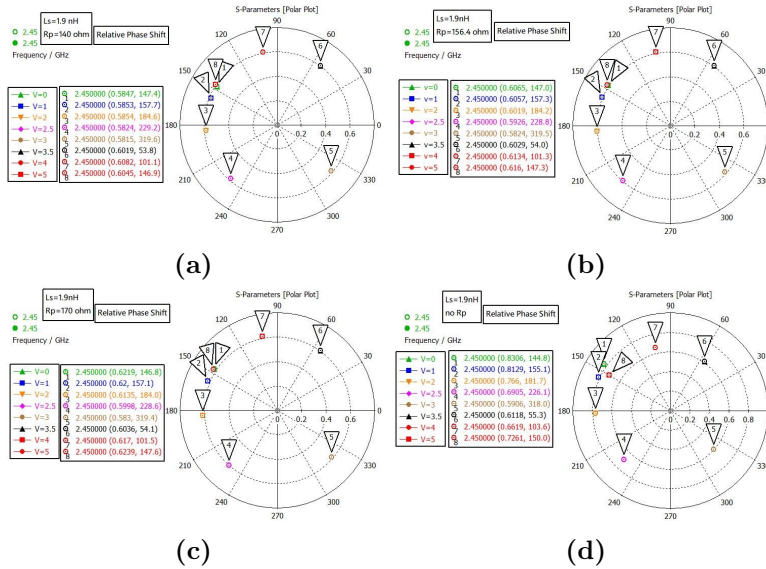


Figure 3.38: Relative Phase Shift results for Load Network with $L_S = 1.9 \text{ nH}$ and (a). $R_P = 140 \Omega$ (b). $R_P = 156.4 \Omega$ (c). $R_P = 170 \Omega$ (d). no R_P

Table 3.17 below summarizes all above results:

Table 3.17: Tabular results for proposed phase shifter with load network with $L_S = 1.9nH$ and $R_P = 140, 156.4, 170\Omega$ and removing R_P

R_P (Ω)	140	156.4	170	no R_P
Insertion Loss (dB)	Min:-4.32 Max:-4.7	Min:-4.2 Max:-4.69	Min:-4.09 Max:-4.68	Min:-1.61 Max:-4.57
Insertion Loss Variation (ΔIL) (dB)	0.38	0.49	0.6	2.96
Maximal Relative Phase Shift (Degree)	359.5	360.3	360.8	365.2
Return Loss (dB)	<-20	<-20	<-20	<-20
Bandwidth (MHz)	382	377.5	376.6	327.7

Obviously, for same inductance, $L_S = 1.9nH$, by increasing R_P max and min insertion loss and bandwidth decrease while insertion loss variation and maximal relative phase shift increase. Return loss for all cases performs better than -20 dB.

Simulation Results of using $L_S = 2nH$ and $R_P = 140, 156.4, 170\Omega$ and removing R_P

For inductance value of $L_S = 2nH$, Insertion loss (S_{21}), Return loss (S_{21}) and relative phase shift ($\angle S_{21}$) are depicted as below :

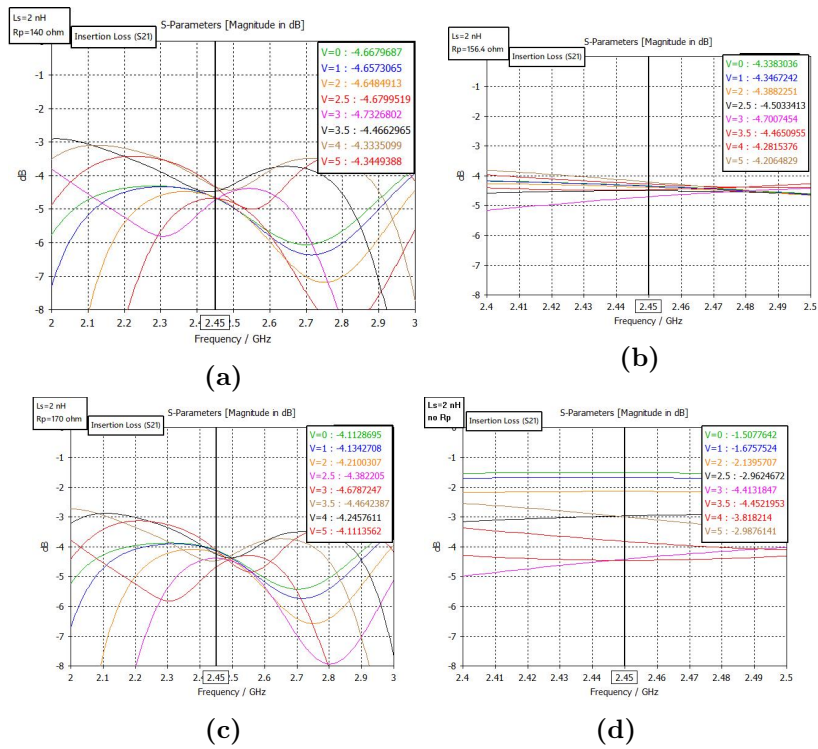


Figure 3.39: Insertion Loss results for Load Network with $L_S = 2 \text{ nH}$ and (a). $R_P = 140 \Omega$ (b). $R_P = 156.4 \Omega$ (c). $R_P = 170 \Omega$ (d). no R_P

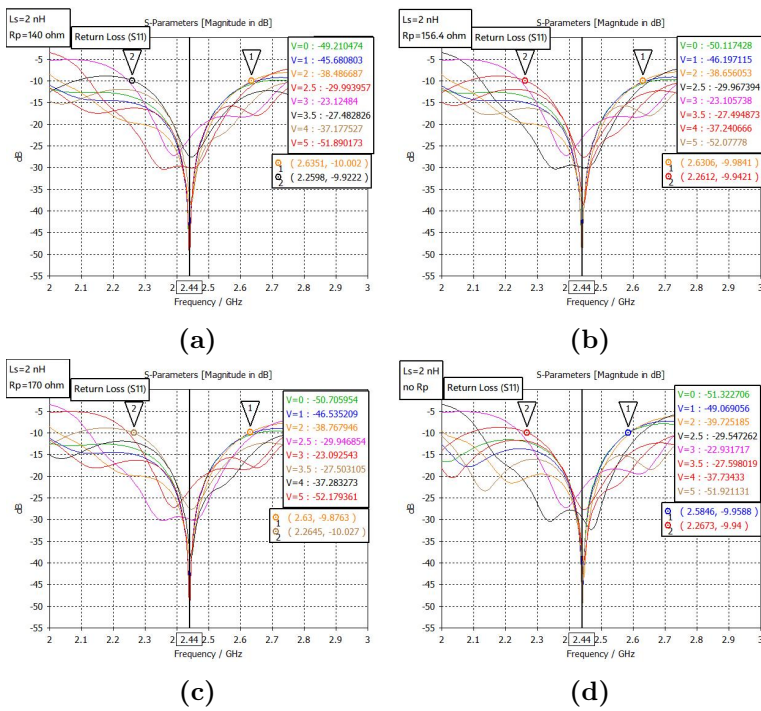


Figure 3.40: Return Loss results for Load Network with $L_S = 2nH$ and (a). $R_P = 140\Omega$ (b). $R_P = 156.4\Omega$ (c). $R_P = 170\Omega$ (d).no R_P

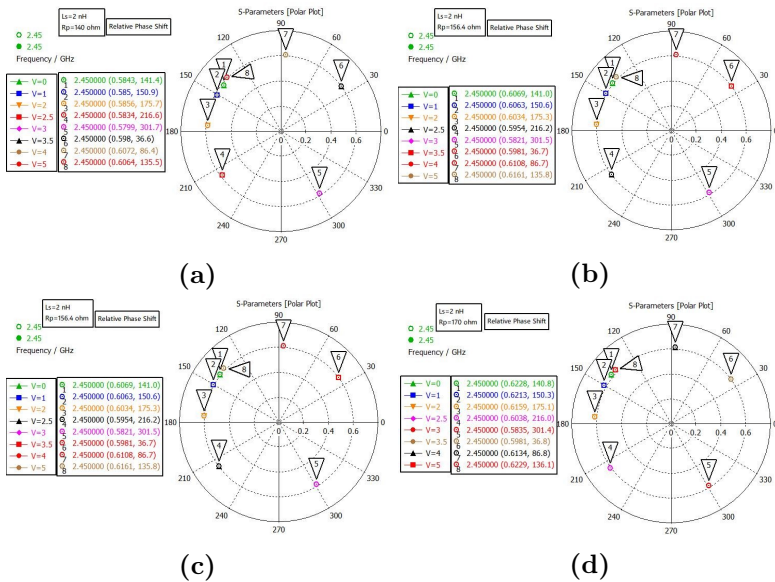


Figure 3.41: Relative Phase Shift results for Load Network with $L_S = 2nH$ and (a). $R_P = 140\Omega$ (b). $R_P = 156.4\Omega$ (c). $R_P = 170\Omega$ (d).no R_P

Table 3.18 below summarizes all above results:

Table 3.18: Tabular results for proposed phase shifter with load network with $L_S = 2nH$ and $R_P = 140, 156.4, 170\Omega$ and removing R_P

R_P (Ω)	140	156.4	170	no R_P
Insertion Loss (dB)	Min:-4.33 Max:-4.73	Min:-4.2 Max:-4.7	Min:-4.11 Max:-4.678	Min:-1.5 Max:-4.45
Insertion Loss Variation (ΔIL) (dB)	0.4	0.5	0.56	2.95
Maximal Relative Phase Shift (Degree)	354.1	354.8	355.3	359.5
Return Loss (dB)	<-20	<-20	<-20	<-20
Bandwidth (MHz)	375.3	369.4	365.5	317.3

As can be seen in Table 3.18, Insertion Loss and insertion loss variation are similar to results of load network with using $L_S = 1.9nH$ while in this case maximal relative phase shift for various values of R_P are lower than full 360° phase shift range. In terms of bandwidth the load network $L_S = 1.9nH$ performs better.

In Conclusion the load network with $L_S = 1.9nH$, in comparison to load network with $L_S = 1.3nH, 1.5nH, 2nH$ has better performance. In following which is the manufacturing and realization of phase shifter, we use this kind of circuit which has $L_S = 1.9nH$ and $R_P = 156.4\Omega$ in the load network.

Chapter 4

Realization And Measurements

Designed phase shifters for using shunt R_P resistance in load network and without using R_P are manufactured. Coupler is made up copper on top of the substrate with constant dielectric of $\epsilon_r = 3.38$ and thickness of $h=0.508$ mm and loss tangent of 0.0028. At each port, an SMA connector is implemented for connecting the device to a network analyzer. Figure below show the layout of the designed phase shifter for without using R_P in the load network.

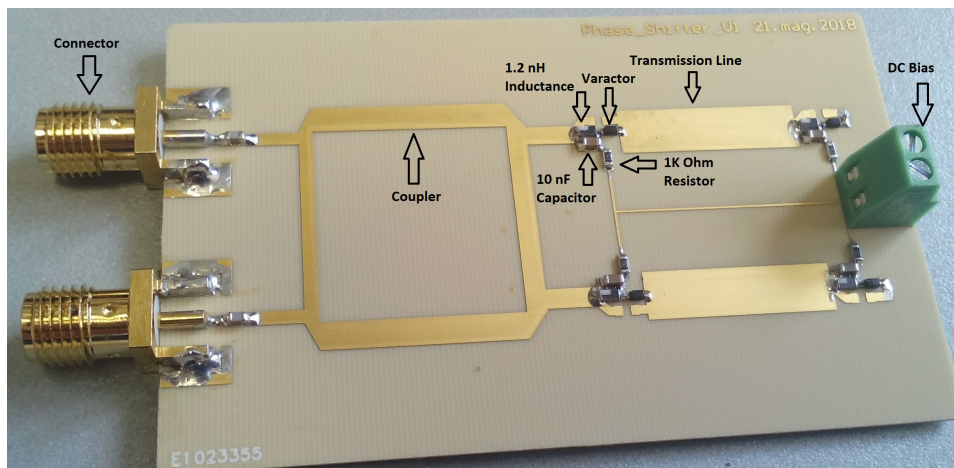


Figure 4.1: Fabricated phase shifter without using R_P in the load network

As can be seen in this Figure 1.2 nH is connected in series with varactor to make a total inductance of 1.9 nH (0.7nH is parasitic inductance of varactor). In order to block DC signal from the RF path and isolate the RF signal from biasing line a 10 nF capacitor and 1K Ω are implemented.

In order to perform measurements Phase Shifter must be connected to

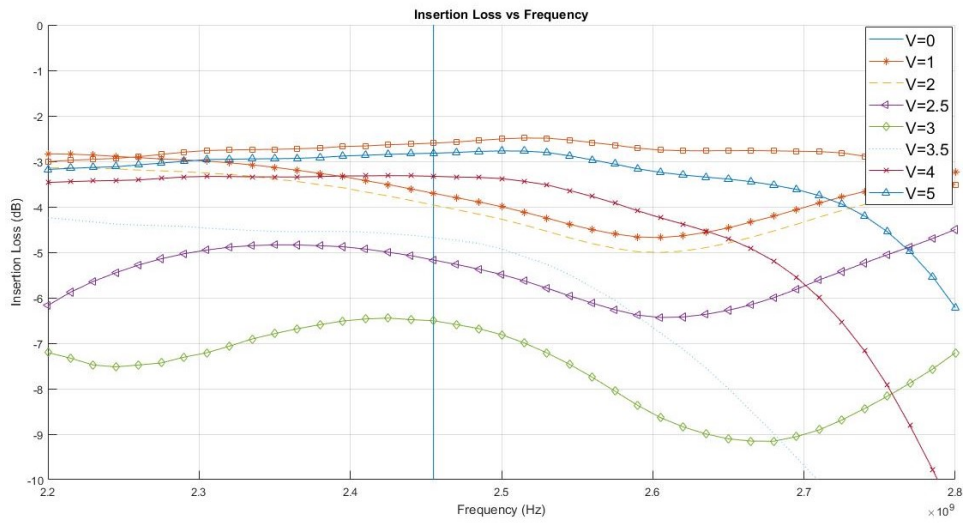
network analyzer to obtain results and evaluate the performance of the phase shifter. Figures 4.2 show the results achieved from network analyzer.

As shown, there is a variation over insertion loss due to removing the shunt R_P resistor resulting variation from -2.5 dB to -6.2 dB. Return loss is better than -20dB as expected and bandwidth covers ISM band which is from 2.4 GHz to 2.5 GHz as calculated in theoretical analysis. For the relative phase shift manufactured phase shifter covers 320° while is less than simulated results in 3.38 but it's much more than the previous proposed phased shifter which is designed for the impedance transforming branch line coupler with $r_Z = 2.5$ with dual varactor connected to output port in Figure 3.2 resulted in 3.11.

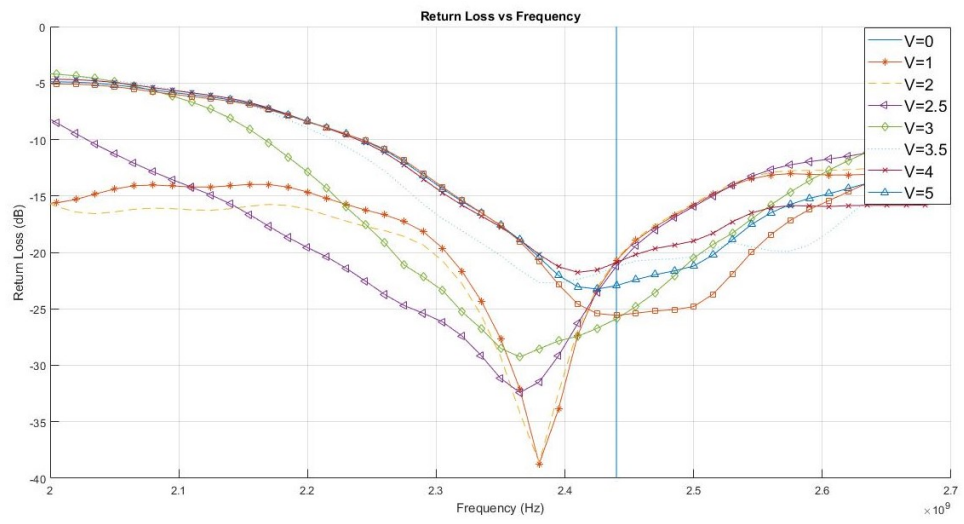
Table below summarizes all information obtained from measurements results.

Table 4.1: Tabular results of measured phase shifter

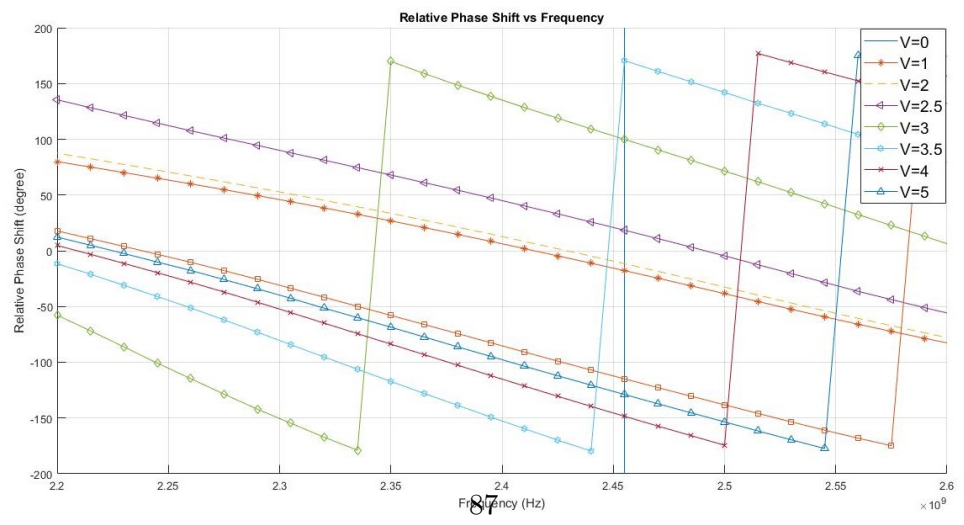
f_0 (GHz)	Insertion Loss (dB)	Insertion Loss Variation	Return Loss (dB)	Relative Phase Shift (Degree)	Bandwidth (MHz)
2.45	Min:-2.5 Max:-6.2	3.7	<-20	320	>300



(a)



(b)



(c)

Figure 4.2: Results of fabricated phase shifter (a). Insertion loss (b). Return Loss (c). Relative phase shift

In order to make a comparison between previous design and improved design Table 4.2 below is created.

Table 4.2: Tabular results comparisons between previous and improved design for without using R_P in load network

	Measurement Results for improved Phase Shifter	Simulation Results for improved Phase Shifter	Simulation Results of Previous Phase Shifter
r_Z	1.3	1.3	2.5
Insertion Loss (dB)	Min:-2.5 Max:-6.2	Min:-1.61 Max:-4.57	Min:-2.92 Max:6.97
Insertion Loss Variation	3.7	2.96	4.05
Return Loss (dB)	<-20	<-20	<-5
Maximal Relative Phase Shift (Degree)	320	365.2	236.6
Bandwidth (MHz)	>360	327.7	<300

As can be seen in Table there is an agreement between simulation and measurement results for the improved phase shifter with $r_Z = 1.3$ and without using R_P in the load network and in comparison to previous design, maximal relative phase shift, insertion loss, return loss, bandwidth have better performances.

Chapter 5

Conclusions And Perspectives

A new reflection type phase shifter has been designed by introducing impedance transforming branch line coupler and two equal load networks consisting of varactor of 1.49 pF to 22.62 pF capacitance range in series with a inductance and a resistor R_P shunted to inductance and varactor which all of them are connected to the output of the coupler. By choosing impedance ratio of $r_Z = 1$ the impedance transforming coupler behaves like conventional 3dB branch line coupler which results 141.5° relative phase shift and insertion loss of -1.8 dB. R_P is used to keep the insertion loss constant by a proper calculation the resistance value of 525.6Ω for $r_Z = 1$ would be achieved. In order to increase the relative phase shift, the impedance ratio of the coupler should be increased but on the other hand insertion loss increases as well due to the parasitic resistance of varactor. By making the try and error approach, the impedance ratio of 2.5 is selected resulting 233° relative phase shift and insertion loss of -4 dB. By changing r_Z to 2.5 the value of R_P is changed to 87.88Ω . Obviously this configuration of phase shifter never satisfies full 360° relative phase shift range.

In order to achieve a full 360° relative phase shift, a new reflection type phase shifter is presented by choosing impedance ratio of $r_Z = 1.3$ and two series resonant varactor interconnected with quarter-wavelength transmission line in the load network which result 360° relative phase shift and insertion loss of -4.7 dB with bandwidth of 377.5 MHz at center frequency of $f_0 = 2.45GHz$. In this case the new value of R_P would be 156.4Ω . By removing the shunt resistance R_P a slight variation over insertion loss appears with minimum and maximum insertion loss of -1.61 and -4.57 dB , but relative phase shift increases to 365.5° while bandwidth decreases to 327.7 MHz.

By introducing a novel approach of phase shifter which is the coupler with $r_Z = 1.3$ and two cascaded varactors, desired results would be ob-

tained. This phase shifter can be exploited in phased array antennas as main components to target any objects in any directions.

Bibliography

- [1] Robert J. Mailloux "*Phased Array Antenna Handbook*" Artech House; 3 edition (November 30, 2017)
- [2] Ehyaie, Danial (2011). *Novel Approaches to the Design of Phased Array Antennas* (Doctoral dissertation). University of Michigan
- [3] Warren L. Stutzman, Gary A. Thiele "*Antenna Theory and Design*" John Wiley & Sons; Second Edition (December 28, 1997)
- [4] A. J. Fenn, D. H. Temme, W. P. Delaney, "*The development of phased-array radar development*", Lincoln Lab. J., vol. 12, pp. 321, 2000
- [5] Iulian Rosu: Phase Shifters <http://www.qsl.net/va3iul/>
- [6] <https://www.chegg.com/homework-help/definitions/phase-shift-4>
- [7] Geethanjali VS, Mohan T, Rao IS. "*Beam forming networks to feed array antennas*". Indian Journal of Science and Technology. 2015 Jan; 8(S2):7881
- [8] Balanis, Constantine A. "*Antenna Theory Analysis and Design*" John Wiley & Sons; 2nd edition (1997)
- [9] <https://www.microwaves101.com/encyclopedias/switched-line-phase-shifters>
- [10] Ivo Lj. Markovi, Milka M. Potrebi, Dejan V. Toi, "*Main-line memristor mounted type loaded line phase shifter realization*". Microelectronic Engineering journal, Vol. 185, Jan. 2018, PP.48-54
- [11] <https://www.microwaves101.com/encyclopedias/loaded-line-phase-shifters>

- [12] V. K. Manoharan, "A novel miniaturized loaded line phase shifter", Journal of Scientific and Industrial Research, vol. 69, Nov 2010
- [13] Shrestha, Bikram "A Reflection Type Phase Shifter for iNET Phase Array Antenna Applications" International Telemetering Conference Proceedings journal, Vol. 46 (2010)
- [14] D. M. Pozar, "Microwave Engineering", 3rd edition, John Wiley & Sons, Inc., New York, 2004
- [15] D. Titz, F. Ferrero, C. Luxey, G. Jacquemod, R. Debroucke, R. Pilard, F. Gianesello, D. Gloria, "Reflection-type phase shifter integrated on Advanced BiCMOS technology in the 60 GHz band", Proc. IEEE Int. New Circuits Syst. Conf., pp. 434-437, 2011-Jun.
- [16] E. Sbarra, L. Marcaccioli, R. Vincenti Gatti, R. Sorrentino, "Kuband analogue phase shifter in SIW technology", Proceedings of the 39th European Microwave Conference, pp. 264-26
- [17] J.-C. Wu, T.-Y. Chin, S.-F. Chang, and C.-C. Chang, "2.45-GHz CMOS reflection-type phase shifter MMICs with minimal loss variation over quadrants of phase shift range" submitted to IEEE Trans. Microwave Theory Tech
- [18] <https://www.microwaves101.com/encyclopedias/438->
- [19] R. W. Beatty, "Insertion loss concepts", Proc. IEEE, vol. 52, pp. 663-671, June 1964
- [20] <http://www.spectrum-soft.com/news/fall2009/vswr.shtm>
- [21] <http://www.antenna-theory.com/definitions/vswr.php>
- [22] D. Yeswanth Sai, Suraya Mubeen, Ch. Pranob Kumar & Ch. Sumaja *Implementation of Phase Shifters in Smart Antennas* IJAEEE, vol.2, pp.57-61, 2013
- [23] phase shifter and I-Q modulator catalog www.admiral-microwaves.co.uk/pdf/herley/herley-catalogue-phase-shifters.pdf
- [24] M.-D. Tsai, A. Natarajan, "60 GHz passive and active RF-path phase shifters in silicon", IEEE Radio Frequency Integrated Circuits Symp. (RFIC) Dig., pp. 223-226, 2009

- [25] nGimat co . "A Low Cost Analog Phase Shifter Product Family for Military, Commercial and Public Safety Applications" Microwave journal, march 2 2006 <http://www.microwavejournal.com/articles/1074-a-low-cost-analog-phase-shifter-product-family-for-military-commercial-and-public-safety-applications>
- [26] Phase shifters from L3 Narda-MITEQ company's website: <https://nardamiteq.com/page.php?ID=22&Z=Phase+Shifters>
- [27] Sheikh, S.I.M.; Gibson, A.A.P.; Basorrah, M.; Alhulwah, G.; Alanizi, K.; Alfarsi, M.; Zafar, J., "Analog/Digital Ferrite Phase Shifter for Phased Array Antennas, " Antennas and Wireless Propagation Letters, IEEE, vol.9, no., pp.319-321, 2010.
- [28] Peter MacNeil textit "A Brief Introduction to the Types of RF Phase Shifters" <https://blog.pasternack.com/phase-shifters/brief-introduction-types-rf-phase-shifters/>
- [29] RF-LAMBDA company's website, "Analog Voltage Control Phase Shifter 60-80MHz 180° Full Band" ,<http://www.rflambda.com/pdf/analogcontrolphaseshifter/RVPT0003MAC.pdf>
- [30] Cheng-Hsing Hsu textit "Microwave Engineering" <http://web.nuu.edu.tw/~hsuch/download/microwave5.pdf>
- [31] D. M. Kerns, textit "Plane-wave scattering-matrix theory of antennas and antenna-antenna interactions" in NBS Monograph, Washington, DC:U.S. Govt. Printing Office, vol. 162, June 1981.
- [32] R. W. Beatty, "Some basic microwave phase shift equations", J. Res. NBS (Radio Science), vol. 68D, pp. 349-353, April 196
- [33] K. Kurokawa, "Power waves and the scattering matrix", IEEE Trans. Microwave Theory Tech. 13(1965) 194202; J.-P. Dupont, Proc. Int. Conf. on Radiation Hazards, Columbia, 1960 (Academic Press, New York, 1961), vol. 2, p. 396
- [34] D. M. Kerns, "Analysis of symmetrical waveguide junctions", J. of Research Nat. Bur. of Standards, vol. 46, pp. 267-282, April 1951.
- [35] Robert William Beatty, "Applications of waveguide and circuit theory to the development of accurate microwave measurement

- methods and standards*”, University of Michigan Library (January 1, 1973)
- [36] J. Reed, G. Wheeler, “*A method of analysis of symmetrical four-port networks*”, IRE Trans. Microwave Theory Tech., vol. MTT-4, pp. 246-252, Oct. 1956.
- [37] T. Lambard, O. Lafond, M. Himdi, H. Jeuland, S. Bolioli, “*A novel analog 360° phase shifter design in Ku and Ka bands*”, Microw. Opt. Technol. Lett., vol. 52, no. 8, pp. 1733-1736, Aug. 2010
- [38] Ian Poole, *Varactor diode tutorial*, <http://www.radio-electronics.com/info/data/semicond/varactor-varicap-diodes/basics-tutorial.php>
- [39] P. Philippe, W. El-Kamali, V. Pauker, “*Physical Equivalent circuit model for planar Schottky varactor diode*”, IEEE Trans. Microwave Theory Tech., vol. MTT-36, pp. 250-255, Feb. 1988
- [40] Varactor Diodes application notes, from skyworks’ company website:<http://www.skyworksinc.com/uploads/documents/200824A.pdf>
- [41] Yadav, R., “*Design of tunable monopole arm planar spiral antenna for cognitive radio*”, Adv. Electr. Eng., 2014, 2014, (1), pp. 110.
- [42] D. Titz, F. Ferrero, C. Luxey, G. Jacquemod, R. Debroucke, R. Pilard, F. Gianesello, D. Gloria, “*Reflection-type phase shifter integrated on Advanced BiCMOS technology in the 60 GHz band*”, Proc. IEEE Int. New Circuits Syst. Conf., pp. 434-437, 2011-Jun
- [43] C. S. Lin, S. F. Chang, C. C. Chang, and Y. H. Shu, “*Design of a reflection-type phase shifter with wide relative phase shift and constant insertion loss*”, IEEE Trans. Microw. Theory Tech., vol. 55, no. 9, pp.1862-1868, Sep. 2007
- [44] A. Vilenskiy and M. Makurin, “*Analog varactor phase shifter*”, IEEE, pp.3820-3825, 18 January 2018
- [45] Q. Liu, Y. Liu, Y. Wu, J. Shen, S. Li, C. Yu, M. Su, “*Generalized impedance-transforming dual-band branch-line couplers for arbitrary coupling levels*”, Progress Electromagn. Res. B, vol. 53, pp. 399-415, 2013.

- [46] R. K. Gupta, S. E. Anderson, and W. J. Getsinger, "Impedance-transforming 3-dB 90 hybrids, IEEE Trans. Microw. Theory Tech., vol. MTT-35, no. 12, pp. 1303-1307, Dec. 1987
- [47] Varactor diode SMVA1248-079LF data sheet from skyworks website: www.skyworksinc.com/Product/1800/SMVA1248-079LF
- [48] B. T. Henoeh and P. Tamm, *A 360 reflection-type diode phase modulator*, IEEE Trans. Microw. Theory Tech., vol. MTT-19, no. 1, pp. 103 -105, Jan. 1971
- [49] R. N. Hardin, E. J. Downey, and J. Munushian, *Electronically variable phase shifter utilizing variable capacitance diodes*, Proc. IRE, vol. 48, no. 5, pp. 944 -945, May 1960
- [50] R. V. Garver, "360° varactor linear phase modulator", IEEE Trans. Microw. Theory Tech., vol. MTT-17, no. 3, pp. 137-147, Mar. 1969
- [51] C. Lin, S. Chang, W. Hsiao, "A full-360 reflection-type phase shifter with constant insertion loss", IEEE Microw. Wireless Compon. Lett., vol. 18, no. 2, pp. 106-108, Mar. 2008.
- [52] j. I. Upsur and B. D. Geller, *Low-loss 360 X-band analog phase shifter*, in IEEE MTT-S Int. Dig., Jun. 1990, pp. 487-490.